# Studies on the Synthesis and Evaluation of Novel Small Interfering RNAs with Halide-based Overhang Nucleobases and Branching Structures

# Studies on the Synthesis and Evaluation of Novel Small Interfering RNAs with Halide-based Overhang Nucleobases and Branching Structures

# (ハロアルキル修飾型 siRNA および分岐型 siRNA の合成とその特性評価)

**2019**

**The United Graduate School of Agricultural Science, Gifu University**

**Science of Biological Resources**

**(Gifu University)**

**Akash Chandela**

# Studies on the Synthesis and Evaluation of Novel Small Interfering RNAs with Halide-based Overhang Nucleobases and Branching Structures

# (ハロアルキル修飾型 siRNA および分岐型 siRNA の合成とその特性評価)

**Akash Chandela**

# Contents

# Abbreviations

| | |
|---|---|
| 9-BBN | 9-Borabicyclo[3.3.1]nonane |
| Ago | Argonaute |
| APS | Ammonium peroxodisulfate |
| bd siRNA | Bident siRNA |
| CPG | Controlled pore glass |
| DCM | Dichloromethane |
| DIPEA | N, N-diisopropylethylamine |
| DLS | Dynamic light scattering |
| DMAP | 4-dimethylaminopyrideine |
| DMF | Dimethylformamide |
| DMSO | Dimethylsulfoxide |
| DMTr | 4,4'-dimethoxy trityl |
| ds | Double strand |
| EDTA | Ethylenediamine-N, N, N', N'-tetraacetic acid |
| MALDI-TOF | Matrix Assisted Laser Desorption Ionization-Time of Flight Mass Spectrometry |
| MeCN | Acetonitrile |
| MEM | Minimum essential medium |
| mRNA | Messenger ribonucleic acid |
| NaH | Sodium hydride |
| n-BuLi | n-butyllithium |
| NMR | Nuclear magnetic resonance |
| OD | Optical density |
| PAGE | Poly-Acrylamide Gel Electrophoresis |

# Abbreviations

| | |
|---|---|
| RNA | Ribonucleic acid |
| RP-HPLC | Reverse-phase high performance liquid chromatography |
| ss | Single strand |
| TBAF | Tetrabutylammoniumfluoride |
| TBDMSCl | *tert*-Butyldimethylsilyl chloride |
| TBE | Tris-boronic acid-EDTA |
| td siRNA | Trident siRNA |
| TEAA | Triethylamine-acetic acid |
| TEMED | N,N,N',N'-tetramethyl-ethylenediamine |
| THF | Tetrahydrofuran |
| TLC | Thin-layer chromatography |
| Tm | Melting temperature |
| TMSOTf | Trimethylsilyl Trifluoromethanesulfonate |
| Tris | Tris(hydroxymethyl)aminomethane |
| UV-vis | Ultraviolet visible |

# List of Figures

# List of Figures

# List of Tables

# List of Schemes

# Abstract

The cancer epidemic continues to afflict millions of humans world-wide each year and despite a renewed hope with the development of new and improved forms of therapy, a cure for cancer remains an elusive goal. Conventional chemotherapy and radiation treatments are detrimental to the health of patient as well as tumors have evolved to be resistant against such treatments. In order to encounter these short comings, the scientific community has been laying tremendous efforts for target specific therapy. These approaches have led to a renaissance in the translation of new medicines from pre-clinical to bedside use. Significantly, gene therapy has recently gained widespread traction in cancer research in the advent of the first RNA interference (RNAi) application in humans. RNAi regulates gene expression in a sequence specific manner with the use of non-coding doublestranded RNA substrate, namely short-interfering RNA (siRNA), which triggers the degradation of a targeted complementary mRNA strand within the catalytic site of a protein complex named, the RNA-Induced Silencing Complex (RISC). In this manner, malignant mRNA expression is silenced, thereby inhibiting the translation of proteins that can lead to the production of pathological disorders such as cancer.

In spite of their therapeutic ability, several challenges still possess potential difficulties in utilizing these nucleic acid-based drugs towards the development of a rational cancer-targeting gene therapy. For instance, native siRNAs are unstable, hydrolytically labile with probably low cell permeability, which limits their pharmaceutical importance as a potent in clinical applications.

In this thesis, we present the synthesis and characterization of halide-based nucleoside analogs introduced at the 3'-dangling ends of the modified siRNAs. With this study, we aim to reveal the correlation between the altered interactions of the haloalkyl-nucleobase

modified 3'-overhang with the PAZ domain of Argonaute protein and the silencing activity. Moreover, how these chemical modifications affect the thermodynamic stability as well as exonuclease resistance of the modified siRNA have been evaluated. Lastly, in order to consolidate our hypothesis of hydrogen bond induced improved binding of the haloalkyl analogs with the hydrophobic pocket of the PAZ domain, molecular modelling and protein binding assay have been performed.

In another part of this study, we have designed, synthesized and evaluated the properties of novel branched siRNAs, which is a very first kind of such study with a trebling solid-support. The aim of this work is to provide a rational assembly of larger siRNAs to escape the critical renal filtration and, modify them towards potential gene silencing and nuclease resistant reagents.

Significantly, synthesis and characterization of the modified siRNAs with 3'-overhang halo-alkyl nucleobase is described and discussed in Chapter 2 for the yielding potential siRNAs with improved exonuclease resistance and gene silencing. The novel branched siRNAs, namely trident siRNA (td siRNA) have been reported for enhanced exonuclease resistance as well as improved gene silencing, upon introduction of such structures with the sense strand. Structural analysis revealed a more compact assembly of these molecules. In Chapter 4 of this thesis, the synthesis of haloaryl analogs have been described, which have been designated as the next candidates for the evaluation of PAZ interaction associated gene silencing with overhang modified siRNAs. Lastly, Chapter 5 highlights the notable inferences from these results and collective summary. This thesis represents an important contribution towards this ultimate goal, in an effort to improvise siRNA mediated RNAi through chemical modifications to potentially eradicate major diseases like cancer.

# Chapter 1

## General Introduction

### 1.1. RNA Interference

The finding of the RNA interference (RNAi) phenomenon and the recognition of the small interfering RNA (siRNA) molecule as an RNAi trigger have rationalized the study of gene function and provided a technological tool for modulating the specific gene regulation. RNAi can be defined as a conserved self-defence mechanism found is most eukaryotes where double-stranded RNA (dsRNA) triggers a series of biochemical events and results in sequence-specific suppression of gene expression (Fire *et al.*, 1998; Fire, 1999; Mello and Conte, 2004). This ability of selectively silencing gene expression has characterized this tool as a major development in the next generation of pharmaceutics as a new class genetic therapeutics. Additionally, this discovery is aimed at revolutionizing the posttranscriptional gene regulation and target the diseases which have been classified as undruggable (Wu *et al.*, 2014).

The pathway of RNAi machinery is processed in a series of events. Initially, a ribonuclease (RNase) III-like enzyme called Dicer reduces long double-stranded RNA (dsRNA) and complex hairpin precursors into small interfering RNAs (siRNAs) that degrade mRNA and microRNAs (miRNAs) that attenuate translation, respectively (Fire *et al.*, 1998; Elbashir *et al.*, 2001a; Hammond *et al.*, 2001). In general, RNAi pathway can be comprehensively defined as a simplistic model consisting of two steps, each involving a ribonuclease machine. In the first step, the goal is to generate siRNAs from the processing of dsRNA or microRNA primary transcript by the RNase III enzymes Dicer and Drosha. dsRNA binding proteins (dsRBD) Pasha, Loquacious, and R2D2 are cofactors for the processing events (Murchison and Hannon, 2004).

In the second step, the siRNA and miRNA duplex are recognized by the Argonaute protein and, are loaded onto the effector RNA-induced silencing complex (RISC). During the RISC assembly, the dsRNA is unwound in a strand specific manner. This single-stranded siRNA is guided to mRNA targets having complementary bases through the Watson-Crick base pairing. Eventually, the function of gene silencing is achieved through the nucleolytic degradation of the targeted mRNA by the endonucleolytic activity of the RNaseH enzyme Argonaute. The siRNA causes the gene silencing due to the cleaving of the target mRNA whereas, in the case of miRNAs, if the duplex contains mismatches at the scissile site, the mRNA is not cleaved. And, gene silencing is attained as a result of translational inhibition.

## 1.2. miRNA based gene silencing

Nucleic acid based therapeutics witnessed a great development with the identification of endogenous small RNA molecules, miRNAs, which had an acute impact on the RNA silencing research. Initial reports came in *C. elegans* , where *lin*-4 and *let*-7 miRNAs, were found to be required for proper larval development. miRNAs are single-stranded oligoribonucleotides ~22 bases in length that are processed from ~70 nt hairpin precursor miRNAs (pre-miRNAs) (Murchison and Hannon, 2004; P.N. Pushparaj, J.J. Aarthi, J.Manikandan, 2008; Chakraborty *et al.*, 2017). The miRNA precursors are noncoding transcripts that are predicted to form stem-loop structures containing characteristic bulges and internal mismatches within the folded molecule. These pre-miRNAs are result of the processing of long primary RNA transcripts (pri-miRNAs) in the nucleus by the RNase III enzyme Drosha (DRSH-1).

Exportin-5 enzyme mediates the export of the pre-miRNAs to the cytoplasm, where they are processed by Dicer (DCR-1) to form the mature ~22 nt miRNAs. Mature miRNAs are loaded onto Argonaute (ALG-1/2) proteins to form the miRNA induced silencing complex

(miRISC). Distinctively, miRNAs utilize the imperfect base pairing to recognize target mRNAs and suppress their expression. Cofactors associated with miRISC induce destabilization or translational repression of bound target mRNAs. However, previous reports also stated that a well-characterized let-7 miRNA, which naturally directs translational attenuation, can also lead to the cleavage of mRNA because of the sequence being completely complementary to the target (Hutvágner and Zamore, 2002; Murchison and Hannon, 2004; Pfeifer and Lehmann, 2010).

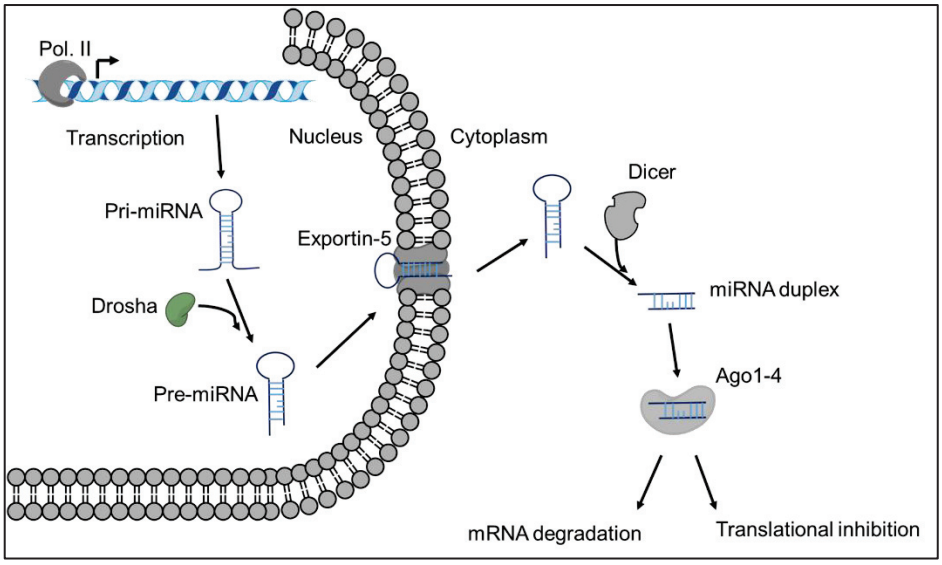


**Fig. 1.1.** Schematic representation of miRNA mediated RNAi.

## 1.3. Small Interfering RNA mediated gene silencing

siRNAs are another class of short, double-stranded regulatory RNAs that mediate gene silencing through catalytic cleavage of the target mRNA. It contains two signature characteristics: a two nucleotide 3'-end overhang and a phosphorylated 5'-end (Elbashir *et al.*, 2001a, 2001b). The synthesis of these siRNAs result from the processing of long non-coding RNAs (lncRNAs) with the dicer endoribonuclease. This siRNA is 21-23 nucleotide long and consists of the functional and non-functional strands. The functional strand, also known as the

guide or antisense strand, contains the seed region from 2nd – 8th nucleotide which is completely complementary to the target mRNA (Fig. 2A). The non-functional strand is called passenger or sense strand, which gets cleaved during the event of mature siRNA formation.

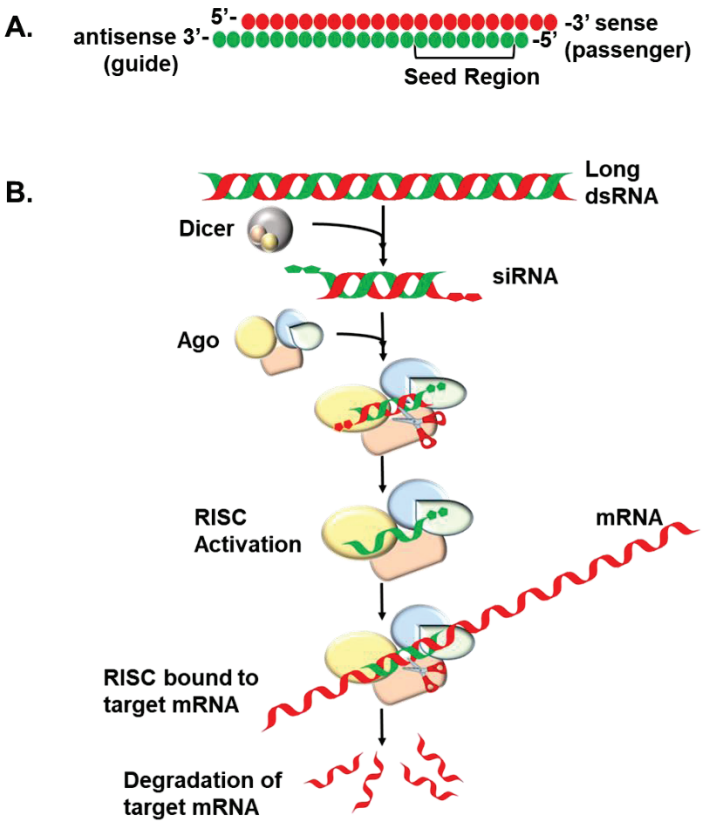


**Fig. 1.2. A.** Structure of siRNA and **B.** siRNA mediated RNAi.

The siRNA is then recognized by the Argonaute (Ago) protein (detailed explanation in later section) and this loading leads to the degradation of the passenger strand in the series of events. Mature siRNA and Ago protein forms RNA-induced silencing complex (RISC), which leads the guide strand to target mRNA and the endonucleolytic activity of Ago protein directs the chopping of the target mRNA (Fig. 2B). In this manner, the expression of particular genes can be regulated in a sequence-specific manner (Schütze, 2004; Leachman *et al.*, 2008).

However, there are numerous factors which limit the efficient exploitation of these class of drugs. The major challenges are faced with the stability and systemic delivery of these compounds. In the later sections, we will discuss these hurdles in the siRNA mediated gene silencing.

## 1.4. Argonaute Protein

In addition to the small non-coding RNAs, Ago protein is another key factor which drives the whole process of RNAi. The Ago protein loads the siRNA and process it for cleaving the target mRNA or perform translation inhibition. In human, there are eight Ago family members, some of which are investigated intensively. These Ago proteins are evolutionarily conserved and composed of four domains: the N-terminal (N), Piwi/Argonaute/Zwille (PAZ), middle (MID), and P-element induced wimpy testis (PIWI) domains (Wang *et al.*, 2008; Elkayam *et al.*, 2012; Schirle and MacRae, 2012).

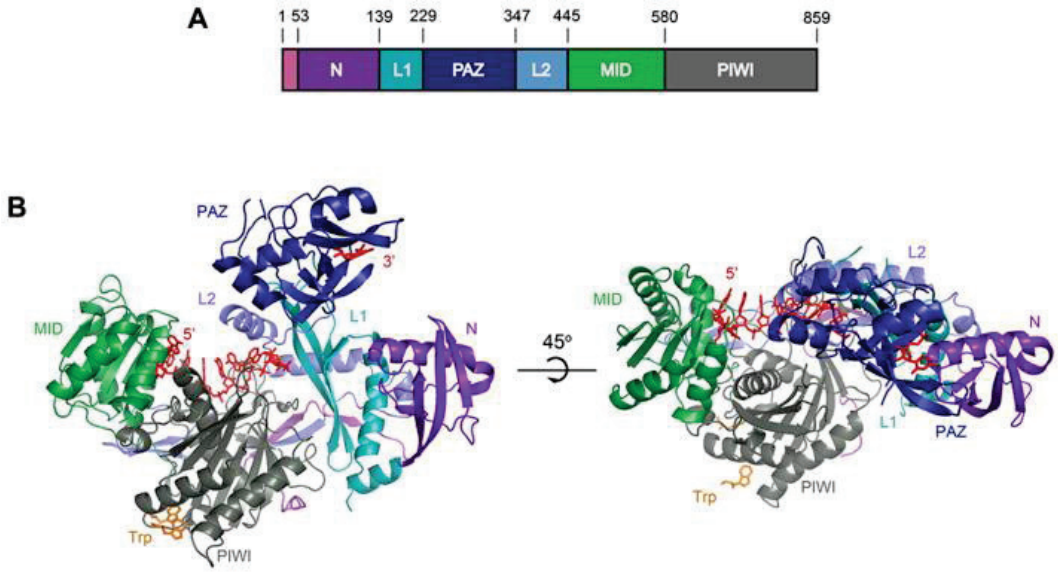


**Fig. 1.3. A.** Assembly of human Ago2 and **B.** Crystal structure of hAgo2.

However, even though Ago1-4 are capable of loading miRNA, endonuclease activity and thus RNAi-dependent gene silencing exclusively belongs to Ago2. Previous reports have revealed that the 5'-OH of the synthetic guide strand is phosphorylated by the cellular kinases in cells, and the resulting 5'-phosphate of the guide strand is recognized by the MID domain and tightly anchored in the Ago protein. It has also been reported that the PAZ domain contains a nucleic acid binding site which recognizes the 3'-end of the guide strand. PIWI domain is responsible for the endonucleolytic cleavage of the target mRNA. Whereas, the function of N-terminal is still unknown (Matranga *et al.*, 2005; Frank *et al.*, 2010; Kandeel and Kitade, 2013). Moreover, it was also suggested that, in the series of biochemical events to cause mRNA degradation, the guide strand is repetitively released and again anchored with the Ago protein in RISC. Hence, many studies have been directed to investigate the role of the 2-nt overhang at the 3'-end to ascertain the relationship between the binding affinity with the PAZ domain and the resultant gene silencing activity.

### *Role of PAZ-domain*

Several lines of evidence suggested that PAZ domain consists an RNA binding site. The structural studies have further confirmed the existence of the central pocket for the binding of nucleic acids, which was examined to be conserved with the free and RNA bound proteins. The 2-nt were reported to be buried in this hydrophobic pocket consisting of aromatic and basic residues (Lingel *et al.*, 2003; Song *et al.*, 2003; Ma *et al.*, 2004; Valenzuela *et al.*, 2016). Major interactions stated with such structural studies showed that the hydrogen bonding arising out of electrostatic interaction and van der Waals interaction, were two critical forces to affect the binding of the 2-nt overhang with the PAZ domain. Hence, providing the scope for further investigation with numerous modifications at the dangling ends.

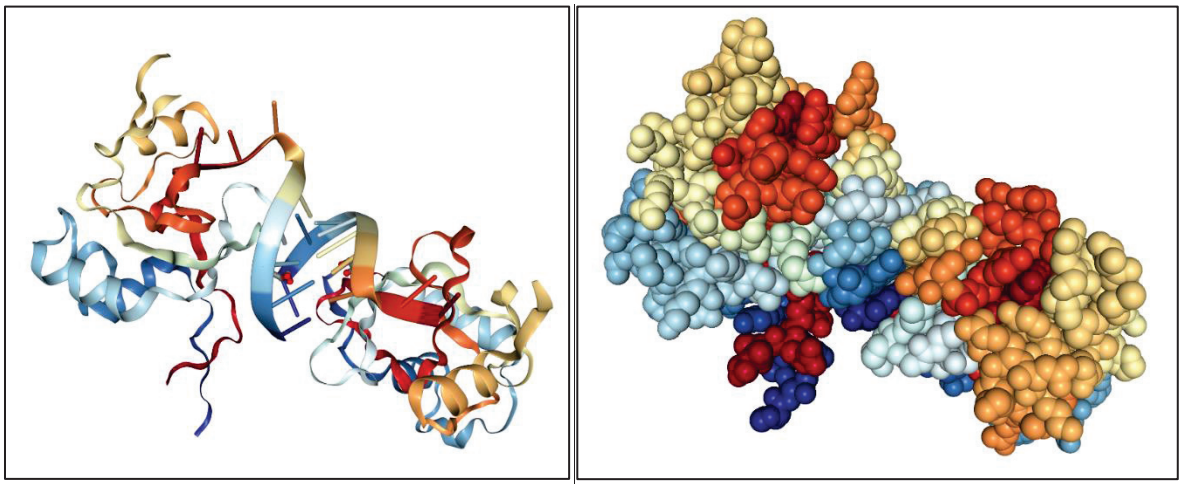

**Fig. 1.4.** Tertiary structure of PAZ domain (PDB ID- 1SI3).

## 1.5. Challenges in siRNA mediated RNAi

Although the application of siRNAs sounds useful in therapeutic practice, natural siRNAs have to face numerous challenges for efficient functioning. A great deal of research is being led in this direction to overcome these limitations and produce potential siRNA based therapeutics. The major problems with unmodified siRNAs are their vulnerability to hydrolytic degradation by nuclease in serum, another significant issue is that they act as potent triggers of the innate immune response, particularly when associated with delivery vehicles that facilitate intracellular uptake (Paroo and Corey, 2004; Pecot *et al.*, 2011; Haussecker, 2014; Borna *et al.*, 2015; Wang *et al.*, 2017). Unmodified siRNAs can also induce off-target effects, as they interfere with natural miRNA pathways. The delivery of siRNAs is another substantial challenge, as these molecules cannot easily pass through cell membranes owing to their size and negative charge.

These factors complicate the translation of siRNA therapeutics to clinical application. These challenges have been classified as extracellular and intracellular barriers in the siRNA

mediated gene silencing, as shown in Fig. 1.5. The extracellular barriers comprise of the degradation by nucleases, renal clearance, and uptake by the reticuloendothelial systems. Many chemical modifications have evidently enhanced the stability of siRNAs and protected against hydrolysis by the nucleases (Ueno *et al.*, 2008, 2009; Chernikov *et al.*, 2017; Gvozdeva *et al.*, 2018). Small size and molecular weight lower than 40 kDa render the siRNA prone to the kidney filtration process. Therefore, carrier systems with a hydrodynamic size of over 6 nm and increased the molecular weight are required (Zuckerman *et al.*, 2012; Bienk *et al.*, 2016). Immunostimulation is another barrier in the delivery of siRNA as it leads to degradation of siRNA after recognition as an alien moiety by the macrophages and kupffer cells (Whitehead *et al.*, 2011; Khairuddin *et al.*, 2012). In order to tackle this issue, 2'-position of the ribose sugar had been modified with 2'-O-methyl and 2'-fluoro groups to suppress the immune response and improve serum provide stability (Valenzuela *et al.*, 2014; Haraszti *et al.*, 2018).

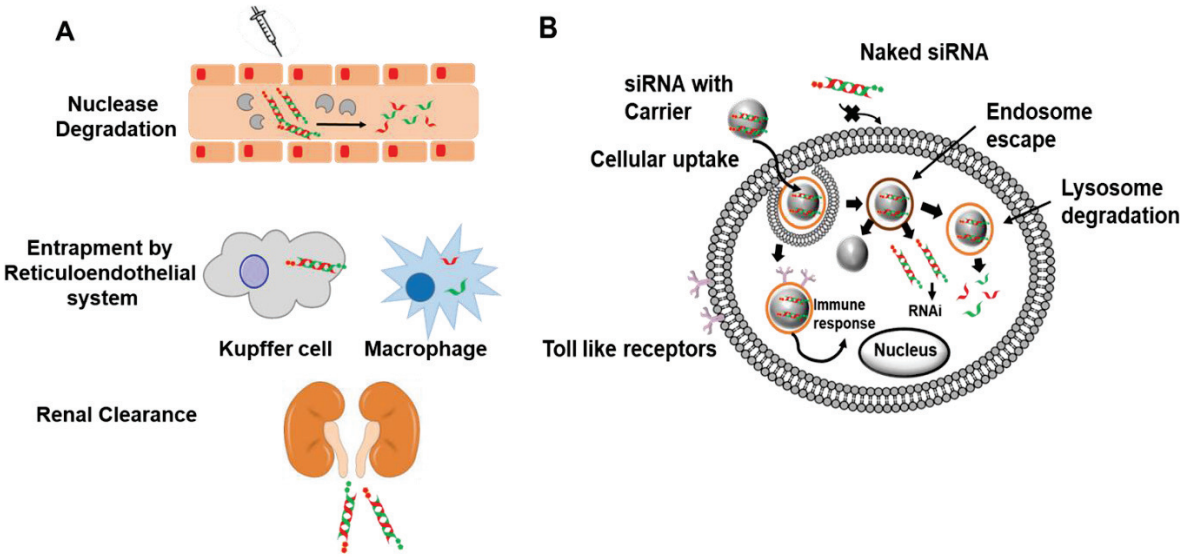


**Fig. 1.5.** Challenges in siRNA administration. **A.** Extracellular barriers; **B.** Intracellular barriers.

Intracellular barriers inhibit the siRNA to permeate the lipid bilayers due to charge repulsion. Hence, cationic delivery systems are utilized for the transport of siRNA inside the cell via endocytosis. The endosomal pH is lower than that of the cytosol and the release can be mediated through a proton pump, inability to do so leads to degradation by the lysosome limiting the bioavailability of siRNA to interact with RISC machinery in the cytosol (Ma, 2014; Tuttolomondo *et al.*, 2017).

## 1.6. Chemical modifications of siRNAs

Currently, the most mature nucleic acid based therapeutic approach focus on the use of chemically modified siRNAs, which can address some of the problems discussed in preceding section. These chemical modifications can be broadly divided into three types i.e. (1) backbone modification, (2) sugar modification and (3) base modification (Fig. 1.6).

The natural siRNAs are unstable and prone to hydrolytic degradation. Synthetic siRNAs provide better stability with essential chemical modifications. The database of chemical modification types seems ever expanding and continuous efforts have provided the basis for the determination of effective chemical modifications in siRNAs to simultaneously reduce siRNA immunogenicity (Whitehead *et al.*, 2011), miRNA-like off-targeting (Gresham, 2003), to enhance nuclease resistance/bio-availability in vivo (Ambardekar *et al.*, 2011; Chernikov *et al.*, 2017; Gvozdeva *et al.*, 2018), and silencing duration while preserving siRNA potency.

The modification of phosphodiester backbone with phosphorothioate or boranophosphate leads to higher nuclease resistance and cell internalisation. The 2'-OH substitution with 2'-OMe and 2'-F have been reported for immunostimulation (Robbins *et al.*, 2007; Whitehead *et al.*, 2011; Eberle *et al.*, 2014). The base modifications have not been extensively utilized, but they have shown better stability and base pairing ability against the natural counterparts.

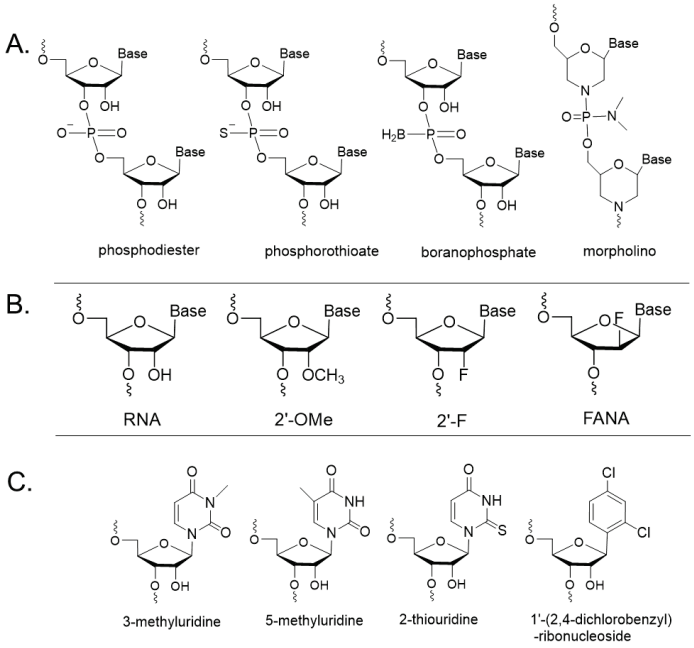


**Fig. 1.6.** Chemical modifications with siRNAs. **A.** backbone; **B.** sugar; **C.** base modification.

## 1.7. Drug delivery

Chemical modifications alone doesn't cater the problems associated with the systemic administration of the siRNAs. These concerns have remarkably increased the advances in the design and development of advanced carrier systems for targeted delivery of the siRNA drugs via systemic delivery (Chandela and Ueno, 2019). Initial progress in this direction saw the incorporation of lipid-based carrier systems with further shift towards the conjugation of cell penetrating peptides, aptamers and other fatty acids (Wang *et al.*, 2010). Shielding the drugs with pegylation and forming complexes of few nanometers were considered in due course of drug delivery system developments.

Many groups have reported systemic delivery of siRNA with different carrier systems such as bioconjugates, complexes and nanoparticles (Crombez *et al.*, 2009; Wagner, 2012;

Zuckerman *et al.*, 2012; Bienk *et al.*, 2016; Liu and Peng, 2016; Kruspe and Giangrande, 2017; Tushir-Singh, 2017). Recent developments have been the combinatorial formulation of carriers to form complexes on the nanoscale for the systemic delivery of siRNA therapeutics. This technique involves the construction of carrier systems with the conjugation of two or more delivery systems in combination, for overcoming the challenges in administration by utilizing the characteristic merits of each of the delivery systems (Zhou *et al.*, 2008; Yang *et al.*, 2015; Li *et al.*, 2016; Peng *et al.*, 2017).

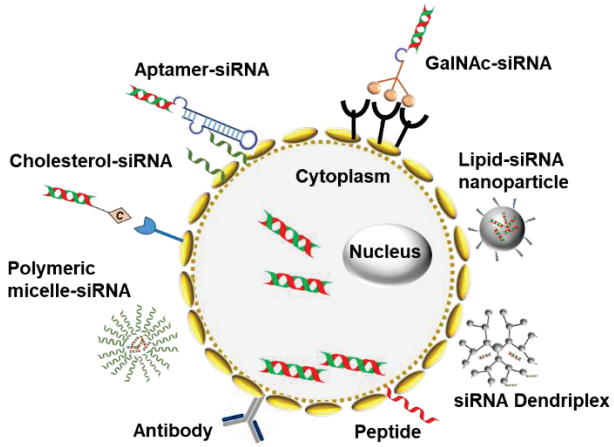


**Fig. 1.7.** Various carriers for delivery of siRNA drugs.

Furthermore, lately, dendrimer based delivery systems have gained importance among the scientific community. These dendrimers are small and compact structures which can either encapsulate siRNAs or surface immobilized with siRNAs for delivery to the target organ site. The cationic charge of dendrimers neutralize the anionic nature of the siRNAs and enhance membrane permeability. Moreover, a new class of structures have been designed based on the single unit of dendrimer, i.e. dendron. Bola-amphiphilic dendrons have been reported to deliver siRNAs inside the cell and release into the cytoplasm on association with the reactive oxygen species (Liu *et al.*, 2016; Eldredge *et al.*, 2018).

A vast domain of delivery systems have been analysed and are still under evaluation for efficient administration of these siRNA therapeutics. Continuous developments in this direction, will soon witness astounding results and are desired to bring revolution in the field of siRNA based genetic therapeutics.

## 1.8. Clinical-trial status of siRNA therapeutics

With advanced research and extensive efforts in formulating nucleic acid-based therapeutics, siRNA treatment has been studied for various diseases (Pruijn, 2006; de França *et al.*, 2010; Cryan *et al.*, 2013). Many of such drugs have been studied with lipid-based carrier systems but recent developments have witnessed the conjugate based delivery to the liver as well as cationic peptides for efficient endosomal escape. Some of the major diseases which have been targeted with siRNA drugs have been listed in the following table (Table 1.1).

**Table 1.1.** List of targets for RNAi Therapeutics.

| Disease | Target | Reference |
|---|---|---|
| Age-related Macular Degeneration | Vascular endothelial growth factor | (Garba and Mousa, 2010) |
| Acute Kidney Injury | P53 | (Molitoris *et al.*, 2009) |
| Colorectal Cancer with Hepatic Metastases | Macrophage migration inhibitory factor | (He, 2017) |
| Glaucoma | β2 adrenergic receptor | (Martínez *et al.*, 2014) |
| Dry Eye Disease | Transient Receptor Potential Vanilloid 1 | (Moreno-Montañés *et al.*, 2018) |
| Chronic Myeloid Leukemia | BCR-ABL gene | (Valencia-Serna *et al.*, 2014) |
| Hepatocellular Carcinoma | Kinetochore-associated protein 2 | (Makita *et al.*, 2017) |
| Hypercholesterolemia | Pproprotein convertase subtilisin-kexin type 9 | (Kosmas *et al.*, 2018) |
| Pachyonychia Congenita | Keratin 6a | (Leachman *et al.*, 2008) |
| Primary Hyperoxaluria Type1 (PH1) | Alanine-glyoxylate aminotransferase | (Liebow *et al.*, 2017) |

Significant amount of siRNA based drugs have long been under clinical trials. Some of those with remarkable outcomes have been discussed here and shown in the following table. (Table 1.2). Bevasiranib was the first siRNA-based drug to enter the clinical trials for the treatment of age-related macular degeneration (AMD) (Garba and Mousa, 2010). Drugs targeting the RTP801 gene are also for the treatment of AMD (Nguyen et al., 2012). Treatment

for respiratory syncytial nasal virus infection was administered therapeutically in single and multiple dose regimens using the ALN-RSV01 conjugate (Alvarez et al., 2009). Acute renal failure and kidney injury have been evaluated as critical ailments after cardiac surgery. QPI-1002, a siRNA-based drug, has been analyzed for curing these problems (Demirjian et al., 2017). PCSK9 silencing using a siRNA drug significantly reduced the level of blood LDL cholesterol in healthy patients and provided evidence for their safe administration against hypercholesterolaemia (Fitzgerald et al., 2014). Cancer cells have been reported to overexpress VEGF; hence, siRNA drug targeting inhibition of this gene has notably demonstrated anti-cancerous activity with sufficient tolerance to the drug (Fitzgerald et al., 2017). Mutation in the transthyretin (TTR) gene results in elevated levels of amyloid and accumulation of these fibrils in various tissues results in heart failure, central nervous system breakdown, and postural hypotension (Rizk and Tüzmen, 2017).

These developments have led to the successful formulation of the drug patisiran by the trade name ONPATTRO, which the first siRNA drug for the treatment of the polyneuropathy of hereditary transthyretin-mediated (TTR) amyloidosis in adults, was recently approved by the Food and Drug Administration (FDA) in 2018. This drug treats numerous problems such as degradation by nucleases, off-target effects, and low cell membrane permeability of siRNAs impede the translation of siRNA-based drugs to clinical applications. However, there are other drugs which are awaiting trial recruitment for investigating their action in disease treatment. Therefore, this field provides enormous potential to extend new domains into genetic therapeutics for numerous undruggable targets.

**Table 1.2.** Clinical trial status of siRNA dugs.

| Drug | Target | Condition | Phase/Status | Investigator (Reference) |
|---|---|---|---|---|
| TKM-080301 | Polo-kinase-1 | Cancer Neuroendocrine Tumors Adrenocortical Carcinoma | I, II/Completed | Arbutus Biopharma Corporation, United States (Demeure *et al.*, 2016) |
| AGN211745 | VEGFR1 | Choroid Neovascularization AMD | II/Terminated | Allergan, Ireland (Barakat and Kaiser, 2009) |
| ALN-PCS02 | PCSK9 | Elevated LDL-Cholesterol | I/Completed | Alnylam Pharmaceuticals, United States (Fitzgerald *et al.*, 2014) |
| ALN-RSV01 | RSV-N Gene | Respiratory Syncytial Virus Infections | II/Completed | Alnylam Pharmaceuticals, United States (J. *et al.*, 2016) |
| ALN-TTR01 | TTR | Transthyretin mediated Amyloidosis | II/Completed | Alnylam Pharmaceuticals, United States (Coelho *et al.*, 2011) |
| ALN-TTRSC | TTR | Acute Kidney Injury | II/Completed | Alnylam Pharmaceuticals, United States (T. *et al.*, 2013) |
| Atu027 | PKN3 | Advanced Solid Tumors | I/Completed | Silence Therapeutics GmbH, Germany (Strumberg *et al.*, 2011) |
| Atu027-I-02 | PKN3 | Metastatic Pancreatic Cancer | II/Completed | Silence Therapeutics GmbH, Germany (Schultheis *et al.*, 2016) |
| Bevasiranib | VEGF | Age-related macular degeneration (AMD) | III/Terminated | Opko Health Inc., United States (Garba and Mousa, 2010) |
| CALAA-01 | RRM2 | Cancer Solid Tumors | I/Terminated | Calando Pharmaceuticals, United States (Zuckerman *et al.*, 2014) |
| PF-04523655 | RTP801 | Choroidal Neovascularization Diabetic Retinopathy Diabetic Macular Edema | II/Completed | Quark Pharmaceuticals, Israel (Nguyen et al., 2012) |

## 1.9. Motivation

RNAi is a conventional phenomenon for the regulation of gene expression but this can be utilized as a technological tool for the treatment of epigenetic ailments with the specific gene suppression. Synthetic siRNAs are the ideal candidates for mediating the gene silencing as they are a defined class of reagent that can be subjected to desired chemical modification to construct highly potent molecules for nucleic acid therapeutics. In addition, siRNA is a powerful tool for studying the loss-of-function phenotypes in mammalian cells. And, the high potency of siRNA, its ease of use make it possible to carry out genome-wide gene silencing experiments to gain new insight in critical biological processes and to identify novel therapeutic targets.

Although, numerous chemical modifications have been performed with the siRNAs, but the introduction of halide-based groups at the 3'-dangling ends have never been performed on a comparative basis. The hypothesis of enhanced interaction of such overhangs with the PAZ domain due to electrostatic interaction resulting in hydrogen bond formation with such highly electronegative moieties forms the basis of this study. With different analogs, the electronegativity as well as van der Waals radii changes, such physicochemical properties are interesting for the comparative study and also, how these kind of interactions actually correlate with the silencing activity, seemed intriguing as a researcher.

Furthermore, delivery carriers have been employed to shield the siRNAs against nuclease degradation and increase their size to perform efficient systemic administration by escaping the renal filtration, which flushes out molecules with around 40 kDa of molecular weight. Notably, dendrimer based carriers have not been extensively exploited in this regard. Hence, it’s fascinating to trident siRNAs using the divergent synthesis approach of dendrimer. In this

manner, self-assembled siRNAs with molecular weight of over 42 kDa could be synthesized as trident siRNAs. There is no any evidence of such a synthesis using a trebling solid-support unit. Hence, this could be a great contribution in the field of nucleic acid based therapeutics with such novel branching structures.

Therefore, all these factors cumulatively played a part in the formulation and designing such a novel theme. Lastly, these kind of minimally modified siRNAs with self-assembled delivery systems could yield in further designing of other delivery systems.

## 1.10. Objectives

The objectives of this dissertation are (1) synthesis of the halide-based nucleobase analogs for introduction at 3'-overhangs of small interfering RNAs and characterize the modified siRNAs for PAZ-domain interaction associated gene silencing, and (2) novel synthesis of the branched siRNAs with a divergent approach and evaluate their properties for gene silencing and nuclease resistance with such structural variation.

# Chapter 2

## Synthesis and characterization of small interfering RNAs with haloalkyl groups at their 3’-dangling ends

### 2.1 Introduction

The siRNA 3'-overhang of the guide strand, which is bound by the Ago PAZ domain during loading, is conveniently tolerant to chemical modification. This reflects a limited role of PAZ binding during target cleavage (Ma et al., 2004) where the 3'-overhang is released from the PAZ domain (Tomari and Zamore, 2005; Wang et al., 2009b). This renders siRNA 3'-overhangs relatively safe to modify, even with bulky modifications incompatible with the size of the PAZ binding pocket. This provides an opportunity for many research groups, including ours, to study and exploit this interaction between the 3'-dangling end of siRNA and the PAZ domain of hAgo2 for improved gene silencing.

With the aim of enhancing the nuclease resistance and the RNAi activity of siRNAs, various 3'-modified siRNAs have been synthesized and characterized (Inada *et al.*, 2015; Xu *et al.*, 2015; Valenzuela *et al.*, 2016). The previous report on the synthesis and characterization of the RNAi activities of siRNAs containing acetal-type nucleoside analogs with several alkyl groups instead of bases at their 3'-dangling ends formed the basis of this study. We found that the siRNA containing 2,2,2-trifluoroethyl β-D-ribofuranoside (**1**) at the 3'-dangling end was the most potent among the synthesized siRNAs. Next, we considered that, as the fluorine atom acts as the hydrogen bond acceptor, the hydrogen bonds between fluorine atoms and amino acid residues in the hydrophobic pocket of the PAZ domain might be preferred to elicit RNAi activity.

Based on these background information, in this study, we designed and synthesized the siRNAs containing the acetal-type nucleoside analogs with the haloalkyl groups, 2,2,2-

trichloroethyl β-D-ribofuranoside (**2**) and 2,2,2-tribromoethyl β-D-ribofuranoside (**3**), at their 3'-dangling ends. We envisioned that, as the chlorine and bromine atoms are less electronegative and more hydrophobic than the fluorine atom, we would be able to obtain new knowledge that would be useful for designing new siRNAs by comparing the properties of modified siRNAs. In this study, we evaluated the thermal stabilities, RNAi activities, and nuclease resistance properties of the modified siRNAs. In addition, we analyzed the interaction between the 3'-dangling ends and the PAZ domain by molecular modeling and enzyme-linked immunosorbent assay (ELISA).

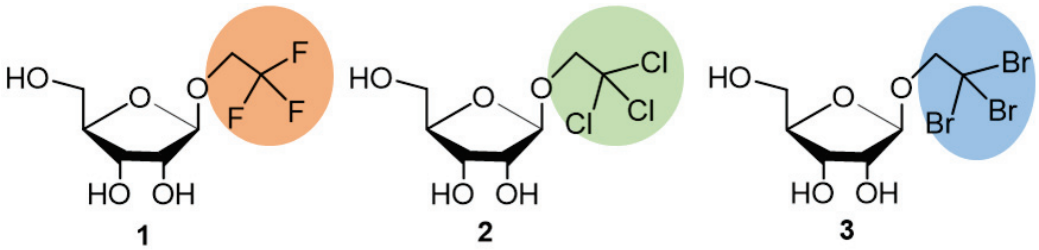


**Fig. 2.1.** Structures of modified haloalkyl nucleoside analogs.

## 2.2 Experimental strategy

*Mechanism of* β-*selective substitution at 1-position of* D-*ribofuranose*

Prior reports with the synthesis of a photo-cross-linking microRNA (miRNA) probe consisting of the nucleoside analog 1- *O*-[4-(3-trifluoromethyl-3H-diazirin-3-yl)]benzyl-β-D-ribofuranose, showed the substitution of the natural base with an aryl residue via an acetal linkage. We considered that different substituents could be β-selectively introduced at the 1-position of D-ribofuranose via an acetal linkage by using 1-*O*-acetyl-2,3,5-tri-*O*-benzoyl- β -D-ribofuranose as a starting material. The mechanism of TMS triflate activated introduction of haloalkyl bases has been described in Fig. 2.2.

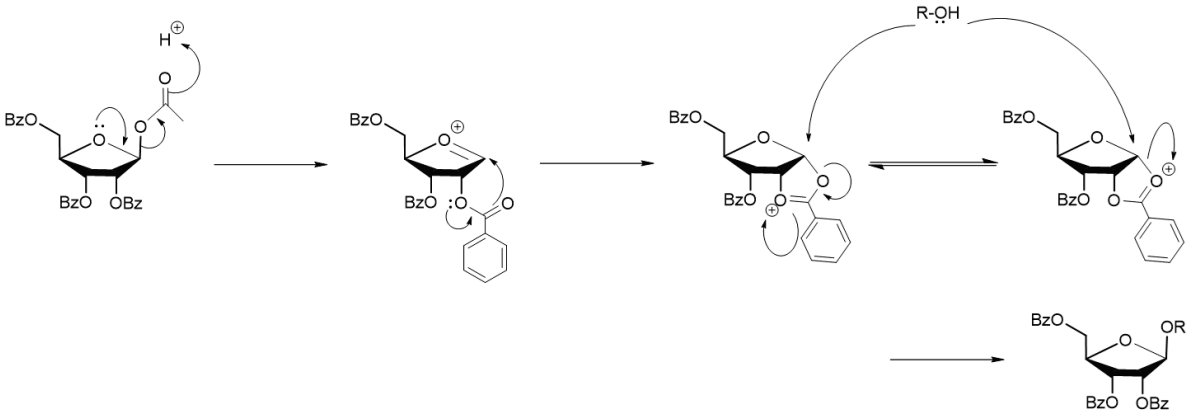


**Fig. 2.2.** Mechanism of β-selective substitution at 1-*O*-position of rifuranose.

## 2.3. Results and Discussion

### 2.3.1. Synthesis of haloalkyl analogs

The phosphoramidites of the nucleoside analogs **2** and **3** were synthesized in a similar manner to the synthesis of that of the nucleoside analog **1** using the protocol from our previous work. Analog **1** was also freshly synthesized for this study using the synthetic route as shown in Scheme 1.1. The glycosylation reaction of 1-*O*-acetyl-2,3,5-tri-*O*-benzoyl-β-D-ribofuranose (**4**), which is commercially available, with trichloroethanol (**5**) in the presence of trimethylsilyl triflate (TMSOTf) at −30 °C in $CH_2Cl_2$ gave the β-anomer **7** in 79% yield. Subsequently, **7** was debenzoylated in the presence of a catalytic amount of $NaOCH_3$ in $CH_3OH$ to afford the product **2** in 89% yield. Then, the primary hydroxyl group of **2** was protected by a 4,4'-dimethoxytrityl (DMTr) group to give the corresponding 5-*O*-DMTr derivative **9** in 97% yield. Silylation of **9** by *tert*-butyldimethylsilyl chloride (TBDMSCl) yielded the 2-*O*-TBDMS (**12**) and 3-*O*-TBDMS (**11**) derivatives in 26% and 32% yields, respectively. The 2-*O*-TBDMS derivative **12** was phosphitylated by a standard procedure to give the corresponding phosphoramidite **15** in

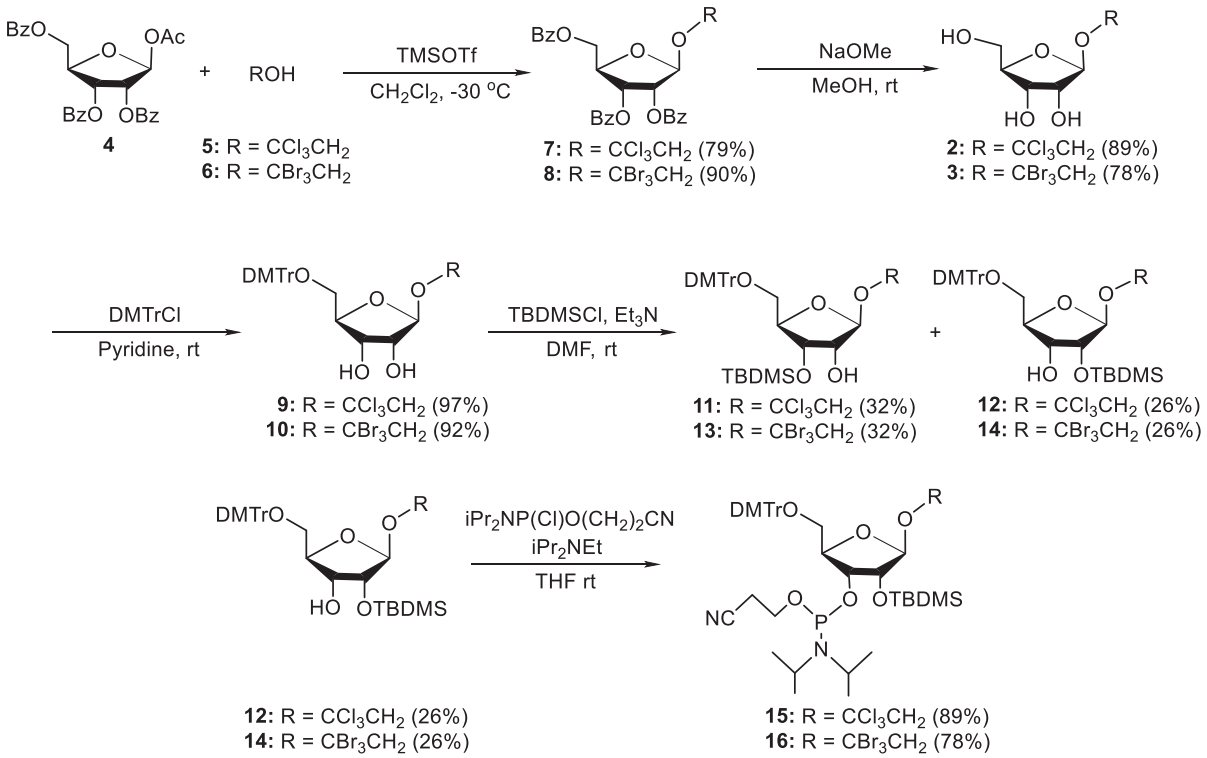


**Scheme 2.1.** Synthetic route for the synthesis of phosphoramidites of haloalkyl analogs.

89% yield. In a similar manner, the phosphoramidite **16** of the tribromoethyl analog **3** was synthesized in 78% final yield.

To incorporate the acetal-type nucleoside analogs **2** and **3** at the 3'-end of an RNA oligomer, compounds **11** and **13** were converted to the corresponding succinates, which were then reacted with controlled pore glass (CPG) to produce the solid supports **17** and **18** in the yields of 58 and 50 μmol/g, respectively (Scheme 2.2).

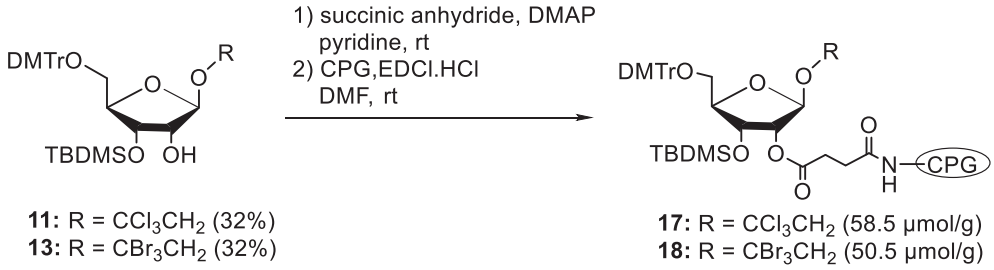


**Scheme 2.2.** Synthetic route for the synthesis of CPG solid-support of haloalkyl analogs.

## 2.3.2. Synthesis of RNAs with modified haloalkyl analogs

RNAs containing the analogs **2** and **3** were synthesized using the phosphoramidites **15** and **16,** and the solid supports **17** and **18** by a DNA/RNA synthesizer. After purification via polyacrylamide gel electrophoresis (PAGE), the RNAs were analyzed for mass by matrix-assisted laser desorption/ionization time-of-flight mass spectrometry (MALDI-TOF/MS).

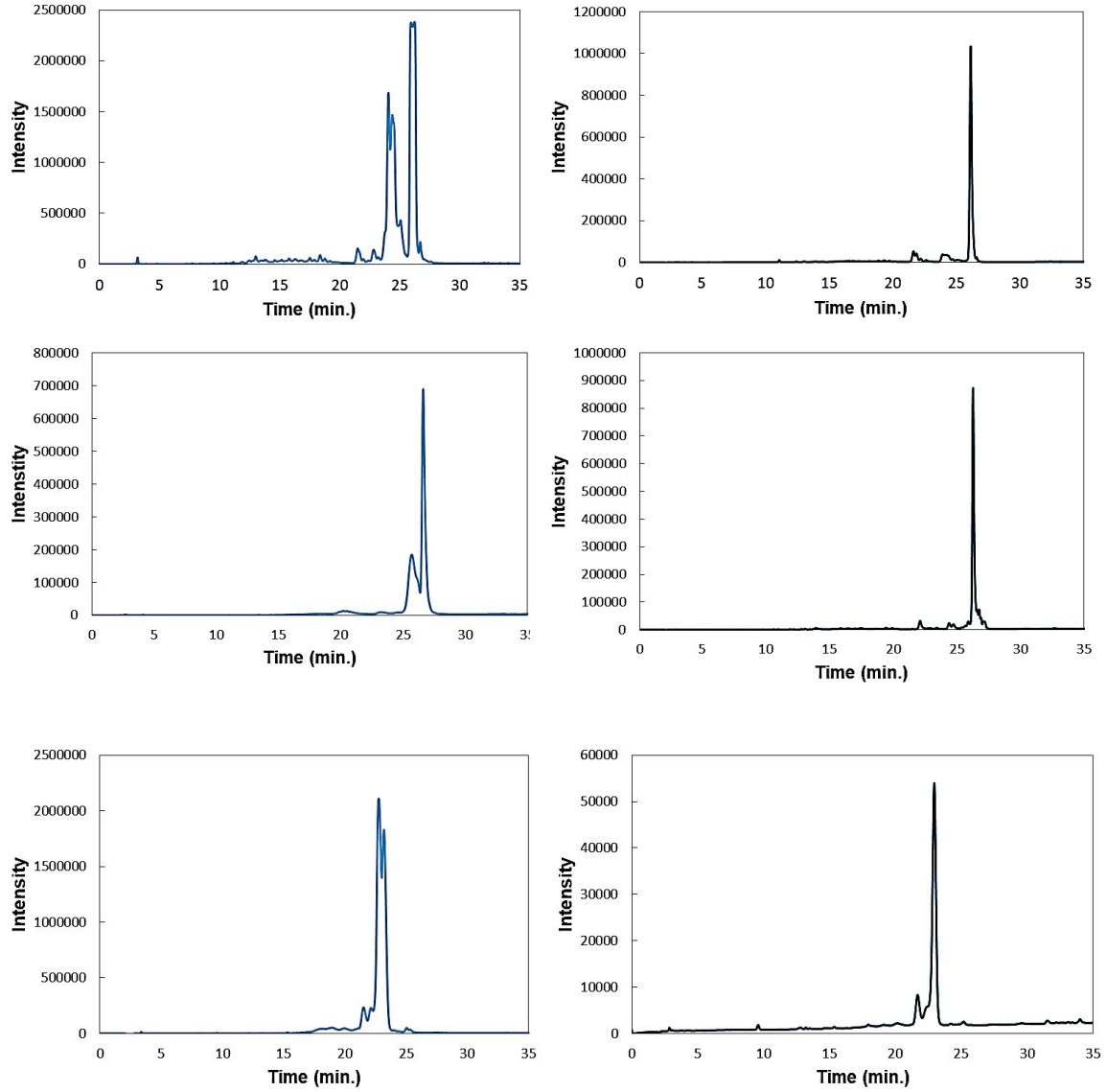


**Fig. 2.3.** HPLC chromatogram of crude and purified tribromoethyl modified RNA.

All RNAs showed the corresponding molecular ion peaks, while several peaks thought to be attributable to the olefin formation by the E2 elimination reaction on the tribromoethyl moieties were observed in the profiles for crude RNA **7**, RNA **8**, and RNA **13**. The mass spectrum showed a sequence of molecular ion peaks differing exactly around 79 mass units. Hence, this dealkylated product was hypothesized to be formed during oligonucleotide synthesis under basic conditions of the capping solution and raisin removal using ammonia solution. Thus, RNA **7**, RNA **8**, and RNA **13** were further purified by RP-HPLC using gradient method (Fig. 2.3). These RNAs were again analyzed by MALDI-TOF/MS, and the observed molecular weights from these analyses were in agreement with the structures of the RNAs. RNA sequences used in this study are listed in Tables 1 and 3.

### 2.3.3. Lipophilicity of the modified RNAs

To examine the lipophilicity of the RNAs involving the haloalkyl groups, the hydrophobicity was expressed as a function of their retention times on a reversed-phase C-18 HPLC (RP-HPLC) under gradient method. The retention times for each of the RNA **2**, RNA **4**, RNA **6**, and RNA **8** were found to be 11, 15, 18, and 19 min, respectively (Fig. 2.2). The hydrophobic nature have been associated with increased retention time. Thereby, the surge in the retention time with the modified RNAs suggests their enhanced lipophilic nature in comparison to the unmodified RNA. This improved lipophilicity was also hypothesized to enable these analogs to yield higher interactions with the hydrophobic pocket of the PAZ domain. The order of the lipophilicity of the modified RNAs was observed as to increase from the RNA **4** with the trifluoroethyl group to the RNA **8** with the tribromoethyl group, with the RNA **6** having trichloroethyl group showing intermediate nature.

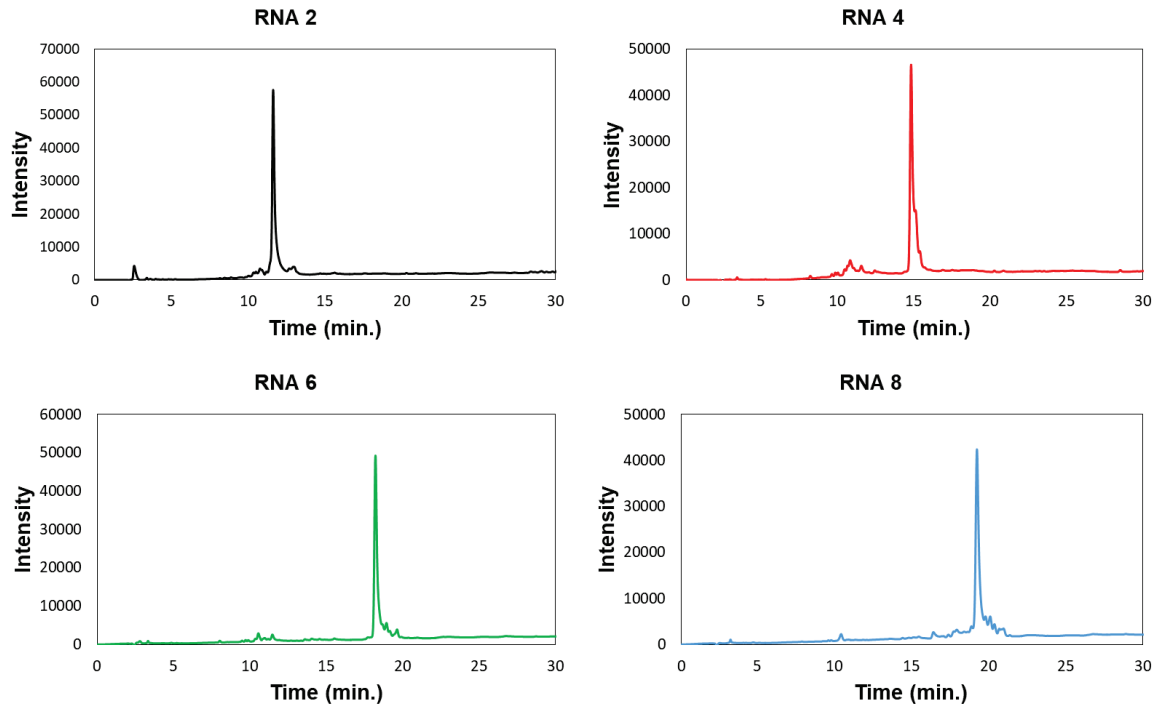


**Fig. 2.4.** HPLC chromatogram for lipophilicity analysis of haloalkyl analog modified RNAs.

## 2.3.4. Thermal stability of the modified RNAs

The thermal stability of siRNA duplexes containing the analogs **1**, **2**, and **3** at their 3'-dangling ends were evaluated by UV melting experiments in a buffer composed of 10 mM sodium phosphate (pH 7.0) and 100 mM NaCl (Fig. 2.5). The melting temperature ($T_m$) values and change in values ($\Delta T_m$) with respect to the unmodified RNA duplex are shown in Table 1. The $T_m$ value of the unmodified siRNA **1** was 78.5 °C, whereas those of the modified siRNAs **2**–**4** were 77.1, 78.0, and 76.4 °C, respectively. Thus, the siRNAs with the haloalkyl groups at the 3'-dangling ends instead of a nucleobase were found to be thermally less stable than the siRNA with natural uridines at the 3'-dangling ends. The order of the thermal stability of the modified siRNAs were as follows: the siRNA **3** with the trichloroethyl group > the siRNA **2** with the trifluoroethyl group > the siRNA **4** with the tribromoethyl group.

**Table 2.1**

Thermal denaturation study of haloalkyl analog modified siRNAs.

| siRNA | RNA | Sequence[a] | $T_m$ (°C) | $\Delta T_m$ (°C)[b] |
|---|---|---|---|---|
| Control | (Buffer) | - | – | – |
| | | Sense strand (Passenger strand) | | |
| siRNA **1** | RNA **1** | 5'- GGCCUUUCACUACUCCUAC**UU**-3' | 78.5±0.2 | – |
| | RNA **2** | 3'-**UU**CCGGAAAGUGAUGAGGAUG-5' | | |
| | | Antisense strand (Guide strand) | | |
| siRNA **2** | RNA **3** | 5'- GGCCUUUCACUACUCCUAC**11**-3' | 77.1±0.1 | −1.4 |
| | RNA **4** | 3'-**11**CCGGAAAGUGAUGAGGAUG-5' | | |
| siRNA **3** | RNA **5** | 5'- GGCCUUUCACUACUCCUAC**22**-3' | 78.0±0.3 | −0.8 |
| | RNA **6** | 3'-**22**CCGGAAAGUGAUGAGGAUG-5' | | |
| siRNA **4** | RNA **7** | 5'- GGCCUUUCACUACUCCUAC**33**-3' | 76.4±0.2 | −2.3 |
| | RNA **8** | 3'-**33**CCGGAAAGUGAUGAGGAUG-5' | | |

[a]The highlighted regions in the overhangs denote the modifications.

[b]$\Delta T_m$ represents [$T_m$ (siRNA$_{mod}$) - $T_m$ (siRNA$_{unmod}$)].

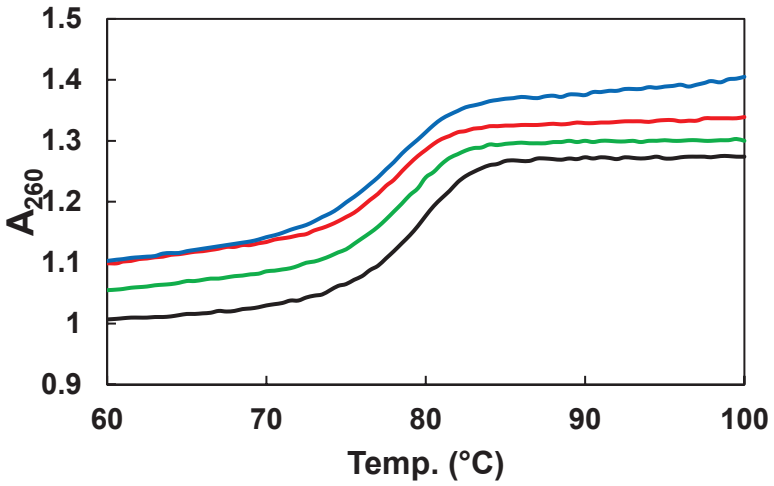


**Fig. 2.5.** UV melting profiles of the modified and unmodified siRNAs. Black: siRNA **1**; Red: siRNA **2**; Green: siRNA **3**; Blue: siRNA **4**.

It is known that the dipole moment of haloalkanes is in the order R-Cl > R-F > R-Br > R-I, where R indicates an alkyl group. Thus, these results suggested that not only lipophilic interactions, but also dipole−dipole interactions among the haloalkyl side chains and the adjacent bases in the dangling ends are important for enhancing the thermal stability of the RNA duplexes.

## 2.3.5. Gene silencing activity of the modified RNAs

The RNAi activities of the unmodified and modified siRNAs were investigated with a dual luciferase reporter assay using HeLa cells, in which the target luciferase genes were constitutively expressed. All siRNAs targeted the *Renilla* luciferase genes, while firefly luciferase genes were used as controls. All siRNAs were transfected using RNAimax. The expression levels of both luciferase genes were analyzed after 12 h and 24 h of incubation of cells transfected with the unmodified and modified siRNAs. The graphical representation of the ratios of Renilla:firefly luciferase activities with respect to the no siRNA control indicating the silencing of target mRNA after 12 h and 24 h of incubation, has been shown in Figs. 2.6 and 2.7, respectively.

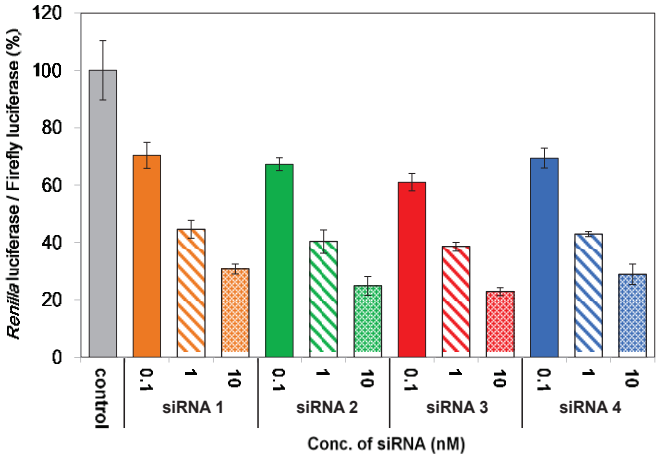


**Fig. 2.6.** RNAi activity of the unmodified and modified siRNAs with 12 h incubation.

**Table 2.2.**

RNAi activity for 12 h incubation with haloalkyl analog modified siRNAs.

| siRNA | Sequence | Upper: 0.1 nM<br>Middle: 1 nM<br>Lower: 10 nM |
|---|---|---|
| Control | (buffer) | 100 ± 10.3 |
| siRNA 1 | Sense strand<br>5'-GGCCUUUCACUACUCCUAC**UU**-3'<br>3'-**UU**CCGGAAAGUGAUGAGGAUG-5'<br>Antisense strand | 70.4 ± 4.5<br>44.6 ± 3.1<br>30.8 ± 1.7 |
| siRNA 2 | 5'-GGCCUUUCACUACUCCUAC**11**-3'<br>3'-**11**CCGGAAAGUGAUGAGGAUG-5' | 64.3 ± 2.3<br>40.4 ± 4.0<br>24.8 ± 3.3 |
| siRNA 3 | 5'-GGCCUUUCACUACUCCUAC**22**-3'<br>3'-**22**CCGGAAAGUGAUGAGGAUG-5' | 61.0 ± 3.0<br>38.6 ± 1.4<br>22.8 ± 1.4 |
| siRNA 4 | 5'-GGCCUUUCACUACUCCUAC**33**-3'<br>3'-**33**CCGGAAAGUGAUGAGGAUG-5' | 69.4 ± 3.5<br>42.9 ± 0.9<br>28.9 ± 3.6 |

Gene expression from cells transfected with each siRNA has been normalized and presented as the percentage from three independent experiments, with three replicate samples per experiment.

The siRNAs modified at the two dangling ends exhibited improved RNAi activities than the unmodified siRNA **1**. The strongest silencing activity was observed for the trichloroethyl−modified siRNA **3**, followed by the trifluoroethyl− and tribromoethyl−modified siRNAs **2** and **4**. Treatment with 10 nM of the siRNAs **2**, **3**, and **4** inhibited gene expression by 75%, 77% and 71%, respectively; whereas, treatment with 10 nM of the unmodified siRNA **1** suppressed gene expression by 69% (Table 1.2).

Moreover, similarly, the cells were transfected with modified siRNAs and incubated for 24 h. And, the results indicated a similar tendency to the observed activity for the 12 h incubation of cells transfected with modified siRNAs. In this case, the treatment with 10 nM of the siRNAs **2**, **3**, and **4** showed reduced gene expression at 14%, 10% and 14%, respectively; whereas, treatment with 10 nM of the unmodified siRNA **1** exhibited gene expression at 21% (Table 1.3). Hence, the inhibition of the gene expression was highly augmented with the increased incubation time of transfected cells.

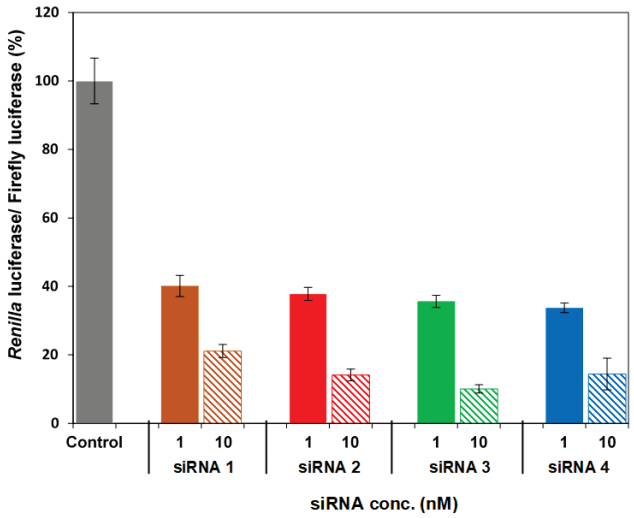


**Fig. 2.7.** RNAi activity of the unmodified and modified siRNAs with 24 h incubation.

**Table 2.3.**

RNAi activity for 24 h incubation with haloalkyl analog modified siRNAs.

| siRNA | Sequence | Upper: 10 nM<br>Lower: 1 nM |
|---|---|---|
| Control | (buffer) | 100±6.7 |
| siRNA 1 | Sense strand<br>5'-GGCCUUUCACUACUCCUAC**UU**-3'<br>3'-**UU**CCGGAAAGUGAUGAGGAUG-5'<br>Antisense strand | <br>21.1±1.9<br>40.1±3.1 |
| siRNA 2 | 5'-GGCCUUUCACUACUCCUAC**11**-3'<br>3'-**11**CCGGAAAGUGAUGAGGAUG-5' | 14.1±1.7<br>37.8±1.9 |
| siRNA 3 | 5'-GGCCUUUCACUACUCCUAC**22**-3'<br>3'-**22**CCGGAAAGUGAUGAGGAUG-5' | 10±1.2<br>35.6±1.8 |
| siRNA 4 | 5'-GGCCUUUCACUACUCCUAC**33**-3'<br>3'-**33**CCGGAAAGUGAUGAGGAUG-5' | 14.4±4.6<br>33.7±1.4 |

Gene expression from cells transfected with each siRNA has been normalized and presented as the percentage from three independent experiments, with three replicate samples per experiment.

## 2.3.6. Molecular modeling study of the modified RNAs

Next, we evaluated the binding energy of the analogs **1**−**3** with the PAZ domain through *ab initio* Fragment Molecular Orbital calculation. For this study, the entry 1SI3 from the Protein Data Bank (PDB) was used and modified with the analogs **1**−**3** without disturbing the complex structure. The modified strands were found to have a different orientation of the analogs **1**−**3** in the hydrophobic pocket. The analogs **1**−**3** showed unrestricted rotation and increased electrostatic interaction with the basic residues, whereas the native bases were found to be stacked over aromatic residues such as F292; this could be due to pi-bond stacking interaction (Fig. 2.8).

The terminal analog displayed improved affinity with residues K313 and H334. Similarly, the second to the last analog exhibited enhanced interaction with the residues R275, K333, and T335. All other forces remain conserved, and only these interactions contributed to the overall enhanced binding energy, as shown in Fig. 2.9-2.10.

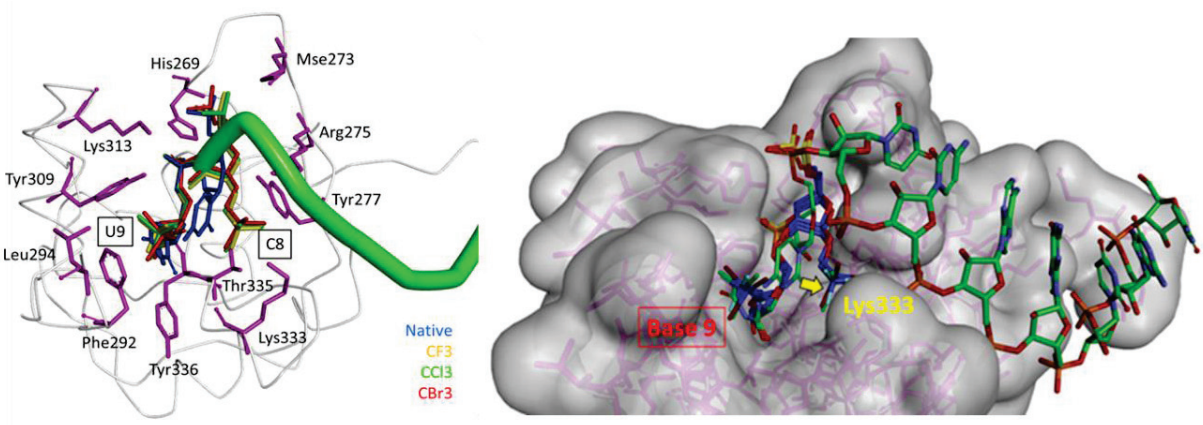


**Fig. 2.8.** Binding of dangling end ribonucleotides (unmodified and modified) in the PAZ hydrophobic pocket.

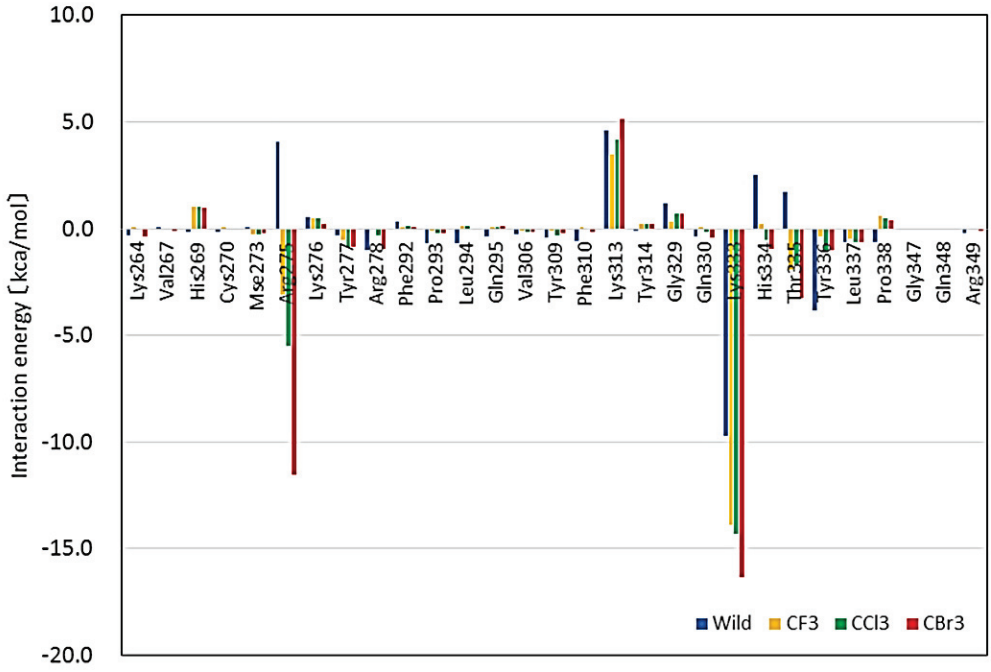


**Fig. 2.9**. Interaction profile of **base 8** (2nd to last) with PAZ domain.

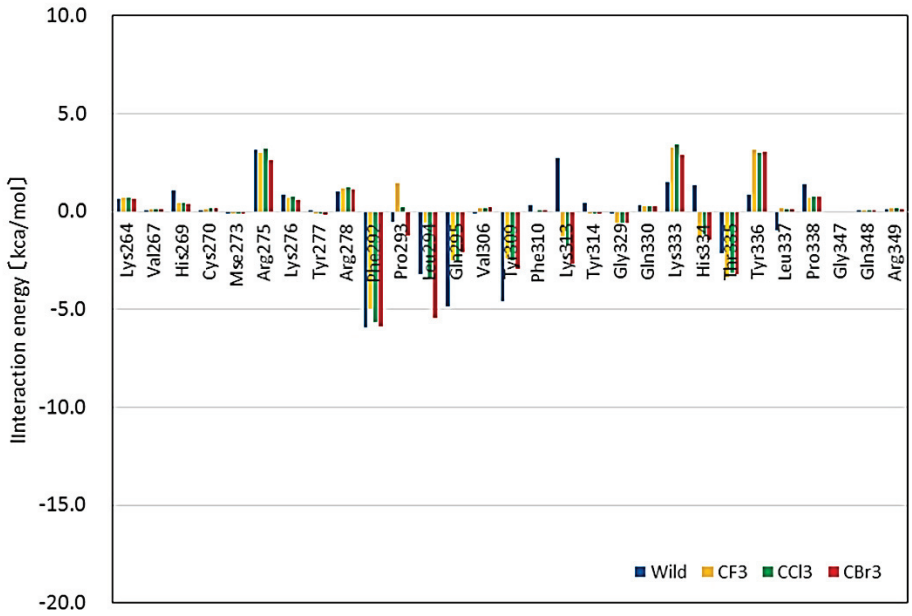


**Fig. 2.10.** Interaction profile of **base 9** (last) with PAZ domain.

These hydrophobic modifications tended to enhance binding of siRNA with certain basic residues, resulting in an overall increase in binding energy. The binding energy was found to be negatively highest (highest binding) for the 2,2,2-trichloroethyl analog−modified siRNA, followed by similar values for the 2,2,2-trifluorethyl and 2,2,2-tribromoethyl analogs (Table 2). All the analogs are found to have enhanced electrostatic interaction, consolidating our hypothesis of H-bond formation with amino acid residues. In addition, the size of analogs affected the van der Waals interaction and thereby caused the trichloroethyl analog to have the best binding to PAZ domain. The results for the binding affinity of the analogs with the PAZ domain were found to be in congruence with the RNAi activity. Therefore, our data indicate that better interaction with the PAZ domain, arising out of hydrogen bonding, is attributed to improved gene silencing.

**Table 2.4**

Binding interaction enthalpy of the modified RNAs.

| | modification | | vdW | electrostatic | ΔE (kcal/mol) |
|---|---|---|---|---|---|
| | 8-base | 9-base | | | |
| Native | rC | rU | −142.33 | −1974.31 | −2116.64 |
| F | $-OCH_2CF_3$ | $-OCH_2CF_3$ | −139.91 | −1993.72 | −2133.63 |
| Cl | $-OCH_2CCl_3$ | $-OCH_2CCl_3$ | −159.02 | −1986.36 | −2145.39 |
| Br | $-OCH_2CBr_3$ | $-OCH_2CBr_3$ | −152.24 | −1983.06 | −2135.30 |

vdW: van der Waals. ΔE: binding energy.

## 2.3.7. Affinity of PAZ domain to the modified dangling ends

To experimentally examine the affinity of the PAZ domain to the modified dangling ends, we carried out ELISA. The sequences of siRNAs used in this study are shown in Table 2.5. The 3'-blunt ends of the sense strands were modified with a biotin tag, while the 3'-ends of the antisense strands had the analogs **1**−**3**. These siRNAs were immobilized on the streptavidin-coated 96-well microplate. The recombinant human Ago2 PAZ domain protein, which was prepared according to the previously reported method, was then added to each well. The protein bound to siRNA was detected using an anti-His tag monoclonal antibody conjugated with horseradish peroxidase (HRP). The activity was measured as a function of absorbance at 450 nm as shown in Fig. 2.11. These results showed the improved binding of the modified siRNAs against the unmodified. And the highest binding affinity to the PAZ domain was observed with the trichloroethyl analog, which falls in congruency with the molecular modeling data. These interactions could also be attributed and related with the nature of gene silencing activity with different analogs having varied binding to PAZ domain.

**Table 2.5**

Sequences of siRNAs used for ELISA.

| siRNA | RNA | Sequence[a] |
|---|---|---|
| | | Sense strand |
| siRNA **5** | RNA **9** | 5'- GGCCUUUCACUACUCCUAC-**Bio**-3' |
| | RNA **2** | 3'-**UU**CCGGAAAGUGAUGAGGAUG -5' |
| | | Antisense strand |
| siRNA **6** | RNA **9** | 5'- GGCCUUUCACUACUCCUAC-**Bio**-3' |
| | RNA **4** | 3'-**11**CCGGAAAGUGAUGAGGAUG -5' |
| siRNA **7** | RNA **9** | 5'- GGCCUUUCACUACUCCUAC-**Bio**-3' |
| | RNA **6** | 3'-**22**CCGGAAAGUGAUGAGGAUG -5' |
| siRNA **8** | RNA **9** | 5'- GGCCUUUCACUACUCCUAC-**Bio**-3' |
| | RNA **8** | 3'-**33**CCGGAAAGUGAUGAGGAUG -5' |

[a]Bio denotes a biotin residue.

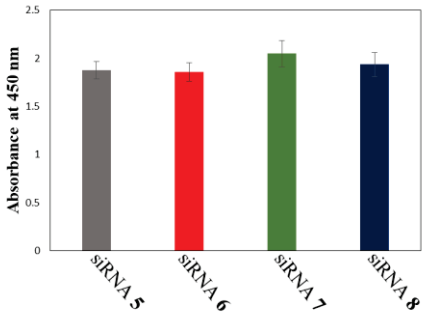


**Fig. 2.11.** ELISA to detect the binding of siRNAs to the recombinant human Ago2 PAZ domain protein.

## 2.3.8. Exonuclease resistance of the modified RNAs

As natural RNAs are easily hydrolyzed by nucleases present inside and outside the cells, the use of natural RNAs as siRNA therapeutics is limited. Thus, synthesis of nuclease−resistant RNAs is important to the development of siRNA drugs. The terminal modifications with the haloalkyl analogs **1**−**3** were expected to result in improved resistance to exonucleases. Thus, we analyzed the nuclease resistance of the modified RNAs by using snake venom phosphodiesterase (SVPD), a 3'-exonuclease.

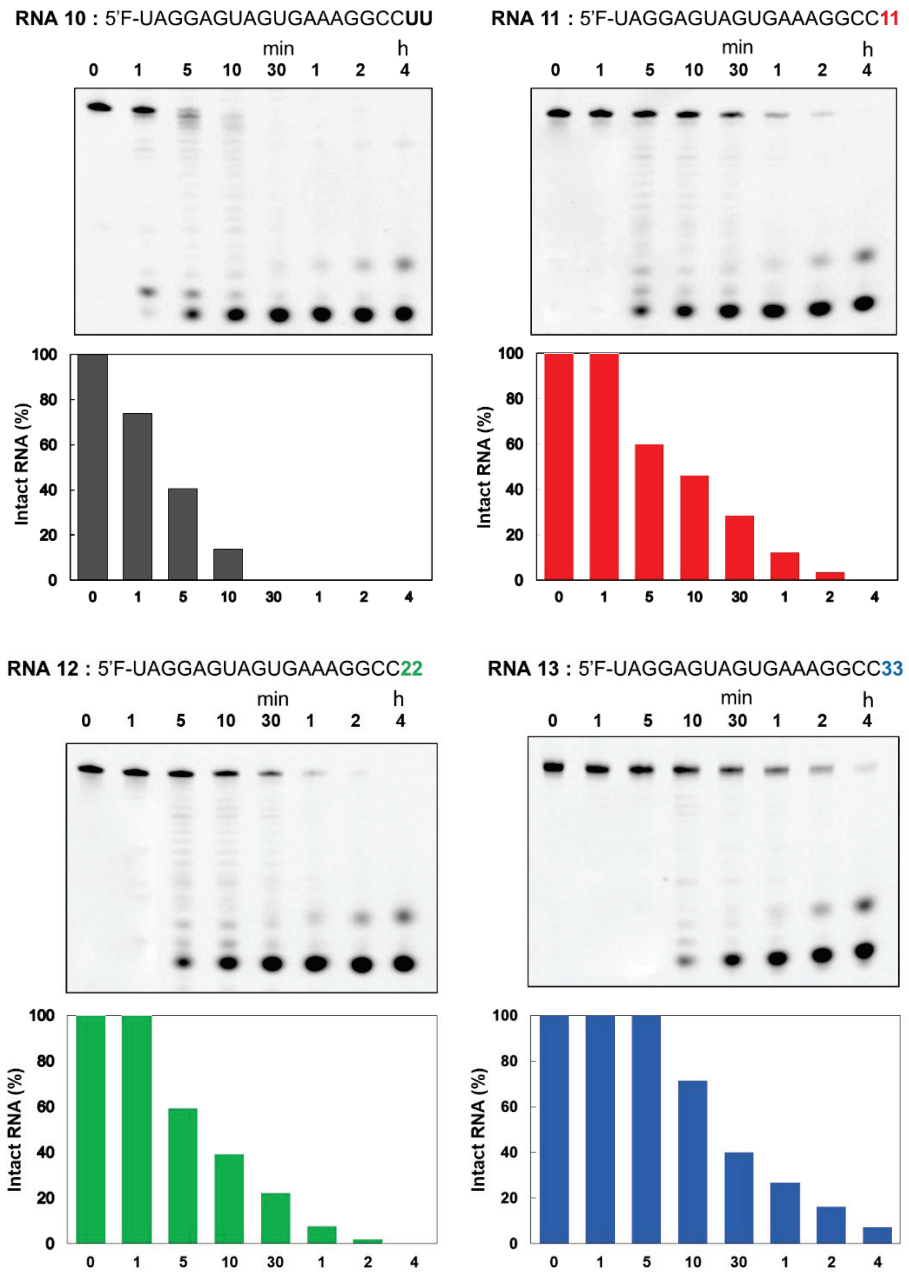


**Fig. 2.12.** 20% denaturing PAGE of RNAs hydrolyzed by SVPD. F denotes a fluorescein.

The unmodified RNA **10** and the modified RNAs **11**−**13** were labeled with fluorescein at the 5'-ends, incubated with SVPD, and then analyzed by denaturing PAGE. As shown in Fig. 2.12, the unmodified RNA was degraded very quickly by the nuclease within 5 minutes of incubation; whereas, the modified RNAs exhibited enhanced stability to the enzyme. The half-

-life ($t_{1/2}$) of unmodified RNA **10** was found to be 3.4 min, while those of the modified RNAs **11**−**13** were 15.5, 12.2, and 28.2 min, respectively. The best resistance was observed with the tribromoethy−modified RNA, followed by trifluoroethyl− and trichloroethyl−modified RNAs, respectively. This result could be attributed to the increased size and unrestricted movement of the molecule, thus protecting the phosphodiester bond and improving nuclease resistance.

## 2.4. Conclusion

We have demonstrated the synthesis of the following siRNAs containing the haloalkyl β-D-ribofuranosides at their 3'-dangling ends: trifluoroethyl β-D-ribofuranoside (**1**), trichloroethyl β-D-ribofuranoside (**2**), and tribromoethyl β-D-ribofuranoside (**3**). We evaluated the thermal stabilities, RNAi activities, and nuclease resistance properties of the modified siRNAs. In addition, we analyzed the interaction between the 3'-dangling ends and the PAZ domain by molecular modeling and ELISA. Administered at 10 nM, the modified siRNAs exhibited improved RNAi activities than the unmodified siRNA **1**. The best activity was observed for the trichloroethyl−modified siRNA **3,** followed by the trifluoroethyl− and tribromoethyl−modified siRNAs **2** and **4**. The incorporation of the analogs notably enhanced the resistance of RNAs to degradation by a 3'-exonuclease compared to that of a natural RNA. The best resistance was observed for the tribromoethyl−modified RNA, followed by the trifluoroethyl− and trichloroethyl−modified RNAs. Thus, incorporation of trichloroethyl β-D-ribofuranoside (**2**) at the 3'-dangling ends of synthetic siRNAs may hold as a promising solution for the application of more potent siRNA drugs.

# Chapter 3

## Novel synthesis and evaluation of branching siRNAs with trebling solid support

### 3.1 Introduction

Branched siRNAs is a very fascinating field of study for this class of therapeutics. Moreover, it's still lurching in the dark during its initial stages of development. Hence, there are not much evidence of such branched structures for siRNAs mediated gene silencing. Several strategies can be used to prepare branched RNA structures (Shchepinov *et al.*, 1997, 1999). Although the synthesis of these compounds is complex and tedious, commercially available synthons have improved the complexity and yields of these structures, but they only provide the branching units as phosphoramidites and not as the one single solid-support.

Previous reports have stated the construction of such architectures through hybridisation of three different RNAs or using the commercially available doubling and tripling synthons for synthesizing the branched structures. Synthetic branched oligonucleotides have been applied for several purposes. Initially, most of the interest in this area was focused on the study of branched oligoribonucleotides as splicing intermediates of eukaryotic mRNAs. Moreover, branched oligonucleotides show high affinity for single-strand oligonucleotides to form alternated strand triplexes (Grøtli *et al.*, 1997; Utagawa *et al.*, 2007). Recently, branched oligonucleotides have been used as building blocks in the synthesis of new nanostructures. Multilabelled oligonucleotides containing branching points have been described to increase the sensitivity of hybridization experiments (Aviñó *et al.*, 2011; Chang *et al.*, 2012; Sajeesh *et al.*, 2014). But, we focussed on the simultaneous synthesis of three arms of RNA on a single solid-support to yield compact branched structures with the aim to escape the renal filtration during systemic administration.

Here, we synthesized the branched RNA structures using the modified solid-support achieved by divergent synthesis approach (Fig 3.1). Next, we evaluated the thermodynamic stability, hydrodynamic size, RNAi activity and 3'-exonuclease resistance of the branched siRNAs. Given that the use of symmetric branching units is compatible with most of the modifications described to enhance the inhibitory capacity of siRNA, the molecules described here may provide a starting point for further modifications.

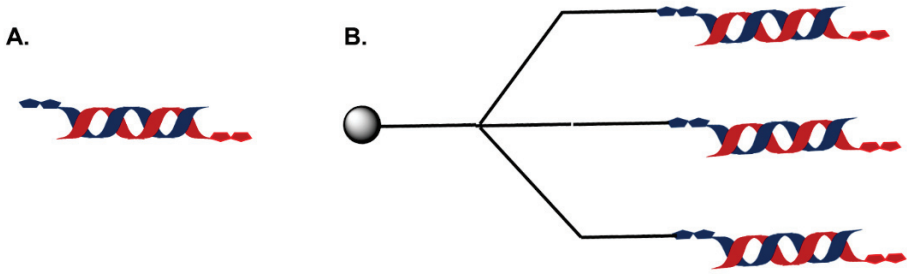


**Fig. 3.1.** Structure of the siRNA for RNAi, A. Duplex siRNA, B. Trident siRNA (this study).

## 3.2. Experimental Strategy

*Steric hindrance due to bulky groups*

Pentaerythritol, which is commercially available, has been widely utilized to accommodate branching structures, e.g. branched oligonucleotides as DNA probes. We also used it as the starting material for the synthesis of our modified CPG solid-support. Interestingly, over the series of organic reactions, the desired trebling solid-support was prepared and incorporated for RNA synthesis (Scheme 3.1). But, the close proximity of the three DMTr (trityl) groups proved troublesome for the efficient synthesis of the full length target sequences. The structural analysis using the ChemBioDraw software, provided the evidence of this accumulation of bulkyl groups giving rise to the steric hindrance (Fig 3.2).

Therefore, we thrived for more elongated arms of the solid support through double C-O coupling in repetitive manner. Additionally, the structural analysis of the new solid-support

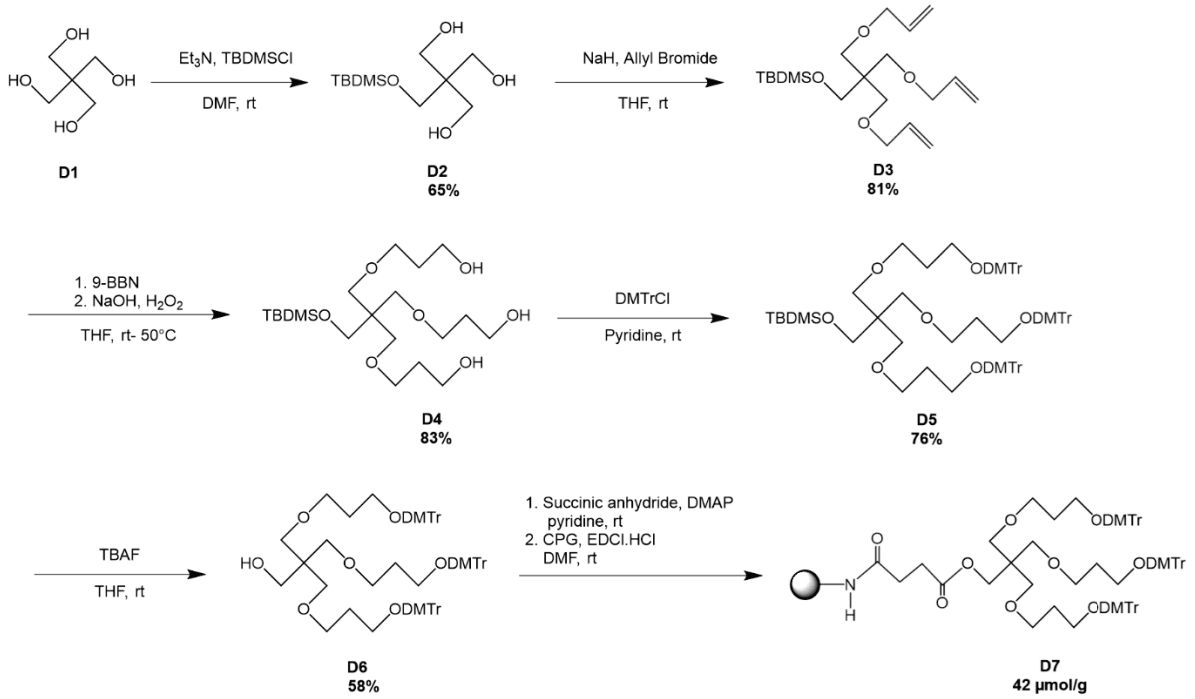


**Scheme 3.1.** Synthetic route for the trebling solid-support with single coupling.

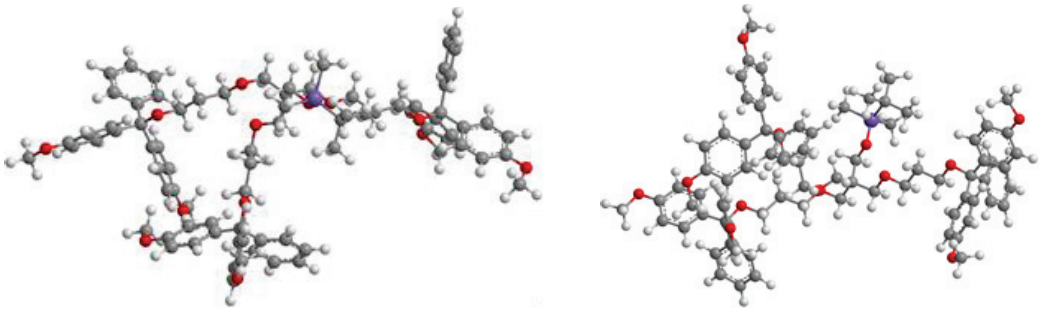

**Fig. 3.2.** Structure of the solid-support with single coupling.

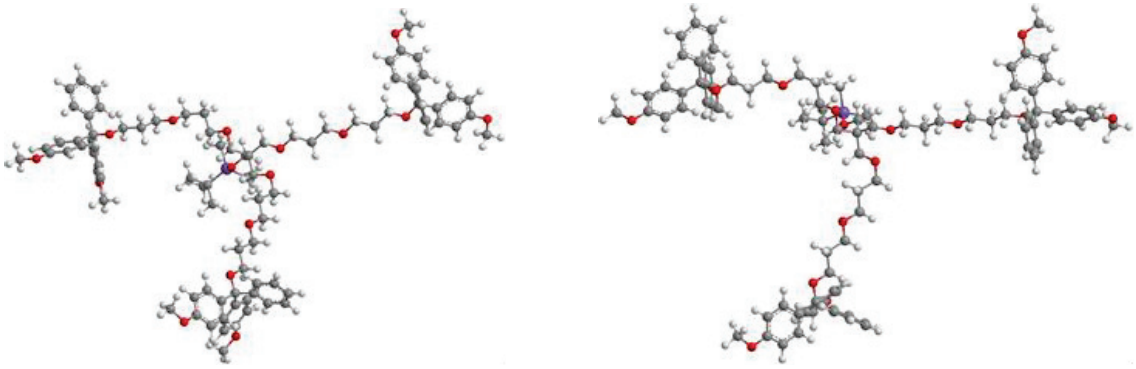

**Fig. 3.3.** Structure of the solid-support with double coupling.

showed dispersed distribution of the bulky trityl groups, favouring efficient synthesis of the target RNAs (Fig 3.3).

## 3.3. Results and Discussion

### 3.3.1. Synthesis of trebler solid support

The modified solid-support, **D'8** for the synthesis of branching oligonucleotides was obtained through the divergent synthesis approach. The synthetic route has been shown in Scheme 3.1. The initial challenges in the synthesis of trebling solid-support unit led to the amended scheme with double repetitive coupling for the elongation of the arms. Commercially available pentaerythritol (**D1**) was mono-protected with the silyl-ether, *tert*-butyldimethylsilyl chloride (TBDMSCl) to afford **D2** in 66% yield. Thereupon, allylation of the remaining hydroxyl groups was performed with allyl bromide in the presence of NaH to give **D3** in 81% yield. Subsequently, **D4** was obtained in 83% yield through anti-Markovnikov hydroboration oxidation of **D3** with 9-BBN. Another cycle of allylation and hydroboration oxidation furnished the elongated arms with **D'5** and **D'6** in 64% and 93% yield, respectively. Finally, the hydroxyl groups of **D'6** were protected by a 4,4'-dimethoxytrityl (DMTr) group to give the corresponding DMTr derivative **D'7** in 90% yield. Next, deprotection of the silyl group was performed with **D'7** to afford **D'8** in 91% yield. Lastly, the solid-support for oligonucleotide synthesis was attained by converting compound **D'8** to the corresponding succinate, which was then reacted with controlled pore glass (CPG) to produce the solid supports **D'9** with 27.4 μmol/g of loading activity (Scheme 3.2).

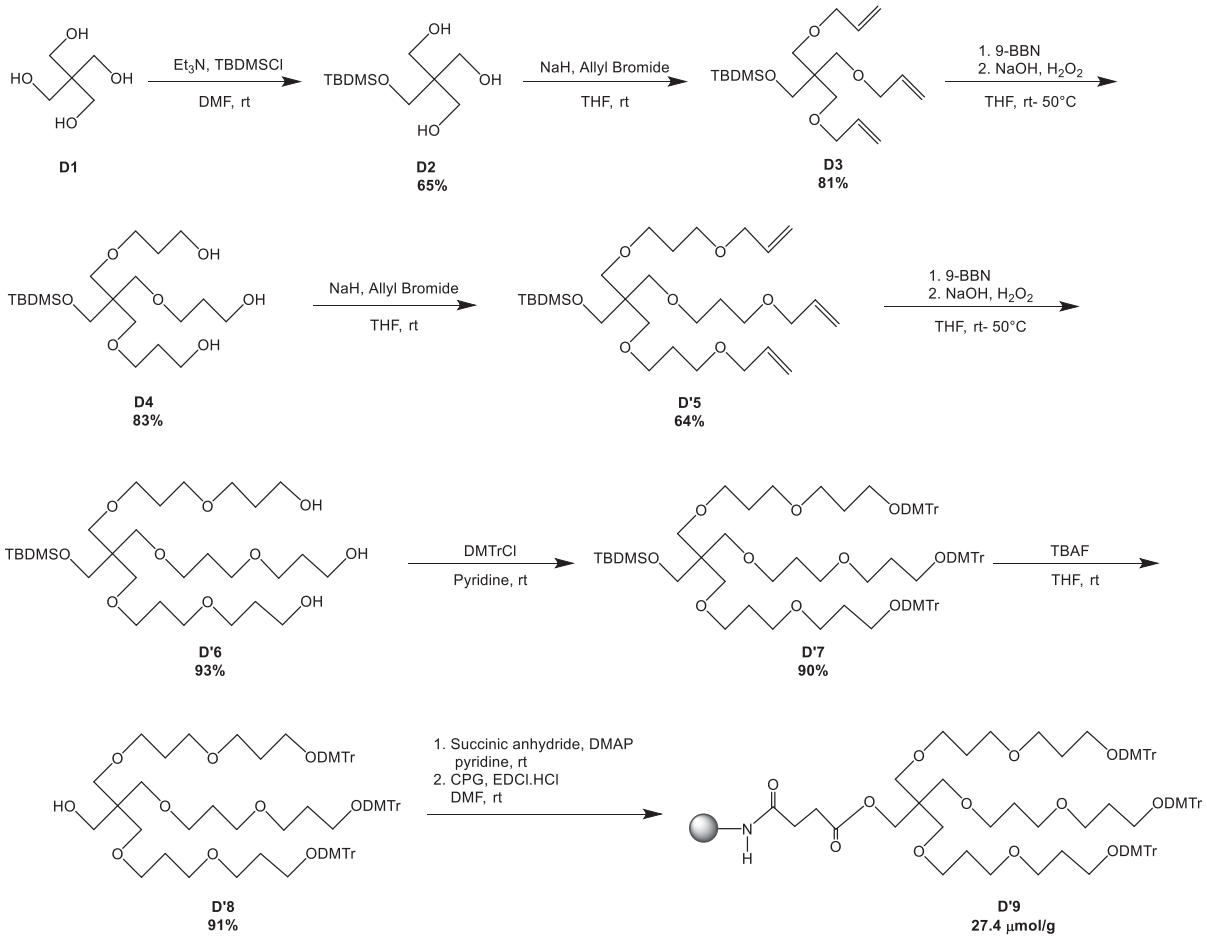


**Scheme 3.2.** Synthetic route for the trebling solid-support with double coupling.

## 3.3.2. Synthesis of branched oligonucleotides

The modified trebling solid-support **D'9** and native RNA phosphoramidites were used to synthesize the trident siRNAs by a DNA/RNA synthesizer. The RNAs were synthesized with a modified cycle using increased coupling time of the phosphoramidite on a DMT-ON mode for obtaining the target full length sequences. The coupling efficiency reported for the synthesis from the trityl monitor was found to be 93%. But, with the incorporation of the $C_{18}$ spacer phosphoramidite following the trebling solid-support, yielded trident RNAs (td RNAs) with the overall coupling efficiency of 100%.

Mass analysis of these trident RNAs revealed unconsolidated peaks. Further screening with RP-HPLC showed the presence of bident and trident mixture. Lastly, purification via polyacrylamide gel electrophoresis (PAGE) produced two distinctive bands which were analyzed for mass by matrix-assisted laser desorption/ionization time-of-flight mass spectrometry (MALDI-TOF/MS). All RNAs showed the corresponding molecular ion peaks.

**Table 3.1**

Mass of branched RNAs

| RNA | Sequence | Calculated | Observed |
|---|---|---|---|
| td #1 | 5'-GGCCUUUCACUACUCCUAC**UU**-**D'9-**3' | 20194.0765 | 10095.4459 $[M-2H]^{2-}$ |
| bd #1 | 5'-GGCCUUUCACUACUCCUAC**UU**-**D'9-**3' | 13624.252 | 6811.5224 $[M-2H]^{2-}$ |
| td #2 | 5'-GGCCUUUCACUACUCCUAC**UU**-**$C_{18}$- D'9-**3' | 21226.969 | 10611.8783 $[M-2H]^{2-}$ |
| bd #2 | 5'-GGCCUUUCACUACUCCUAC**UU**- **$C_{18}$-D'9-**3' | 14312.847 | 7155.3966 $[M-2H]^{2-}$ |
| td #3 | 5'-GUAGGAGUAGUGAAAGGCCUU- **$C_{18}$-D'9-**3' | 22.154.763 | 11298.5687 $[M-2H]^{2-}$ |
| bd #3 | 5'-GUAGGAGUAGUGAAAGGCCUU- **$C_{18}$-D'9-**3' | 14931.3763 | - |
| td #4 | 5'-**F**GGCCUUUCACUACUCCUAC**UU**-**D'9-**3' | 22842.3487 | 11406.6375 $[M-2H]^{2-}$ |
| bd #4 | 5'-**F**GGCCUUUCACUACUCCUAC**UU**-**D'9-**3' | 15389.7668 | 7702.6526 $[M-2H]^{2-}$ |

### 3.3.3. HPLC analysis of the branched RNAs

The synthesized branched RNAs were analyzed with reverse phase high performance liquid chromatography (RP-HPLC) for investigating the efficiency of the synthesis of full length targets. The evaluation with crude RNAs yielded broad peaks with an observable hinge. Further purification with PAGE showed two different sets of RNAs, classified as the bident and trident branched RNAs (Fig. 3.4).

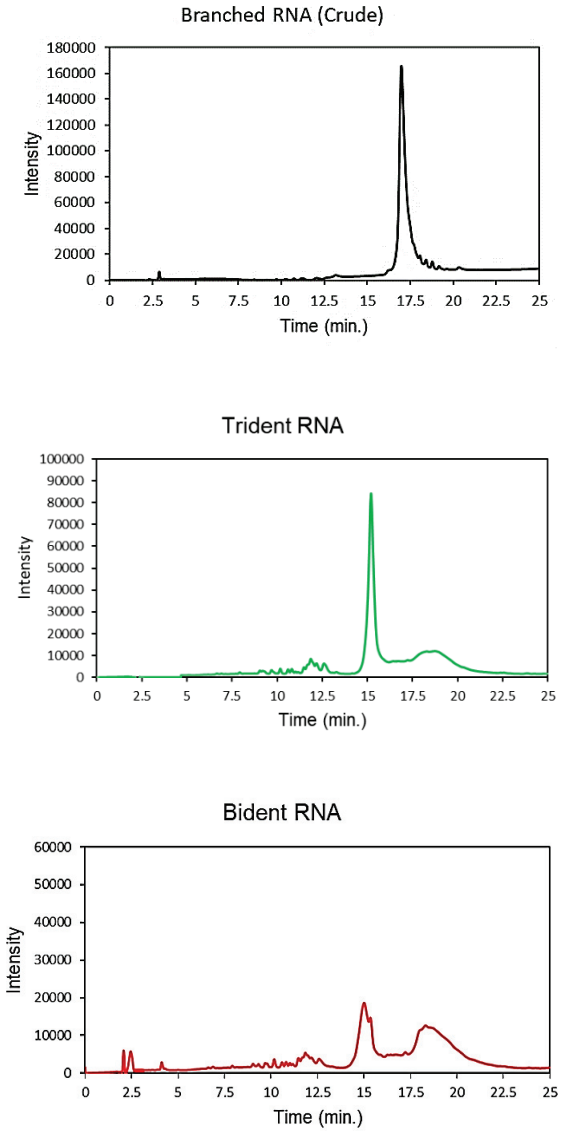


**Fig. 3.4.** HPLC chromatograms of the crude and PAGE purified RNAs.

### 3.3.4. Physical characterization of branched siRNAs

To evaluate the impact of branching on the structural conformation of siRNAs, we measured their hydrodynamic diameters using Dynamic Light Scattering (DLS). The mean hydrodynamic diameters were found to be 2.80 nm, 5.70 nm and 6.87 nm for duplex siRNA, bident siRNA and trident siRNA, respectively (Fig. 3.5). These results indicate that the bident siRNA forms a close to linear geometry for such an arrangement of siRNAs, but the trident siRNAs form more compact structure in comparison to its other counterparts.

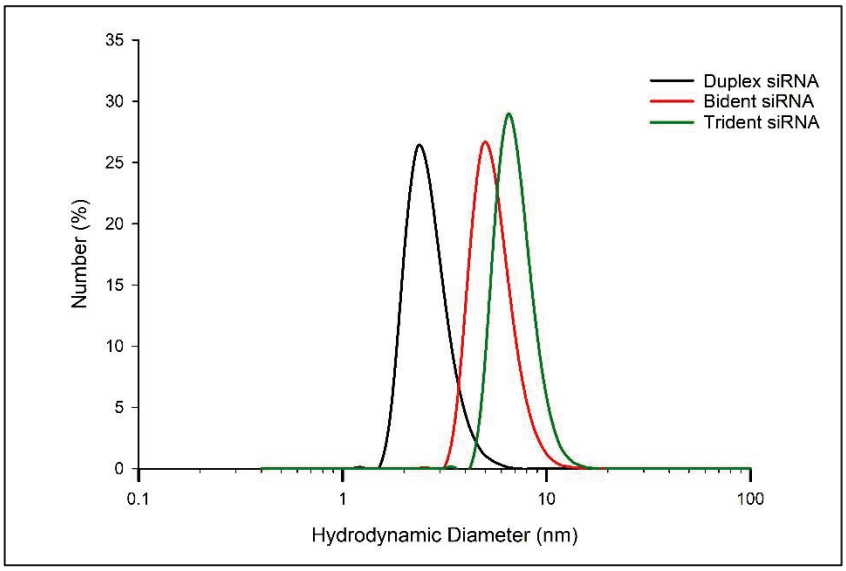


**Fig. 3.5.** Hydrodynamic diameter of duplex and branched siRNAs.

### 3.3.5. Thermodynamic stability of branched siRNAs

The thermodynamic stability of the branched siRNAs (td siRNAs), were evaluated with the sense strand forming the td RNA and the antisense 3'-overhang modified with the previously stated haloalkyl nucleobase analogs. Two different assemblies of the td siRNAs were utilized in this experiment, i.e. td RNA with $C_{18}$ spacer introduced after the solid-support and without any spacer. The modified branched siRNAs were subjected to evaluation by UV

melting experiments in a buffer composed of 10 mM sodium phosphate (pH 7.0) and 100 mM NaCl, in each case (Fig. 3.6-3.7). The melting temperature ($T_m$) values and change in values ($\Delta T_m$) with respect to the unmodified RNA duplex are shown in Tables 3.2 & 3.3.

In the case of td siRNA without $C_{18}$ spacer, the $T_m$ value of the unmodified siRNA **1** was found to be 77.8 °C, whereas those of the modified siRNAs **2**−**4** were 76.8, 77.1, and 77.4 °C, respectively. And, with the modified td siRNAs **1-3**, the $T_m$ values were found to be 76.8, 77.3,

**Table 3.2**

Thermal denaturation study of without $C_{18}$ spacer td siRNA.

| siRNA | ON | Sequence | $T_m$ (°C) | $\Delta T_m$ (°C) |
|---|---|---|---|---|
| **Control** | **Buffer** | - | - | - |
| | | Sense strand | | |
| **#1** | **#1** | 5'-GGCCUUUCACUACUCCUAC**UU**-3' | | |
| | **#2** | 3'-**UU**CCGGAAAGUGAUGAGGAUG-5' | 77.8 ± 0.2 | - |
| | | Antisense strand | | |
| **#2** | **#1** | 5'-GGCCUUUCACUACUCCUAC**UU**-3' | 76.8 ± 0.2 | -1.1 |
| | **#3** | 3'-**11**CCGGAAAGUGAUGAGGAUG-5' | | |
| **#3** | **#1** | 5'-GGCCUUUCACUACUCCUAC**UU**-3' | 77.1 ± 0.2 | -0.7 |
| | **#4** | 3'-**22**CCGGAAAGUGAUGAGGAUG-5' | | |
| **#4** | **#1** | 5'-GGCCUUUCACUACUCCUAC**UU**-3' | 77.4 ± 0.2 | -0.5 |
| | **#5** | 3'-**33**CCGGAAAGUGAUGAGGAUG-5' | | |
| **td siRNA #1** | **td #1** | 5'-GGCCUUUCACUACUCCUAC**UU-D'9**-3' | 76.8 ± 0.2 | -1.0 |
| | **#3** | 3'-**11**CCGGAAAGUGAUGAGGAUG-5' | | |
| **td siRNA #2** | **td #1** | 5'-GGCCUUUCACUACUCCUAC**UU- D'9**-3' | 77.3 ± 0.2 | -0.5 |
| | **#4** | 3'-**22**CCGGAAAGUGAUGAGGAUG-5' | | |
| **td siRNA #3** | **td #1** | 5'-GGCCUUUCACUACUCCUAC**UU- D'9**-3' | 77.7 ± 0.2 | -0.1 |
| | **#5** | 3'-**33**CCGGAAAGUGAUGAGGAUG-5' | | |

[a]The highlighted regions in the overhangs denote the modifications. [b]$\Delta T_m$ represents [$T_m$ ($siRNA_{mod}$) - $T_m$ ($siRNA_{unmod}$)].

77.7 °C, respectively (Table 3.2). Thus, the modified td siRNAs were reported with higher thermal stability in comparison to the duplex siRNAs.

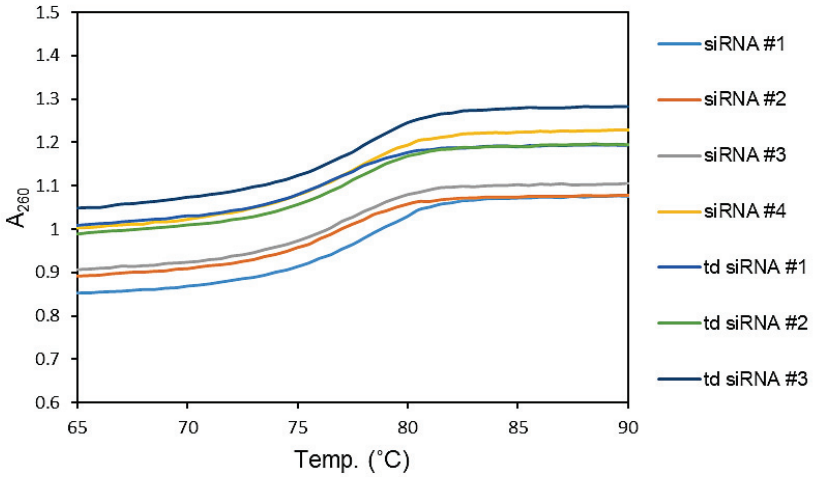


**Fig. 3.6.** UV melting profiles of the modified and unmodified td siRNAs (without C $_{18}$ spacer).

Moreover, similar set of experiments with the modified td siRNAs incorporated with $C_{18}$ spacer, revealed much better stability over the preceding counterparts. In this case, the $T_m$ value of the unmodified siRNA **1** was found to be 77.6 °C, whereas those of the modified siRNAs **2**–**4** were 77.0, 77.1, and 77.2 °C, respectively. And, with the modified td siRNAs **4**–**6**, the $T_m$ values were found to be 77.0, 77.5, 77.5 °C, respectively (Table 3.3). Thus, here also, the modified td siRNAs were reported with higher thermal stability in comparison to the duplex siRNAs.

This increased thermodynamic stability of the branched siRNAs against the duplex structures could be the result of their compact structures as the difference in values is minimally low. Therefore, we can state that these branched siRNAs provide better thermal stability with only slight deviation from the unmodified duplex siRNAs.

**Table 3.3**

Thermal denaturation study of $C_{18}$ spacer td siRNAs.

| siRNA | ON | Sequence | $T_m$ (˚C) | $\Delta T_m$ (˚C) |
|---|---|---|---|---|
| **Control** | **Buffer** | - | - | - |
| **#1** | | Sense strand | | |
| | **#1** | 5'-GGCCUUUCACUACUCCUAC**UU**-3' | 77.6 ± 0.2 | - |
| | **#2** | 3'-**UU**CCGGAAAGUGAUGAGGAUG-5' | | |
| | | Antisense strand | | |
| **#2** | **#1** | 5'-GGCCUUUCACUACUCCUAC**UU**-3' | 77.0 ± 0.4 | -0.7 |
| | **#3** | 3'-**11**CCGGAAAGUGAUGAGGAUG-5' | | |
| **#3** | **#1** | 5'-GGCCUUUCACUACUCCUAC**UU**-3' | 77.1 ± 0.3 | -0.5 |
| | **#4** | 3'-**22**CCGGAAAGUGAUGAGGAUG-5' | | |
| **#4** | **#1** | 5'-GGCCUUUCACUACUCCUAC**UU**-3' | 77.2 ± 0.4 | -0.4 |
| | **#5** | 3'-**33**CCGGAAAGUGAUGAGGAUG-5' | | |
| **td siRNA #4** | **td #2** | 5'-GGCCUUUCACUACUCCUAC**UU**- **$C_{18}$-D**'9-3' | 77.0 ± 0.2 | -0.7 |
| | **#3** | 3'-**11**CCGGAAAGUGAUGAGGAUG-5' | | |
| **td siRNA #5** | **td #2** | 5'-GGCCUUUCACUACUCCUAC**UU**- **$C_{18}$-D**'9-3' | 77.5 ± 0.3 | -0.2 |
| | **#4** | 3'-**22**CCGGAAAGUGAUGAGGAUG-5' | | |
| **td siRNA #6** | **td #2** | 5'-GGCCUUUCACUACUCCUAC**UU-$C_{18}$- D**'9-3' | 77.5 ± 0.3 | -0.1 |
| | **#5** | 3'-**33**CCGGAAAGUGAUGAGGAUG-5' | | |

[a]The highlighted regions in the overhangs denote the modifications. [b]$\Delta T_m$ represents [$T_m$ ($siRNA_{mod}$) - $T_m$ ($siRNA_{unmod}$)].

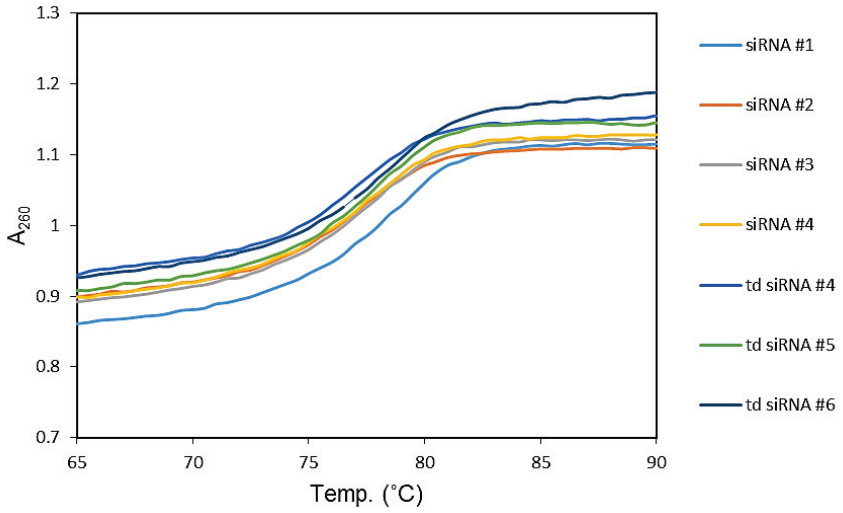


**Fig. 3.7.** UV melting profiles of the modified and unmodified td siRNAs (with $C_{18}$ spcaer) .

### 3.3.5. Gene silencing activity of branched siRNAs

The RNAi activities of the unmodified and modified td siRNAs were investigated with a dual luciferase reporter assay using HeLa cells, in which the target luciferase genes were constitutively expressed. All modified td siRNAs targeted the *Renilla* luciferase genes, while firefly luciferase genes were used as controls. All td siRNAs were transfected using RNAimax. The expression levels of both luciferase genes were analyzed 24 h of incubation of transfected cells with the modified td siRNAs. The silencing activity was expressed as the the ratios of Renilla:firefly luciferase activities with respect to the no siRNA control.

To evaluate the silencing activity, two different sets of td siRNAs were included in this study. Firstly, the td siRNAs with td RNA as the passenger strand and the antisense being the modified strand. Secondly, the td siRNAs with the guide strand forming the branching structure and the sense being the 3'-overhang modified. The two cases differed quite significantly in respect to the exhibited silencing activities (Table 3.4).

**Table 3.4**

RNAi activity for 24 h incubation with td siRNAs.

| siRNA | Sequence | Upper: 10 nM<br>Lower: 1 nM |
|---|---|---|
| Control | (buffer) | 100±9.3 |
| siRNA 1 | Sense strand<br>5'-GGCCUUUCACUACUCCUAC**UU**-3'<br>3'-**UU**CCGGAAAGUGAUGAGGAUG-5'<br>Antisense strand | <br>19.9±1.4<br>31.5±4.5 |
| td siRNA 7 | 5'-GGCCUUUCACUACUCCUAC**UU**- $C_{18}$-**D**'9-3'<br>3'-**UU**CCGGAAAGUGAUGAGGAUG-5' | 18.4±1.0<br>38.7±1.8 |
| td siRNA 4 | 5'-GGCCUUUCACUACUCCUAC**UU**- $C_{18}$-**D**'9-3'<br>5'-GGCCUUUCACUACUCCUAC**11**-3' | 22.1±1.1<br>45.9±4.2 |
| td siRNA 5 | 5'-GGCCUUUCACUACUCCUAC**UU**- $C_{18}$-**D**'9-3'<br>5'-GGCCUUUCACUACUCCUAC**22**-3' | 22.0±2.2<br>39.9±2.6 |
| td siRNA 6 | 5'-GGCCUUUCACUACUCCUAC**UU**- $C_{18}$-**D**'9-3'<br>3'-**33**CCGGAAAGUGAUGAGGAUG-5' | 22.1±2.0<br>56.0±3.3 |
| td siRNA 8 | 5'-GGCCUUUCACUACUCCUAC**UU**-3'<br>3' **D**'9-$C_{18}$-**UU**CCGGAAAGUGAUGAGGAUG-5' | 42.1±4.4<br>76.3±5.0 |
| td siRNA 9 | 5'-GGCCUUUCACUACUCCUAC**11**-3'<br>**D**'9-$C_{18}$-**UU**CCGGAAAGUGAUGAGGAUG-5' | 33.9±1.5<br>70.1±4.0 |
| td siRNA 10 | 5'-GGCCUUUCACUACUCCUAC**22**-3'<br>**D**'9-$C_{18}$-**UU**CCGGAAAGUGAUGAGGAUG-5' | 30.7±4.7<br>59.1±3.2 |
| td siRNA 11 | 5'-GGCCUUUCACUACUCCUAC**33**-3'<br>**D**'9-$C_{18}$-**UU**CCGGAAAGUGAUGAGGAUG-5' | 28.0±3.3<br>71.0±5.1 |

Gene expression from cells transfected with each siRNA has been normalized and presented as the percentage from three independent experiments, with three replicate samples per experiment.

The observed results indicate that these branched structures are compatible with the siRNA mediated gene silencing. Also, the incorporation of the passenger strand as the branching

RNA reveals more promising silencing activity, in comparison to the guide strand constituting branching structure, as shown in Fig. 3.8. Moreover, all of the td siRNAs **4-6** showed comparable activity by inhibiting 78% gene expression in the case of analog modified td siRNAs whereas 81% inhibition was observed with the unmodified branched td siRNA **7,** at 10 nM concentration.

On the contrary, the gene silencing was considerably reduced for td siRNAs **8-11**. At 10 nM concentration, the unmodified td siRNA **8** showed 58% inhibition whereas td siRNAs **9-11**, which were modified with the analogs at the dangling end showed 68%, 69% and 72% inhibition, respectively. Hence, it can be inferred that the branching structures are tolerant for siRNA mediated RNAi, if the branching RNA backbone constitutes passenger strand, as it could not restrict the recognition of the termini of guide strand by the Ago protein.

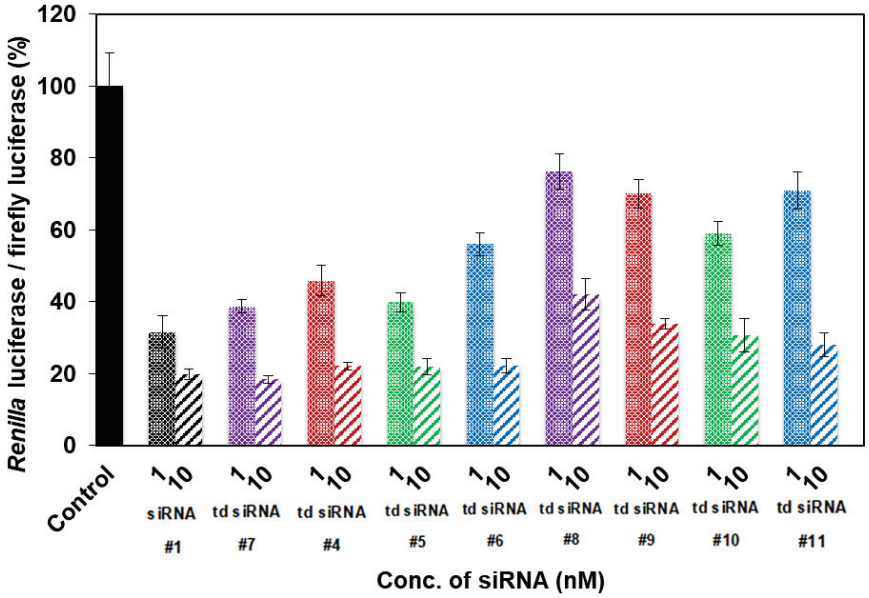


**Fig. 3.8.** RNAi activity of the unmodified and modified td siRNAs.

### 3.3.6. Exonuclease resistance of the branched siRNAs

Unmodified siRNAs are unstable in serum due to degradation by nucleases (De Paula et al. 2007). Thereby, raising the necessity of chemically modified synthetic siRNAs which are nuclease resistant and act as ideal candidates in siRNA therapeutics. In this study, the branched siRNAs possess a caged 3'-end which might be beneficial for providing resistance against the 3'-exonucleases. Thus, we analysed the branched RNAs for resistance against snake venom phosphodiesterase (SVPD), a 3'-exonuclease.

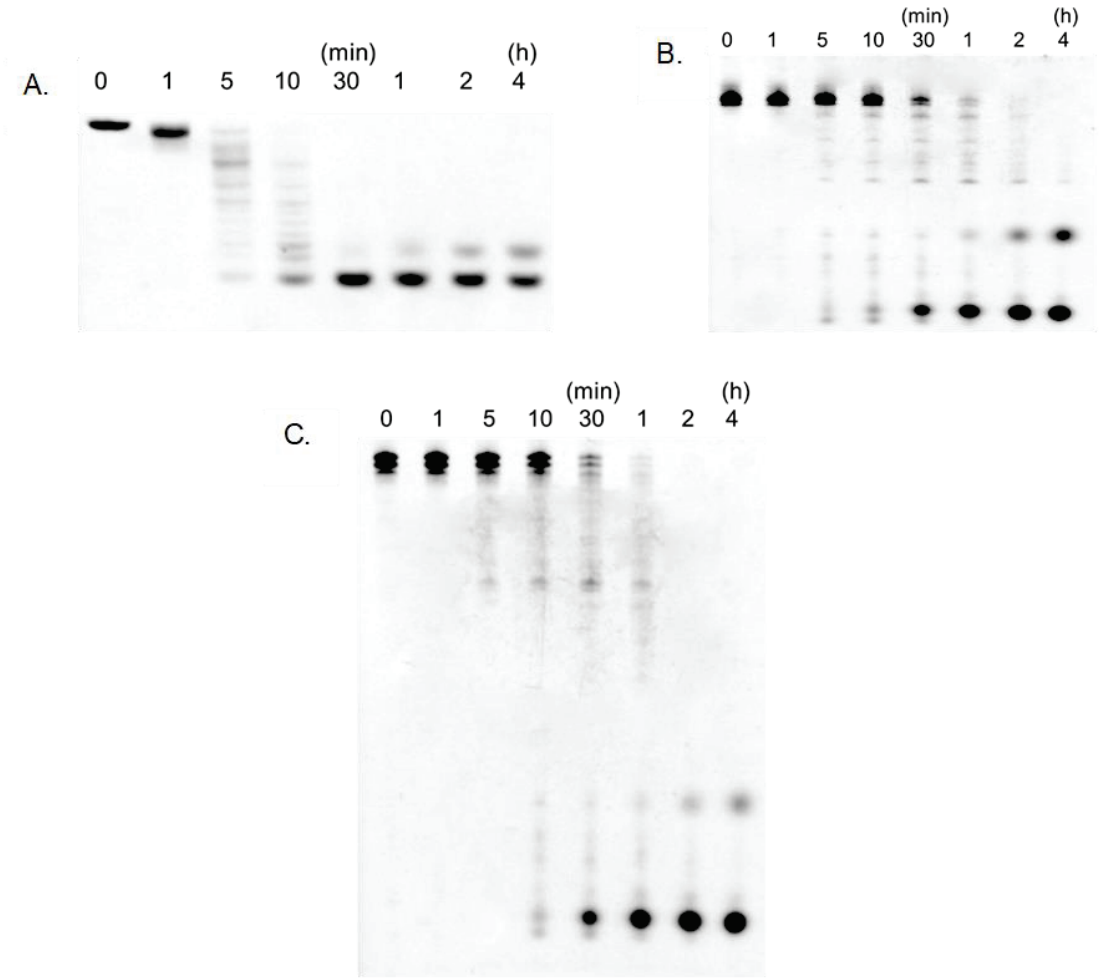


**Fig. 3.9.** A. 20% denaturing PAGE of RNA hydrolyzed by SVPD. B & C. 6% denaturing PAGE of bd RNA and td RNA hydrolyzed by SVPD.

The unmodified RNA **10** and the modified branched RNAs, td 4 and bd 4 were labelled with fluorescein at the 5'-ends, incubated with SVPD, and then analyzed by denaturing PAGE. As shown in Fig. 3.9, the unmodified RNA was degraded instantaneously in the presence of nuclease with fairly no full length RNA at 5 minutes of incubation; whereas, the modified branched RNAs exhibited enhanced stability to the exonuclease enzyme. The bd RNA and td RNA, both showed the presence of RNAs even upon treatment with the enzyme for 30 minutes. Therefore, it can be easily inferred from these observations that the branched RNAs provide better stability against the exonucleases in the serum.

## 3.4. Conclusion

For several years, research has focused on chemical modifications and delivery technologies to improve the pharmacokinetic properties of siRNA. Many of the chemically modified siRNA with interesting inhibitory capacity contain one or multiple modifications in the sugar, nucleobases, and phosphate linkages or at the 3′- or 5′-ends. In addition to these modifications, duplex architecture of siRNA itself is also relevant, and several modifications have been reported to show satisfactory inhibitory capacity. However, here we have demonstrated that branched siRNA is compatible with RNAi and that, with increased branching, they form more compact structures. Although these branched siRNAs did not significantly enhance the silencing activity, but they showed comparable inhibition of gene expression as the unmodified siRNAs. Also, they showed significantly improved exonuclease resistance and thermodynamic stability was also conserved. Although, the activity has not been altered significantly, but the formulation of such branched siRNAs and their compatibility with siRNA mediated RNAi signify them as potent building block for further developments with branched siRNAs, in this direction. Moreover, these structures can be utilized with further in-built cationic modifications

for improvising it as a self-assembled carrier for siRNA therapeutics. In vivo experiments with these structures will considerably help in validating their potential as rational candidates for escaping the renal filtration system. Therefore, branched siRNAs with such a trebling solid-support, could help in providing potential solutions to the problems in siRNA drug delivery.

# Chapter 4

## Synthesis of 2'-OMe haloaryl analogs: next candidate for 3'-dangling ends

### 4.1 Introduction

We have already discussed about the halide-based analogs for introduction at the dangling ends of the siRNAs (Chandela *et al.*, 2019). But, those studies were only confined to the aliphatic chains. Moreover, the presence of aromatic residues in the hydrophobic pocket of the PAZ domain, imparts upon us the task of investigating the effect of aromatic bases at the 3'-overhang position. Prior studies have stated the introduction of aromatic molecules like naphthalene, anthracene, etc. with reduced activity when included in the guide strand. This background knowledge leaves us with the scope to modify the overhang with haloaryl nucleobases and deduce the effect of aromatic moiety in combination with the halide group.

Therefore, with this study, we look forward to the class of haloaryl nucleobases substituted for the natural bases at the dangling end, to impact the silencing activity with PAZ associated interaction. In this study, we present the design and synthesis of 1-(phenoxy)-2-methoxy-β-D-ribofuranoside, 1-(4-fluorophenoxy)-2-methoxy-β-D-ribofuranoside and 1-(4-chlorophenoxy)-2-methoxy-β-D-ribofuranoside as the new candidates through a fresh synthetic route to yield the 2'-OMe substituted analogs (Fig. 4.1). We hypothesize these analogs to add further dimensions to the siRNA mediated gene silencing with modified overhangs constituting these novel molecules.

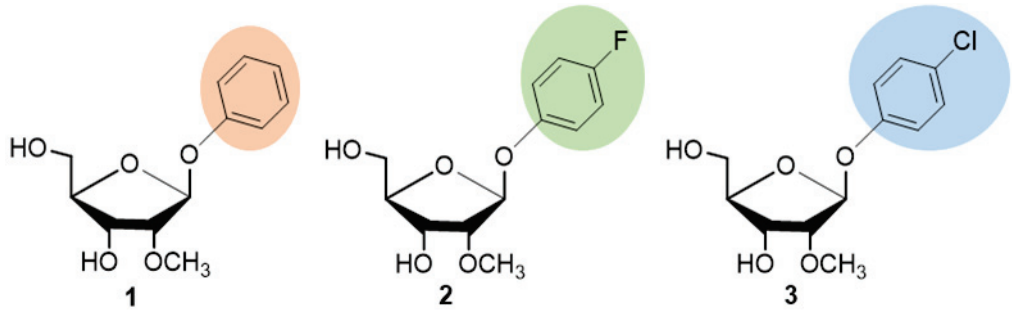


**Fig. 4.1.** Structure of the 2'-OMe haloaryl nucleoside analogs.

## 4.2. Experimental strategy

*Inseparable 2'-silylated and 3'-silylated products with ribofuranose*

In the chapter 2, the silylation of DMTr derivative of the 1-*O* substituted haloalkyl analogs yielded 2-*O*-TBDMS and 3-*O*-TBDMS compounds for the further synthesis of phosphoramidites and solid-supports. But, in the case of haloaryl analogs, the high hydrophobicity of the resulting mixtures proved extremely difficult for the purification of the two silyl protected derivatives (Fig. 4.2). Therefore, we modified our previous synthetic route and introduced the 2'-OMe as it has already been stated that there are no any notable interactions with the 2'-OH. In this manner, we synthesized these new candidates for our study.

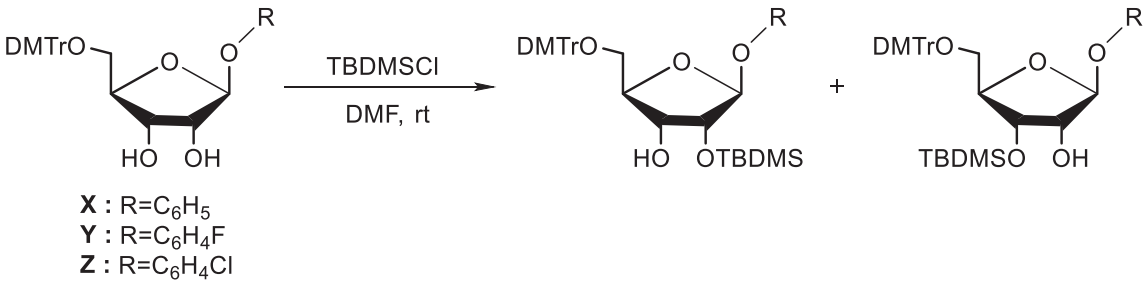


**Fig. 4.2.** Challenging conversion of haloaryl analogs to two silyl derivatives.

## 4.3. Results and Discussion

### 4.3.1. Synthesis of 2'-OMe haloaryl analogs phosphoramidites

The phosphoramidites of the nucleoside analogs 1,**2** and **3** were synthesized with a new improvised protocol. The new synthetic route has been shown in Scheme 4.1. The initial steps remained the same, the substitution at 1-position of ribofuranose was attained by the glycosylation reaction of commercially available, 1-*O*-acetyl-2,3,5-tri-*O*-benzoyl-β-D-ribofuranose (**4**), with phenol (**5**) in the presence of trimethylsilyl triflate (TMSOTf) at −30 °C in $CH_2Cl_2$ to give the β-anomer **8** in 81% yield. Next, debenzoylation of compound **8** was carried out in the presence of catalytic amount of $NaOCH_3$ in $CH_3OH$ to afford the product **1** in 90% yield. Subsequently, 1,3-dichloro-1,1,3,3-tetraisopropyldisiloxane ($TIPDSCl_2$) was used to simultaneously protect the 3'-OH and 5'-OH of the ribofurnaose to produce **11** in 89% yield. Next, 2'-OH of compound **11** was modified to 2'-OMe in the presence of $CH_3I$ and NaH through Williamson ether synthesis mechanism, to afford **14** in 49% yield. The low yield resulted due to the simultaneous desilylation under these conditions with DMF as solvent. Whereas, in the case of 4-chlorophenoxy as nucleobase analog, the application of THF as solvent, reduced the deprotection of silyl group. In the next step, desilylation of **14** was performed with $Et_3 \cdot 3HF$ at 35°C to give **17** in 82% yield. Later, the primary hydroxyl group of **17** was protected by a 4,4'-dimethoxytrityl (DMTr) group to give the corresponding 5'-*O*-DMTr derivative **20** in 84% yield. Finally, the phosphoramidite **23** was produced upon phosphitylation of **20** in 76% yield. Similarly, the phosphoramidites for 4-fluorophenoxy and 4-chlorophenoxy base analogs were afforded in the total yield of 17% and 18%, respectively.

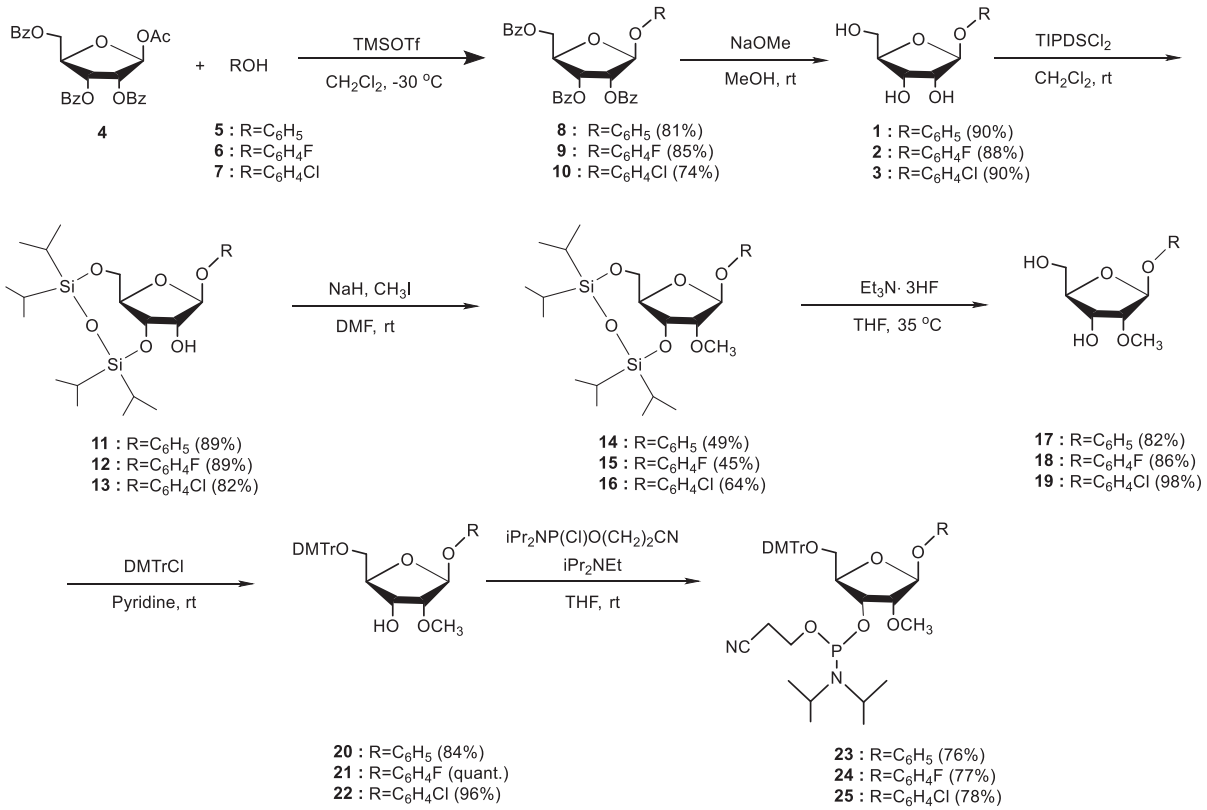


**Scheme 4.1.** Synthetic route for the synthesis of phosphoramidites of 2'-OMe haloaryl analogs analogs.

### 4.3.2. Synthesis of solid-support for 2'-OMe haloaryl analogs

The solid support synthesis for incorporating 2'-OMe haloaryl analogs **1**, **2** and **3** at the 3'-end of an RNA oligomer, compounds **20-22** were converted to the corresponding succinates, which were then reacted with controlled pore glass (CPG) to produce the solid supports **26-28** in the yields of 16.7, 33.7,13.7 µmol/g, respectively (Scheme 4.2).

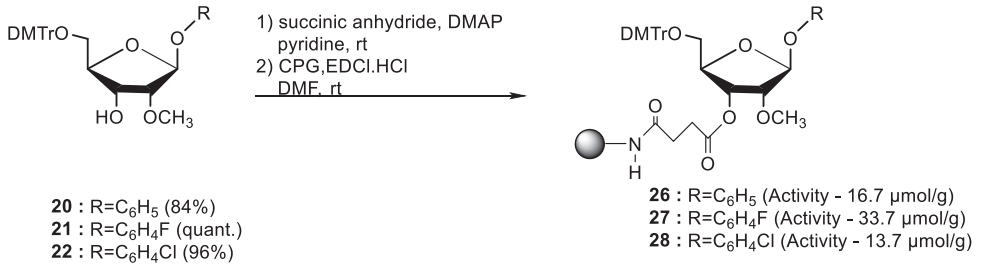


**Scheme 4.2.** Synthetic route for the synthesis of solid-support of 2'-OMe haloaryl analogs.

## 4.4. Conclusion

In the recent time, RNAi has emerged as a potential tool for sequence specific gene regulation. siRNA being the key moiety in this phenomenon provides a wide scope for enhancing the silencing activity with useful chemical modifications. Interaction of these siRNAs with the PAZ domain plays a critical role in the gene silencing. Therefore, in continuation of our previous studies with haloalkyl nucleobases introduced at the 3'-overhang of the modified siRNAs, we have recognized the next candidates as 2'-OMe haloaryl analogs to study their impact on the stability and activity of the modified siRNAs.

# Chapter 5

## Summary

### 5.1. Synthesis and characterization of haloalkyl modified siRNAs

RNAi interference is a technological tool which bestow us with the opportunity to develop a new class of genetic therapeutics which can specifically target even the undruggable targets. The two key moieties, siRNA and Ago2 protein plays a crucial role in the RNAi machinery for degrading the target mRNAs. The hydrophobic pocket of the PAZ domain of Ago protein have been reported for accommodating the 2-nt overhang of the guide strand. Therefore, with this study we explore the interaction of the 3'-overhangs with the PAZ domain upon modification with highly electronegative and hydrophobic halides to correlate it with the silencing activity and provide a strong base for future endeavors in this direction.

The synthesis of the haloalkyl analogs was obtained with the substitution of 1-position of ribose sugar with the haloalkyls in a conformation specific manner. The modified analogs were afforded as 2,2,2-trifluoroethyl β-D-ribofuranoside (TFE), 2,2,2-trichloroethyl β-D-ribofuranoside (TCE) and 2,2,2-tribromoethyl β-D-ribofuranoside (TBE), which were further reacted to give the phosphoramidites and the CPG solid-supports for the oligonucleotide synthesis. The synthesized RNAs were confirmed with mass spectrometry and utilized for the physicochemical characterization.

The thermodynamic studies revealed the higher stability of TCE modified siRNAs, closely followed by the TFE and TBE modified siRNAs. These observations are in congruency with the dipole moment of these halide compounds and forms the basis of our argument. Moreover, as per the hypothesis, the hydrophobicity of the resulting RNAs were found to be escalated. The gene silencing activity also showed that at the concentration of 10 nM, the TCE modified

siRNAs showed considerably high activity, followed by the TFE and TBE modified siRNAs against the unmodified siRNA.

Interestingly, the molecular modelling study and the protein binding assay exhibited a slightly increased interaction of these modified siRNAs in respect to the unmodified siRNA. The highest affinity was observed with the TCE modified siRNAs, with the TFE and TBE modified following the list and unmodified being the least bounded to the protein. Moreover, these modified RNAs also mediated enhanced nuclease resistance against the 3'-exonuclease. Hence, these haloalkyl analogs present us with astounding outcomes, which designate them as the potential candidates for further extrapolating such an interaction enhanced gene silencing activity.

## 5.2. Novel synthesis and evaluation of branched siRNAs for RNAi activity

The advances with the siRNA based nucleic acid therapeutics have reached new dimensions but the exploitation of critical architecture of branched siRNAs have been meagerly touched upon. These shortcomings in this direction have been the result of their tedious, complicated and difficult synthesis. Therefore, with the current study, we present the novel branched siRNAs which originate from a common trebler solid-support, which the first of this kind of study.

The modified trebling solid-support was designed and synthesized with three elongated arms to accommodate the three bulkyl DMTr (trityl) groups, which was challenging to afford the simultaneous synthesis of the trident RNAs. Finally, the branched RNAs were synthesized with DNA/RNA synthesized with the increased coupling time for the phosphoramidites. And, the resulting RNAs were down-processed to obtain the mixture of bident and trident, which were further purified using PAGE.

The physical characterization of these molecules clearly indicated the compactness of these structures over the duplex siRNAs. The hydrodynamic diameter of the duplex siRNA was 2.80 nm, whereas for the td siRNA, it was found to be 6.87 nm. Next, we analyzed the thermodynamic stability of these modified td siRNAs and found the branched structures exhibiting an enhanced strength. The RNAi activity was also found to be conserved with the branched structures when the branching RNA was constituted with the passenger strand, but the opposite was observed when constituting the branching RNA with the guide strand, and the activity diminished in the latter case. Furthermore, the branched siRNAs exhibited an increased resistivity against the 3'-exonuclease, SVPD. Thereby, making these structures as an ideal candidate for enhanced activity and systemic administration with increased molecular size but compact geometry.

# Chapter 6

## Experimental Section

### 6.1. Materials

### 6.1.1. Apparatus

| | |
|---|---|
| DNA/RNA Synthesizer | NTS-H6 DNA/RNA Synthesizer |
| MALDI/TOF-MS | SHIMADZU AXIMA-CFR Plus |
| NMR-Spectrometry | JEOL ECX-400P, ECA-500 |
| UV-VIS Spectrophotometer | SHIMADZU UV2450 |
| Gel Doc | FUJIFILM LAS4000 |
| Lumiscence Microplate Reader | ATTO Luminescencer JNRII |
| HPLC | SHIMADZU LC Solution<br>LC-20AT<br>SPD-20A<br>CTO-10AS<br>DGU-20A3<br>CBM-20A |
| Dynamic Light Scattering | Malvern Zetasizer nano ZS |
| Thin Layer Chromatography | Merck TLC plates silica gel F254 |
| Column Chromatography | Kanto Chemicals, Silica gel 60N (spherical, neutral) 63-120 μm |
| Disposable syringe | Terumo - 1mL, 10 mL |
| Syringe filter | ABLU PVDF 0.22 μm, 0.45 μm<br>Millipore Millex®-LH PTFE 0.45 μm |

## 6.1.2. Reagents

| Company | Chemical Reagent |
|---|---|
| Aldrich | 1 M TBAF in THF, 0.5 M 9-BBN in THF |
| Kanto Chemicals | THF |
| TCI | Allyl bromide, DMAP, Pentaerythritol, 2,2,2-trichloroethanol, 2,2,2-tribromoethanol, 4-fluorophenol, 4-chlorophenol, Iodomethane, TBDMSCl, TMSOTf, $TIPDSCl_2$. |
| Nacalai Tesque | DMF, Ethanol, $NaHCO_3$, TEA, $H_2SO_4$, $Na_2SO_4$ |
| Wako Chemicals | $CH_2Cl_2$, DMTrCl, Pyridine, Methanol, 1-*O*-acetyl-2,3,5-tri-*O*-benzoyl-β-D-ribofuranose, DIPEA |
| Cambridge Isotope Laboratories | $CDCl_3$, DMSO-d6 |

## 6.1.3. Reagents for oligonucleotide synthesis and analysis

| Company | Chemical Reagent |
|---|---|
| Glen Research | Oxidizing solution, Cap Mix A, Cap Mix B, Deblocking mix, Activator |
| Aldrich | TEA·3HF |
| Nacalai Tesque | Urea, Acrylamide (monomer), TEMED, Sodium dihydrogen phosphate, Disodium phosphate, EtOH, TEA |

| | |
|---|---|
| Wako Chemicals | MeCN (super-dehydrated), Bromophenol blue, N,N'-Methylenbisacrylamide, EDTA • 4Na, APS, Formamide, Boric acid, Tris(hydroxymethyl)aminomethane, Ammonium solution (28%) |
| Promega | Dual-Glo® Luciferase Assay System |
| Invitrogen | Trypsin-EDTA, Lipofectamine RNAimax, Opti-MEM |

## 6.2. Materials

### 6.2.1. Synthesis of haloalkyl nucleoside analogs

**2,3,5-tri-*O*-benzoyl-1-*O*-(2,2,2-trichloroethyl)-β-D-ribofuranose (7)**

To a stirred solution of 1-*O*-acetyl-2,3,5-tri-*O*-benzoyl-β-D-ribofuranose (2.00 g, 3.97 mmol) in dry $CH_2Cl_2$ (20 mL) at −30 ˚C, TMSOTf (1.29 mL, 7.15 mmol) and 2,2,2-trichloroethanol (0.38 mL, 3.97 mmol) were added dropwise. The reaction mixture was stirred for 2 h, quenched by saturated sodium bicarbonate and extracted with $CHCl_3$. The organic layer was washed with aqueous $NaHCO_3$ and brine, dried ($Na_2SO_4$) and solvent was evaporated under reduced pressure to afford a crude residue. The crude was purified by silica gel chromatography using hexane/ethyl acetate (5:1) to afford **7** (1.86 g, 3.13 mmol, 79%): $^1$H-NMR (400 MHz, $CDCl_3$) δ 8.08 (dd, *J* = 8.5, 1.1 Hz, 2H), 8.01−8.04 (m, 2H), 7.87−7.90 (m, 2H), 7.56−7.61 (m, 1H), 7.49−7.55 (m, 2H), 7.38−7.46 (m, 4H), 7.33 (t, *J* = 8.0 Hz, 2H), 5.94 (dd, *J* = 6.9, 5.0 Hz, 1H), 5.86 (d, *J* = 5.0 Hz, 1H), 5.56 (s, 1H), 4.75−4.81 (m, 2H), 4.72 (d, *J* = 4.1 Hz, 1H), 4.59 (q, *J* = 5.8 Hz, 1H), 4.31 (s, 1H), 4.18 (s, 1H); $^{13}$C-NMR (101 MHz, $CDCl_3$) δ 166.32, 165.48, 165.27, 133.77, 133.63, 133.39, 129.98, 129.91, 129.72, 129.18, 128.95, 128.69, 128.60, 128.55, 106.27, 96.29, 79.93, 79.70, 77.48, 76.85, 75.49, 72.22, 64.76. HRMS (ESI-TOF) *m/z*: Calcd. for $C_{28}H_{23}Cl_3O_8Na$ $[M+Na]^+$ 615.0369, found 615.0356.

**1-*O*-(2,2,2-Trichloroethyl)- β-D-ribofuranose (2)**

To a stirred solution of **7** (1.83 g, 3.08 mmol) in MeOH (18 mL), a catalytic amount of 28% MeOH solution of sodium methoxide was added. The reaction mixture was stirred at room temperature for 16 h and quenched by using aqueous $NH_4Cl$ (saturated, 1 mL). The solvent was evaporated under reduced pressure and the resulting residue was purified by silica gel

chromatography using $CHCl_3$/MeOH (10:1) to give **2** (0.76 g, 2.7 mmol, 89%): $^1$H-NMR (400 MHz, DMSO-$d_6$) δ 5.19 (d, $J$ = 4.1 Hz, 1H), 5.06 (s, 1H), 4.90 (d, $J$ = 6.9 Hz, 1H), 4.71 (t, $J$ = 5.7 Hz, 1H), 4.17−4.29 (m, 2H), 3.80−3.95 (m, 3H), 3.57 (qd, $J$ = 5.7, 3.5 Hz, 1H), 3.37−3.43 (m, 1H); $^{13}$C-NMR (101 MHz, DMSO-$d_6$) δ 106.99, 97.21, 84.09, 77.84, 74.26, 70.65, 62.80, 40.14, 39.94, 39.73, 39.31, 39.10, 38.89. HRMS (ESI-TOF) *m/z*: Calcd. for $C_7H_{11}Cl_3O_5Na$ $[M+Na]^+$ 302.9561, found 302.9569.

**5-*O*-(4,4'-Dimethoxytrityl)-1-*O*-(2,2,2-trichloroethyl)-β-D-ribofuranose (9)**

To a solution of **2** (0.76 g, 2.69 mmol) in pyridine (15 mL) stirred at room temperature, DMTrCl (1.09 g, 3.23 mmol) was added. The mixture was stirred for 2 h and extracted with EtOAc and aqueous $NaHCO_3$ (saturated). The organic layer was washed with brine, dried ($Na_2SO_4$) and concentrated under vacuum. The residue was purified by silica gel chromatography using hexane/ethyl acetate (2:1) to give **9** (1.53 g, 2.62 mmol, 97%): $^1$H-NMR (400 MHz, $CDCl_3$) δ 7.45−7.47 (m, 2H), 7.34 (qd, $J$ = 4.7, 2.4 Hz, 4H), 7.28−7.30 (m, 1H), 7.20−7.23 (m, 1H), 6.83 (dt, $J$ = 9.5, 2.4 Hz, 4H), 5.23 (s, 1H), 4.32−4.36 (m, 1H), 4.23 (d, $J$ = 5.0 Hz, 1H), 4.12−4.20 (m, 2H), 4.06 (s, 1H), 3.79 (d, $J$ = 4.6 Hz, 7H), 3.31 (dq, $J$ = 21.3, 5.0 Hz, 2H), 2.72 (d, $J$ = 6.9 Hz, 1H); $^{13}$C-NMR (101 MHz, $CDCl_3$) δ 158.65, 149.56, 144.88, 136.05, 130.16, 128.23, 128.05, 127.00, 124.10, 113.33, 107.56, 96.70, 86.34, 82.88, 79.20, 77.48, 76.85, 75.20, 72.75, 64.97, 55.36. HRMS (ESI-TOF) *m/z*: Calcd. for $C_{28}H_{29}Cl_3O_7Na$ $[M+Na]^+$ 605.0874, found 605.0876.

**3-*O*-(*tert*-Butyldimethylsilyl)-5-*O*-(4,4'-dimethoxytrityl)-1-*O*-(2,2,2-trichloroethyl)-β-D-ribofuranose (11) and 2-*O*-(*tert*-Butyldimethylsilyl)-5-*O*-(4,4'-dimethoxytrityl)-1-*O*-(2,2,2-trichloroethyl)-β-D-ribofuranose (12)**

To a stirred solution of **9** (1.515 g, 2.59 mmol) and $Et_3N$ (1.08 mL, 7.77 mmol) in DMF (15 mL) was added TBDMSCl (0.78 g, 5.18 mmol) at room temperature. The reaction mixture was stirred for 16 h at room temperature and partitioned between EtOAc and aqueous $NaHCO_3$ (saturated). The organic layer was washed with brine, dried ($Na_2SO_4$) and evaporated under reduced pressure. The crude was purified by silica gel chromatography using hexane/ethyl acetate (11:1) to yield **11** (0.58 g, 0.83 mmol, 32%) and **12** (0.47 g, 0.67 mmol, 26%). Physical data for **11**: $^1$H-NMR (400 MHz, $CDCl_3$) δ 7.47−7.49 (m, 2H), 7.35−7.38 (m, 4H), 7.28−7.30 (m, 1H), 7.18−7.22 (m, 1H), 6.80−6.85 (m, 5H), 5.32 (s, 1H), 4.37 (dd, *J* = 6.9, 5.0 Hz, 1H), 4.12−4.22 (m, 3H), 4.07 (q, *J* = 2.3 Hz, 1H), 3.79 (d, *J* = 7.3 Hz, 7H), 3.33 (dd, *J* = 10.3, 3.0 Hz, 1H), 3.08 (q, *J* = 5.3 Hz, 1H), 2.80 (d, *J* = 2.3 Hz, 1H), 0.93 (d, *J* = 4.1 Hz, 0H), 0.82 (t, *J* = 3.0 Hz, 10H), 0.01−0.04 (m, 3H), -0.14−-0.10 (m, 3H); $^{13}$C-NMR (101 MHz, $CDCl_3$) δ 158.62, 144.89, 136.20, 136.11, 130.20, 130.16, 128.32, 127.97, 126.93, 113.28, 107.98, 96.94, 86.09, 83.64, 79.49, 77.48, 76.85, 75.26, 72.35, 64.06, 55.36, 25.76, 18.04, -4.77. Physical data for **12**: $^1$H-NMR (400 MHz, $CDCl_3$) δ 7.48−7.50 (m, 2H), 7.34−7.39 (m, 4H), 7.27−7.30 (m, 1H), 6.82 (dq, *J* = 9.5, 2.6 Hz, 5H), 5.20 (d, *J* = 1.4 Hz, 1H), 4.31 (td, *J* = 4.4, 2.6 Hz, 1H), 4.19 (d, *J* = 4.6 Hz, 1H), 4.09−4.16 (m, 3H), 3.79 (d, *J* = 6.4 Hz, 8H), 3.36 (dd, *J* = 10.1, 3.2 Hz, 1H), 3.12−3.16 (m, 1H), 2.48 (d, *J* = 7.8 Hz, 1H), 0.92 (q, *J* = 4.9 Hz, 13H), 0.15−0.18 (m, 8H); $^{13}$C-NMR (101 MHz, $CDCl_3$) δ 158.59, 136.23, 130.24, 129.28, 128.33, 127.98, 126.88, 113.28, 108.23, 86.21, 84.54, 79.60, 77.47, 76.85, 76.45, 72.36, 64.66, 55.34, 25.86, 18.26, -4.47, -4.86; HRMS (ESI-TOF) *m/z*: Calcd. for $C_{34}H_{43}Cl_3O_7SiK$ $[M+K]^+$ 735.1504, found 735.1481.

**2-*O*-(*tert*-Butyldimethylsilyl)-5-*O*-(4,4'-dimethoxytrityl)-3-*O*-[(2-cyanoethoxy)(N,N-diisoprylamino)]phosphanyl-1-*O*-(2,2,2-trichloroethyl)-β-D-ribofuranose (15)**

To a solution of **12** (0.44 g, 0.63 mmol) in THF (5 mL) was added *N,N*-diisopropylethylamine (0.54 mL, 3.15 mmol) and chloro(2-cyanoethoxy)(*N,N*-diisopropylamino)phosphine (0.28 mL, 1.26 mmol) at room temperature. The mixture was stirred for 45 min at room temperature and white precipitate confirmed reaction completion. The reaction mixture was extracted with $CHCl_3$ and aqueous $NaHCO_3$ (saturated). The organic layer was washed with brine, dried ($Na_2SO_4$) and concentrated. The residue was purified by silica gel chromatography using hexane/ethyl acetate (2:1) to afford **15** (0.37 g, 0.44 mmol, 90%): $^{31}$P-NMR (202 MHz, $CDCl_3$) δ 149.974, 149.543. HRMS (ESI-TOF) *m/z*: Calcd. for $C_{43}H_{60}Cl_3O_8NaPSi$ $[M+Na]^+$ 919.2820, found 919.2837.

**2,3,5-tri-*O*-benzoyl-1-*O*-(2,2,2-tribromoethyl)-β-D-ribofuranose (8)**

To a stirred solution of 1-*O*-acetyl-2,3,5-tri-*O*-benzoyl- β-D-ribofuranose (2.02 g, 4.00 mmol) in dry $CH_2Cl_2$ (20 mL) at −30 ˚C, TMSOTf (1.32 mL, 7.2 mmol) and 2,2,2-tribromoethanol (1.13 g, 4.00 mmol) were added slowly. The reaction mixture was stirred for 4 h, quenched by saturated sodium bicarbonate and extracted with $CHCl_3$. The organic layer was washed with aqueous $NaHCO_3$ and brine, dried ($Na_2SO_4$) and solvent was evaporated under reduced pressure to afford a crude residue. The crude was purified by silica gel chromatography using hexane/ethyl acetate (5:1) to afford **8** (2.63 g, 3.62 mmol, 90%): $^1$H-NMR (400 MHz, $CDCl_3$) δ 8.01−8.09 (m, 4H), 7.89 (dd, *J* = 8.5, 1.1 Hz, 2H), 7.49−7.62 (m, 3H), 7.42 (dt, *J* = 18.8, 7.8 Hz, 4H), 7.33 (t, *J* = 7.8 Hz, 2H), 5.96 (dd, *J* = 6.9, 5.0 Hz, 1H), 5.91 (d, *J* = 4.6 Hz, 1H), 5.63 (s, 1H), 4.69−4.82 (m, 2H), 4.62 (q, *J* = 5.6 Hz, 1H), 4.52−4.55 (m, 1H), 4.32−4.35 (m, 1H), $^{13}$C-NMR (101 MHz, $CDCl_3$) δ 165.49, 133.77, 133.63, 133.39, 129.99, 129.94, 129.91, 129.73,

128.96, 128.69, 128.62, 128.55, 106.12, 82.57, 79.91, 77.48, 76.85, 75.52, 72.34, 64.87, 38.65; HRMS (ESI-TOF) *m/z*: Calcd. for $C_{28}H_{23}Br_3O_8Na$ $[M+Na]^+$ 746.8855, found 746.8840.

**1-*O*-(2,2,2-Tribromoethyl)-β-D-ribofuranose (3)**

To a stirred solution of **8** (2.56 g, 3.5 mmol) in MeOH (18 mL), a catalytic amount of 28% MeOH solution of sodium methoxide was added. The reaction mixture was stirred at room temperature for 16 h and quenched by using aqueous $NH_4Cl$ (saturated, 1 mL). The solvent was evaporated under reduced pressure and the resulting residue was purified by silica gel chromatography using $CHCl_3$/MeOH (10:1) to give **3** (1.136 g, 2.74 mmol, 78%): $^1$H-NMR (400 MHz, DMSO-$d_6$) δ 5.20 (d, *J* = 4.6 Hz, 1H), 5.11 (s, 1H), 4.92 (d, *J* = 6.9 Hz, 1H), 4.72 (t, *J* = 5.7 Hz, 1H), 4.38 (d, *J* = 11.9 Hz, 1H), 4.24 (d, *J* = 11.9 Hz, 1H), 3.94 (td, *J* = 7.1, 4.6 Hz, 1H), 3.81−3.88 (m, 2H), 3.56−3.63 (m, 1H), 3.40−3.47 (m, 1H), $^{13}$C-NMR (101 MHz, DMSO-$d_6$) δ 106.73, 84.06, 80.75, 74.29, 70.84, 63.05, 40.66, 40.14, 39.93, 39.72, 39.31, 39.10, 38.89; HRMS (ESI-TOF) *m/z*: Calcd. for $C_7H_{11}Br_3O_5$ $[M+Na]^+$ 434.8054, found 434.8058.

**5-*O*-(4,4'-Dimethoxytrityl)-1-*O*-(2,2,2-Tribromoethyl)-β-D-ribofuranose (10)**

To a solution of **3** (1.1 g, 2.65 mmol) in pyridine (16 mL) stirred at room temperature, DMTrCl (1.08 g, 3.18 mmol) was added. The mixture was stirred for 2 h and extracted with EtOAc and aqueous $NaHCO_3$ (saturated). The organic layer was washed with brine, dried ($Na_2SO_4$) and concentrated under vacuum. The residue was purified by silica gel chromatography using hexane/ethyl acetate (3:1) to give **10** (1.74 g, 2.42 mmol, 92%): $^1$H-NMR (400 MHz, $CDCl_3$) δ 7.45−7.47 (m, 2H), 7.25−7.35 (m, 10H), 7.15−7.22 (m, 1H), 6.82−6.85 (m, 4H), 5.29 (s, 1H), 4.31−4.38 (m, 2H), 4.25−4.28 (m, 1H), 3.79 (d, *J* = 5.0 Hz, 6H), 3.39 (dd, *J* = 9.4, 5.7 Hz, 1H), 3.29 (dd, *J* = 9.4, 5.7 Hz, 1H), $^{13}$C-NMR (101 MHz, $CDCl_3$) δ 158.65, 130.18, 128.23, 128.07,

127.00, 113.35, 107.26, 86.36, 82.77, 77.47, 76.85, 75.27, 73.06, 55.37; HRMS (ESI-TOF) *m/z*: Calcd. for $C_{28}H_{29}Br_3O_7Na$ $[M+Na]^+$ 736.9366, found 736.9361.

**3-*O*-(*tert*-Butyldimethylsilyl)-5-*O*-(4,4'-dimethoxytrityl)-1-*O*-(2,2,2-tribromoethyl)-β-D-ribofuranose (13) and 2-*O*-(*tert*-Butyldimethylsilyl)-5-*O*-(4,4'-dimethoxytrityl)-1-*O*-(2,2,2-tribromoethyl)-β-D-ribofuranose (14)**

To a stirred solution of **10** (1.7 g, 2.37 mmol) and $Et_3N$ (1.00 mL, 7.11 mmol) in DMF (15 mL) was added TBDMSCl (0.72 g, 4.74 mmol) at room temperature. The reaction mixture was stirred for 12 h at room temperature and partitioned between EtOAc and aqueous $NaHCO_3$ (saturated). The organic layer was washed with brine, dried ($Na_2SO_4$) and evaporated under reduced pressure. The crude was purified by silica gel chromatography using hexane/ethyl acetate (11:1) to yield **13** (0.503 g, 0.61 mmol, 26%) and **14** (0.456 g, 0.55 mmol, 23%). Physical data of **13**: $^1$H-NMR (400 MHz, $CDCl_3$) δ 7.48−7.50 (m, 2H), 7.37 (dd, *J* = 9.2, 0.9 Hz, 4H), 7.30 (dd, *J* = 7.1, 5.3 Hz, 2H), 7.15−7.22 (m, 1H), 6.80−6.84 (m, 5H), 5.39 (s, 1H), 4.38 (dd, *J* = 5.7, 3.9 Hz, 2H), 4.32 (s, 1H), 4.10−4.19 (m, 2H), 3.79 (t, *J* = 3.4 Hz, 6H), 3.33 (dd, *J* = 10.3, 3.0 Hz, 1H), 3.12 (q, *J* = 5.2 Hz, 1H), 2.81 (q, *J* = 2.7 Hz, 1H), 0.94 (d, *J* = 4.6 Hz, 1H), 0.82 (d, *J* = 2.7 Hz, 11H), 0.02 (d, *J* = 3.2 Hz, 3H), -0.10 (d, *J* = 5.0 Hz, 3H); $^{13}$C-NMR (101 MHz, $CDCl_3$) δ 158.60, 130.22, 130.18, 128.34, 127.99, 126.93, 113.30, 107.82, 86.12, 83.68, 82.40, 77.48, 76.85, 75.32, 72.48, 64.24, 55.37, 25.77, 18.05, -4.75. Physical data of **14**: $^1$H-NMR (400 MHz, $CDCl_3$) δ 7.48−7.51 (m, 2H), 7.37 (td, *J* = 4.5, 2.6 Hz, 5H), 7.29 (d, *J* = 7.3 Hz, 1H), 7.18−7.21 (m, 1H), 6.83 (q, *J* = 4.3 Hz, 5H), 5.26 (d, *J* = 1.8 Hz, 1H), 4.39 (d, *J* = 11.9 Hz, 1H), 4.33 (q, *J* = 2.0 Hz, 1H), 4.26 (d, *J* = 11.9 Hz, 1H), 4.11−4.18 (m, 3H), 3.79 (d, *J* = 6.9 Hz, 6H), 3.36 (dd, *J* = 10.1, 3.2 Hz, 1H), 3.18 (q, *J* = 5.2 Hz, 1H), 2.49 (d, *J* = 7.8 Hz, 1H), 0.93−0.94 (m, 12H), 0.18 (q, *J* = 3.4 Hz, 6H); $^{13}$C-NMR (101 MHz, $CDCl_3$) δ

158.57, 130.25, 128.33, 127.99, 126.87, 113.29, 107.98, 86.20, 84.50, 82.44, 77.47, 76.84, 76.46, 72.45, 64.78, 55.34, 25.88, 18.26, -4.35, -4.80; HRMS (ESI-TOF) *m/z*: Calcd. for $C_{34}H_{43}Br_3O_7NaSi$ $[M+Na]^+$ 851.0213, found 851.0225.

**2-*O*-(*tert*-Butyldimethylsilyl)-5-*O*-(4,4'-dimethoxytrityl)-3-*O*-[(2-cyanoethoxy)(N,N-diisoprylamino)]phosphanyl-1-*O*-(2,2,2-tribromoethyl)-β-D-ribofuranose (16)**

To a solution of **18** (0.416 g, 0.5 mmol) in THF (5 mL) was added *N,N*-diisopropylethylamine (0.44 mL, 2.5 mmol) and chloro(2-cyanoethoxy)(*N,N*-diisopropylamino)phosphine (0.23 mL, 1.0 mmol) at room temperature. The mixture was stirred for 45 min at room temperature and white precipitate confirmed reaction completion. The reaction mixture was extracted with $CHCl_3$ and aqueous $NaHCO_3$ (saturated). The organic layer was washed with brine, dried ($Na_2SO_4$) and concentrated. The residue was purified by silica gel chromatography using hexane/ethyl acetate (3:1) to afford **16** (0.40 g, 0.38 mmol, 78%): $^{31}$P-NMR (162 MHz, $CDCl_3$) δ 149.62, 149.24. HRMS (ESI-TOF) *m/z*: Calcd. for $C_{43}H_{60}Br_3O_8NaPSi$ $[M+Na]^+$ 1051.1304, found 1051.1292.

**Synthesis of the controlled pore glass (CPG) solid support (17-18)**

*N,N*-Dimethyl-4-aminopyridine (DMAP) (0.195 g, 1.56 mmol), and succinic anhydride (0.312 g, 3.12 mmol ) were added to a solution of **11** (0.55 g, 0.78 mmol) in pyridine (10 mL) under argon atmosphere and the mixture was stirred for 20 h at room temperature. The mixture was extracted with $H_2O$ and EtOAc. The organic layer was washed with sat. $NaHCO_3$ solution, brine, dried over $Na_2SO_4$ and concentrated in vacuo. The residue was purified by column chromatography on silica gel (hexane:ethyl acetate, 2:1) to give succinate mixture as a colorless, viscous liquid. Aminopropyl controlled pore glass (0.45 g, 60 μmol) and 1-ethyl-3-[3-

(dimethylamino)propyl] carbodiimide hydrochloride (50 mg, 0.24 mmol) were added to a solution of succinate in DMF and the mixture was kept at room temperature for 4 days. This resin was washed with pyridine, 15 mL of capping solution (0.1 M DMAP in pyridine: $Ac_2O$, 9:1) were added to the resin and the mixture was kept at room temperature for 1 day. The resin was washed with pyridine, ethanol, acetonitrile and dried under vacuum to give solid support **17**. Similarly, solid support **18** was also synthesized for analog **3**. The amount of nucleoside loaded to the solid support was calculated by release of dimethoxytrityl cation using solution of 70% $HClO_4$: EtOH (3:2, v/v).

**MALDI-TOF/MS analysis of RNAs**

The spectra were obtained with a time-of-flight mass spectrometer equipped with nitrogen laser (337 nm, 3 ns pulse). A solution of 3-hydroxypicolinic acid (3-HPA) and diammonium hydrogen citrate in 0.1 M MeCN/$H_2O$ (1:1, v/v) was used as matrix. Data of synthetic RNAs: RNA **1** *m/z* = 6507.00 (calcd for $C_{194}H_{245}N_{65}O_{150}P_{20}$ $[M-H]^-$, 6505.844); RNA **2** *m/z* = 6817.45 (calcd for $C_{203}H_{248}N_{86}O_{144}P_{20}$ $[M-H]^-$, 6816.11); RNA **3** *m/z* = 6483.80 (calcd for $C_{190}H_{243}N_{61}O_{148}P_{20}F_6$ $[M-H]^-$, 6482.75); RNA **4** *m/z* = 6791.73 (calcd for $C_{199}H_{246}N_{82}O_{142}P_{20}F_6$ $[M-H]^-$, 6792.01); RNA **5** *m/z* = 6582.33 (calcd for $C_{190}H_{243}N_{61}O_{148}P_{20}Cl_6$ $[M-H]^-$, 6581.46); RNA **6** *m/z* = 6890.42 (calcd for $C_{199}H_{246}N_{82}O_{142}P_{20}Cl_6$ $[M-H]^-$, 6890.72); RNA **7** *m/z* = 6849.08 (calcd for $C_{190}H_{243}N_{61}O_{148}P_{20}Br_6$ $[M-H]^-$, 6848.18); RNA **8** *m/z* = 7157.45 (calcd for $C_{199}H_{246}N_{82}O_{142}P_{20}Br_6$ $[M-H]^-$ , 7157.45); RNA **9** *m/z* = 6466.14 (calcd for $C_{198}H_{262}N_{64}O_{144}P_{19}S$ $[M-H]^-$, 6464.12); RNA **10** *m/z* = 7353.24 (calcd for $C_{230}H_{273}N_{87}O_{153}P_{21}$ $[M-H]^-$, 7354.57); RNA **11** *m/z* = 7329.17 (calcd for $C_{226}H_{271}N_{83}O_{151}P_{21}F_6$ $[M-H]^-$, 7330.48); RNA **12** *m/z* = 7427.72 (calcd for $C_{226}H_{271}N_{83}O_{151}P_{21}Cl_6$ $[M-H]^-$, 7429.18); RNA **13** *m/z* = 7700.86 (calcd for $C_{226}H_{271}N_{83}O_{151}P_{21}Br_6$ $[M-H]^-$ , 7695.91).

## 6.2.2. Synthesis of branching Dendron solid support

**2-(((tert-Butyldimethylsilyl)oxy)methyl)-2-(hydroxymethyl)propane-1,3-diol (D2)**

To a solution of pentaerythrtol (1.36 g, 10 mmol) and $Et_3N$ (1.54 mL, 11 mmol) in DMF (80 mL) was added TBDMSCl (1.21 g, 8 mmol) and stirred at room temperature. The reaction mixture was stirred for 16 h at room temperature and partitioned between EtOAc and aqueous $NaHCO_3$ (saturated). The organic layer was washed with brine, dried ($Na_2SO_4$) and evaporated under reduced pressure. The crude was purified by silica gel chromatography using chloroform/methanol (20:1) to yield D2 (1.30 g, 5.2 mmol, 65%). $^1$H-NMR (500 MHz, $CDCl_3$), δ 3.72 (d, *J* = 5.7 Hz, 6H), 3.66 (s, 2H), 2.53 (t, *J* = 5.7 Hz, 3H), 0.89 (d, *J* = 11.5 Hz, 9H), 0.08 (d, J = 2.9 Hz, 6H); $^{13}$C-NMR (126 MHz, $CDCl_3$) δ 77.42, 76.90, 65.89, 64.73, 45.20, 25.93, 18.23, -5.59.

**(3-(Allyloxy)-2,2-bis((allyloxy)methyl)propoxy)(tert-butyl)dimethylsilane (D3)**

To a stirred solution of NaH, in 60% oil immersion (0.78 g,19.4 mmol) in THF (50 mL) was added D2 (1.515 g, 4.85 mmol) dissolved in THF (10 mL) at 0°C. The reaction was stirred at 0°C for 30 minutes before adding the allyl bromide (2.46 mL, 29.1 mmol). The reaction mixture was then stirred for 14 h at room temperature and traced with TLC using $KMnO_4$ as the stain for the double bond. Excess of NaH was quenched with MeOH and then partitioned between EtOAc and aqueous $NaHCO_3$ (saturated). The organic layer was washed with brine, dried ($Na_2SO_4$) and evaporated under reduced pressure. The crude was purified by silica gel chromatography using hexane/ethyl acetate (20:1) to yield D3 (1.45 g, 3.92 mmol, 81%). $^1$H-NMR (500 MHz, $CDCl_3$) δ 5.84-5.92 (m, 3H), 5.25 (dq, *J* = 17.2, 1.7 Hz, 3H), 5.11-5.14 (m, 3H), 3.94 (td, *J* = 3.4, 1.5 Hz, 6H), 3.59 (s, 2H), 3.42 (s, 6H), 0.88 (s, 9H), 0.02 (t, *J* = 3.2 Hz,

6H); $^{13}$C-NMR (126 MHz, $CDCl_3$) δ 135.47, 116.18, 77.41, 76.90, 72.42, 69.13, 61.74, 46.20, 29.86, 26.02, 18.38, -5.49.

**3,3'-((2-(((tert-Butyldimethylsilyl)oxy)methyl)-2-((3-hydroxypropoxy)methyl)propane-1,3-diyl)bis(oxy))bis(propan-1-ol) (D4)**

9- Borabicyclo [3.3.1] nonane (9-BBN, 0.5 M in THF, 33.75 mL) was added dropwise to a solution of compound D3 (1.39 g, 3.75 mmol) in THF (15 mL) and stirred for 17 h at room temperature. Water was added to the reaction mixture until effervescence ceased. 3 N NaOH solution (12.6 mL) was added, and then, slowly 30% aqueous hydrogen peroxide solution (6.4 mL) was added while keeping the temperature between 30 and 50 °C. The mixture was stirred and extracted with water and ethyl acetate. The organic layer was washed with neutral phosphate buffer solution and brine, dried over $Na_2SO_4$, filtered, and concentrated. The crude material was purified by column chromatography (4% methanol in chloroform) to afford the desired product D4 (1.32 g, 3.11 mmol, 83%). $^1$H-NMR (500 MHz, $CDCl_3$) δ 3.74 (q, *J* = 5.3 Hz, 6H), 3.58 (t, *J* = 5.4 Hz, 6H), 3.50 (d, *J* = 6.3 Hz, 2H), 3.37 (s, 6H), 3.22 (t, *J* = 5.4 Hz, 3H), 1.77-1.82 (m, 6H), 0.88 (s, 10H), 0.03 (s, 6H); $^{13}$C-NMR (126 MHz, $CDCl_3$) δ 77.41, 76.90, 70.69, 70.62, 61.92, 61.79, 45.60, 31.86, 25.98, 18.38, 14.33, -5.56.

**6,6-bis((3-(Allyloxy)propoxy)methyl)-2,2,3,3-tetramethyl-4,8,12-trioxa-3-silapentadec-14-ene (D'5)**

To a stirred solution of NaH, in 60% oil immersion (0.46g, 11.48 mmol) in THF (30 mL) was added **D4** (1.22 g, 2.87 mmol) dissolved in THF (6 mL) at 0°C. The reaction was stirred at 0°C for 30 minutes before adding the allyl bromide (1.46 mL, 17.22 mmol). The reaction mixture was then stirred overnight at room temperature and traced with TLC using $KMnO_4$ as

the stain for the double bond. Excess of NaH was quenched with MeOH and then partitioned between EtOAc and aqueous $NaHCO_3$ (saturated). The organic layer was washed with brine, dried ($Na_2SO_4$) and evaporated under reduced pressure. The crude was purified by silica gel chromatography using hexane/ethyl acetate (10:1) to yield **D'5** (1.00 g, 1.85 mmol, 64%). $^1$H-NMR (500 MHz, $CDCl_3$) δ 5.91 (qd, *J* = 11.1, 5.4 Hz, 3H), 5.26 (dq, *J* = 17.2, 1.7 Hz, 3H), 5.16 (dd, *J* = 10.3, 1.1 Hz, 3H), 3.96 (td, *J* = 3.4, 2.1 Hz, 6H), 3.53 (s, 2H), 3.50 (t, *J* = 6.6 Hz, 6H), 3.45 (t, *J* = 6.3 Hz, 6H), 3.34 (s, 6H), 1.80-1.85 (m, 6H), 0.88 (s, 9H), 0.01 (d, *J* = 2.9 Hz, 6H); $^{13}$C-NMR (126 MHz, $CDCl_3$) δ 135.17, 116.82, 77.42, 76.90, 72.02, 69.51, 68.38, 67.71, 61.82, 46.18, 30.25, 26.03, 18.40, -5.47.

**10-(((tert-Butyldimethylsilyl)oxy)methyl)-10-((3-(3-hydroxypropoxy)propoxy)methyl)-4,8,12,16-tetraoxanonadecane-1,19-diol (D'6)**

9- Borabicyclo [3.3.1] nonane (9-BBN, 0.5 M in THF, 14.85 mL) was added dropwise to a solution of compound **D'5** (0.9 g, 1.65 mmol) in THF (10 mL) and stirred for 18 h at room temperature. Water was added to the reaction mixture until effervescence ceased. 3 N NaOH solution (5.6 mL) was added, and then, 30% aqueous hydrogen peroxide solution (6.4 mL) was added carefully, while keeping the temperature between 30 and 50 °C. The mixture was stirred and extracted with water and ethyl acetate. The organic layer was washed with neutral phosphate buffer solution and brine, dried over $Na_2SO_4$, filtered, and concentrated. The crude was purified by column chromatography (4% methanol in chloroform) to afford the desired product **D'6** (0.92 g, 1.53 mmol, 93%). $^1$H-NMR (500 MHz, $CDCl_3$) δ 3.76 (q, *J* = 5.5 Hz, 6H), 3.60 (t, *J* = 5.7 Hz, 6H), 3.49-3.52 (m, 8H), 3.44 (t, *J* = 6.3 Hz, 6H), 3.33 (s, 6H), 2.61 (t, *J* = 5.4 Hz, 3H), 1.81 (td, *J* = 12.7, 6.3 Hz, 12H), 0.88 (s, 9H), 0.02 (d, *J* = 2.9 Hz, 6H); $^{13}$C-NMR

(126 MHz, $CDCl_3$) δ 77.42, 76.90, 70.24, 69.47, 68.53, 68.25, 62.06, 61.74, 46.17, 32.18, 30.14, 26.02, 18.40, -5.48.

**12,12-bis((3-(3-(bis(4-methoxyphenyl)(phenyl)methoxy)propoxy)propoxy)methyl)-1,1-bis(4-methoxyphenyl)-15,15,16,16-tetramethyl-1-phenyl-2,6,10,14-tetraoxa-15-silaheptadecane (D'7)**

To a solution of D**'6** (0.84 g, 1.40 mmol) in pyridine (30 mL) stirred at room temperature, DMTrCl (1.71 g, 5.04 mmol) was added. The mixture was stirred for 12 h and extracted with EtOAc and aqueous $NaHCO_3$ (saturated). The organic layer was washed with brine, dried ($Na_2SO_4$) and concentrated under vacuum. The residue was purified by silica gel chromatography using hexane/ethyl acetate (5:1) to give **D'7** (1.90 g, 1.26 mmol, 90%):$^1$H-NMR (500 MHz, $CDCl_3$) 7.42 (d, *J* = 7.4 Hz, 6H), 7.29-7.32 (m, 13H), 7.28 (s, 2H), 7.25 (s, 2H), 7.18 (t, *J* = 7.2 Hz, 3H), 6.79-6.81 (m, 13H), 3.77 (s, 18H), 3.53 (t, *J* = 6.0 Hz, 8H), 3.43 (t, J = 6.6 Hz, 6H), 3.38 (t, *J* = 6.3 Hz, 6H), 3.30 (s, 6H), 3.12 (t, *J* = 6.3 Hz, 6H), 1.73-1.87 (m, 12H), 0.86 (s, 9H), -0.01 (s, 6H); $^{13}$C-NMR (126 MHz, $CDCl_3$) δ 158.46, 145.44, 136.76, 130.15, 128.34, 127.82, 126.71, 113.10, 85.86, 77.42, 76.91, 69.45, 68.53, 68.30, 60.53, 60.47, 55.31, 30.60, 30.25, 26.03, 21.20, 14.35, -5.46.

**3-(3-(3-(bis(4-Methoxyphenyl)(phenyl)methoxy)propoxy)propoxy)-2,2-bis((3-(3-(bis(4-methoxyphenyl)(phenyl)methoxy)propoxy)propoxy)methyl)propan-1-ol (D'8)**

To a stirred solution of **D'7** (1.81 g, 1.19 mmol) in THF (12 mL) was added TBAF (1 M in THF, 2.38 mL) at room temperature. The reaction mixture was stirred for 18 h at room temperature and partitioned between EtOAc and aqueous $NaHCO_3$ (saturated). The organic layer was washed with brine, dried ($Na_2SO_4$) and evaporated under reduced pressure. The crude

was purified by silica gel chromatography using hexane/ethyl acetate (2:1) to yield **D'8** (1.50 g, 1.08 mmol, 91%). $^{1}$H-NMR (500 MHz, $CDCl_3$) δ 7.41-7.43 (m, 6H), 7.29-7.32 (m, 13H), 7.28 (s, 2H), 7.25 (s, 2H), 7.18 (t, *J* = 7.2 Hz, 3H), 6.79-6.82 (m, 13H), 3.77 (s, 18H), 3.65 (d, J = 6.3 Hz, 2H), 3.53 (t, *J* = 6.6 Hz, 6H), 3.44 (s, 1H), 3.42 (t, *J* = 5.7 Hz, 9H), 3.39 (s, 2H), 3.39 (s, 6H), 3.12 (t, *J* = 6.3 Hz, 6H), 3.00 (t, *J* = 6.3 Hz, 1H), 1.82-1.87 (m, 6H), 1.74-1.79 (m, 6H); $^{13}$C-NMR (126 MHz, $CDCl_3$) δ 158.46, 145.43, 136.74, 130.15, 128.32, 127.82, 126.72, 113.10, 85.86, 77.41, 76.90, 71.59, 68.84, 68.34, 68.04, 60.43, 55.32, 44.91, 30.55, 30.11.

**Synthesis of the controlled pore glass (CPG) solid support (D'9)**

*N,N*-Dimethyl-4-aminopyridine (DMAP) (0.23 g, 1.84 mmol), and succinic anhydride (0.37 g, 3.68 mmol ) were added to a solution of D'8 (1.28 g, 0.92 mmol) in pyridine (10 mL) under argon atmosphere and the mixture was stirred for 20 h at room temperature. The mixture was extracted with $H_2O$ and EtOAc. The organic layer was washed with sat. $NaHCO_3$ solution, brine, dried over $Na_2SO_4$ and concentrated in vacuo. The residue was purified by column chromatography on silica gel (hexane:ethyl acetate, 2:1) to give succinate mixture as a colorless, viscous liquid in 82% yield. Aminopropyl controlled pore glass (0.49 g, 60 μmol) and 1-ethyl-3-[3-(dimethylamino)propyl] carbodiimide hydrochloride (46 mg, 0.24 mmol) were added to a solution of succinate (0.36 g, 0.24 mmol) in DMF and the mixture was kept at room temperature for 4 days. This resin was washed with pyridine, 15 mL of capping solution (0.1 M DMAP in pyridine: $Ac_2O$, 9:1) were added to the resin and the mixture was kept at room temperature for 1 day. The resin was washed with pyridine, ethanol, acetonitrile and dried under vacuum to give solid support D'9. The amount of nucleoside loaded to the solid support was calculated by release of dimethoxytrityl cation using solution of 70% $HClO_4$: EtOH (3:2, v/v).

## 6.2.3. Synthesis of 2'-OMe haloaryl nucleoside analogs

**2,3,5-Tri-*O*-benzoyl-1-*O*-(phenyl)-β-D-ribofuranose (8)**

To a stirred solution of 1-*O*-acetyl-2,3,5-tri-*O*-benzoyl-β-D-ribofuranose (2.52 g, 5.00 mmol) in dry $CH_2Cl_2$ (20 mL) at −30 ˚C, TMSOTf (1.60 mL, 9.00 mmol) and phenol (0.47 g, 5.00 mmol) were added. The reaction mixture was stirred for 14 h, quenched by saturated sodium bicarbonate and extracted with $CHCl_3$. The organic layer was washed with aqueous $NaHCO_3$ and brine, dried ($Na_2SO_4$) and solvent was evaporated under reduced pressure. The crude was purified by silica gel chromatography using hexane/ethyl acetate (5:1) to afford **8** (2.17 g, 4.03 mmol, 81%): $^1$H-NMR (500 MHz, $CDCl_3$) δ 8.03 (t, *J* = 6.9 Hz, 2H), 7.88-7.96 (m, 5H), 7.41-7.61 (m, 7H), 7.29-7.36 (m, 5H), 7.02 (dd, *J* = 17.5, 7.7 Hz, 3H), 6.03 (dd, *J* = 7.2, 4.9 Hz, 1H), 5.93 (d, *J* = 4.6 Hz, 1H), 5.91 (s, 1H), 4.82-4.85 (m, 1H), 4.72 (dd, *J* = 12.0, 4.0 Hz, 1H), 4.54 (dd, J = 12.0, 4.6 Hz, 1H); $^{13}$C-NMR (126 MHz, $CDCl_3$) δ 166.26, 165.53, 165.34, 156.36, 133.75, 133.62, 133.16, 129.99, 129.91, 129.89, 129.70, 129.64, 129.20, 129.01, 128.68, 128.54, 128.38, 122.65, 116.58, 103.75, 79.73, 77.42, 76.90, 75.94, 72.25, 64.23.

**1-*O*-(Phenyl)- β-D-ribofuranose (1)**

To a stirred solution of **8** (2.09 g, 3.88 mmol) in MeOH (12 mL) and $CH_2Cl_2$ (8 mL), a catalytic amount of 28% MeOH solution of sodium methoxide was added. The reaction mixture was stirred at room temperature for 18 h and quenched by using aqueous $NH_4Cl$ (saturated, 1 mL). The solvent was evaporated under reduced pressure and the resulting residue was purified by silica gel chromatography using $CHCl_3$/MeOH (10:1) to give **1** (0.79 g, 3.49 mmol, 90%): $^1$H-NMR (500 MHz, DMSO-$d_6$) δ 7.26-7.30 (m, 2H), 6.97 (dd, *J* = 7.4, 5.7 Hz, 3H), 5.43 (s, 1H), 5.31 (d, *J* = 4.6 Hz, 1H), 5.00 (d, *J* = 6.3 Hz, 1H), 4.65-4.69 (m, 1H), 3.95-4.01 (m, 2H), 3.88

(td, $J$ = 5.7, 4.0 Hz, 1H), 3.53 (qd, $J$ = 5.7, 4.0 Hz, 1H), 3.37 (t, $J$ = 5.2 Hz, 1H); $^{13}$C-NMR (126 MHz, DMSO- $d_6$) δ 156.67, 129.48, 121.56, 116.28, 105.26, 84.59, 74.66, 70.64, 62.81, 40.02, 39.85, 39.68, 39.35, 39.19, 39.02.

**3,5-*O*-(Tetraisopropyldisiloxane)-1-*O*-(phenyl)-β-D-ribofuranose (11)**

To a solution of **1** (0.74 g, 3.27 mmol) in pyridine (12 mL) stirred at room temperature, $TIPDSCl_2$ (1.12 mL, 3.60 mmol) was added. The mixture was stirred for 4 h and extracted with $CHCl_3$ and water. The organic layer was washed with aqueous $NaHCO_3$ (saturated), brine, dried with $Na_2SO_4$ and co-evaporated with toluene under vacuum to remove excess pyridine. The residue was purified by silica gel chromatography using hexane/ethyl acetate (10:1) to give **11** (1.37 g, 2.92 mmol, 89%). $^1$H-NMR (500 MHz, $CDCl_3$) δ 7.27-7.29 (m, 2H), 6.96-7.01 (m, 3H), 5.62 (s, 1H), 4.68 (t, $J$ = 5.4 Hz, 1H), 4.26 (d, $J$ = 4.6 Hz, 1H), 4.08-4.13 (m, 1H), 3.99 (dd, $J$ = 11.5, 4.0 Hz, 1H), 3.75 (dd, $J$ = 11.2, 9.5 Hz, 1H), 3.09 (s, 1H), 1.03-1.11 (m, 32H); $^{13}$C-NMR (126 MHz, $CDCl_3$) δ 156.42, 129.61, 122.22, 116.52, 104.25, 83.39, 77.41, 77.16, 76.90, 76.21, 74.79, 65.95, 17.62, 17.57, 17.54, 17.48, 17.37, 17.17, 17.12, 13.47, 13.43, 13.00, 12.75.

**2-*O*-Methyl-3,5-*O*-(tetraisopropyldisiloxane)-1-*O*-(phenyl)-β-D-ribofuranose (14)**

To a stirred solution of 11 (1.30 g, 2.77 mmol) in DMF (15 mL) was added NaH (60% in oil, 0.33 g, 8.25 mmol) at 0 ˚C. After 15 minutes, the reaction mixture was brought to room temperature and iodomethane (0.86 mL, 13.85 mmol) was added. The reaction mixture was stirred for 15 h at room temperature and partitioned between $CHCl_3$ and water. The organic layer was washed with aqueous $NaHCO_3$ (saturated), brine, dried with $Na_2SO_4$ and evaporated under reduced pressure. The crude was purified by silica gel chromatography using

hexane/ethyl acetate (20:1) to yield **14** (0.65 g, 1.35 mmol, 49%). $^{1}$H-NMR (500 MHz, $CDCl_3$) δ 7.25 (s, 1H), 6.98 (q, *J* = 8.4 Hz, 4H), 5.53 (s, 1H), 4.67 (q, *J* = 4.0 Hz, 1H), 4.10 (qd, *J* = 5.5, 3.0 Hz, 1H), 3.96 (dd, *J* = 12.6, 2.9 Hz, 1H), 3.87 (td, *J* = 12.5, 5.0 Hz, 2H), 3.63 (s, 3H), 1.02-1.11 (m, 28H); $^{13}$C-NMR (126 MHz, $CDCl_3$) δ 156.54, 129.59, 122.09, 116.53, 102.73, 84.75, 81.67, 77.42, 76.91, 73.27, 63.34, 59.70, 17.69, 17.58, 17.55, 17.49, 17.42, 17.24, 17.17, 13.63, 13.37, 12.90, 12.80.

**2-*O*-Methyl-1-*O*-(phenyl)-β-D-ribofuranose (17)**

To a solution of **14** (0.60 g, 1.24 mmol) in THF (10 mL) stirred at room temperature, TEA·3HF (0.24 mL, 1.48 mmol) was added. The reaction mixture was stirred for 18 h at 40 ˚C and quenched with $NaHCO_3$ (saturated, 1 mL). $CHCl_3$ was added to the reaction mixture and reduced under vacuum. The residue was purified by silica gel chromatography using $CHCl_3$ /methanol (12:1) to give **17** (0.24 g, 1.01 mmol, 82%): $^{1}$H-NMR (500 MHz, $CDCl_3$) δ 7.30 (t, *J* = 8.0 Hz, 2H), 7.03 (t, *J* = 8.3 Hz, 3H), 5.68 (s, 1H), 4.46-4.50 (m, 1H), 4.09-4.11 (m, 1H), 3.95 (d, *J* = 5.2 Hz, 1H), 3.82 (td, *J* = 7.9, 4.2 Hz, 1H), 3.63-3.68 (m, 1H), 3.57 (s, 3H), 2.62 (d, *J* = 8.6 Hz, 1H), 1.78 (q, *J* = 4.6 Hz, 1H); $^{13}$C-NMR (126 MHz, $CDCl_3$) δ 156.36, 129.82, 122.58, 116.33, 102.63, 85.94, 84.82, 77.42, 76.91, 70.45, 62.66, 58.88.

**2-*O*-Methyl-5-*O*-(4,4'-dimethoxytrityl)-1-*O*-(phenyl)-β-D-ribofuranose (20)**

To a stirred solution of 17 (0.22 g, 0.90 mmol) in pyridine (8 mL) was added DMTrCl (0.37 g, 1.08 mmol) at room temperature. The reaction mixture was stirred for 15 h at room temperature and partitioned between EtOAc and water. The organic layer was washed with aqueous $NaHCO_3$ (saturated), brine, dried with $Na_2SO_4$ and evaporated under reduced pressure. The crude was purified by silica gel chromatography using hexane/ethyl acetate (1:1) to yield **20** (0.41 g, 0.76 mmol, 84%). $^{1}$H-NMR (500 MHz, $CDCl_3$) δ 7.41 (dd, *J* = 7.4, 2.3 Hz, 2H), 7.27-

7.33 (m, 6H), 7.15 (qd, *J* = 5.2, 3.2 Hz, 3H), 7.08-7.09 (m, 2H), 7.02 (t, *J* = 7.4 Hz, 1H), 6.64-6.68 (m, 4H), 5.75 (s, 1H), 4.37-4.41 (m, 1H), 4.12-4.17 (m, 1H), 4.00 (d, *J* = 4.6 Hz, 1H), 3.73 (d, *J* = 5.2 Hz, 7H), 3.57 (s, 3H), 3.27 (dd, *J* = 10.0, 3.2 Hz, 1H), 3.15 (q, *J* = 5.3 Hz, 1H), 2.53 (d, *J* = 8.6 Hz, 1H); $^{13}$C-NMR (126 MHz, $CDCl_3$) δ 158.41, 157.01, 145.09, 136.17, 136.01, 130.27, 130.16, 129.64, 128.33, 127.79, 126.69, 121.99, 116.30, 113.11, 102.35, 86.04, 84.62, 84.47, 77.41, 77.16, 76.90, 71.29, 64.52, 58.74, 55.30.

**2-*O*-Methyl-5-*O*-(4,4'-dimethoxytrityl)-3-*O*-[(2-cyanoethoxy)(N,N-diisoprylamino)] phosphanyl-1-*O*-(phenyl)-β-D-ribofuranose (23)**

To a solution of **20** (0.27 g, 0.50 mmol) in THF (5 mL) was added *N,N*-diisopropylethylamine (0.44 mL, 2.50 mmol) and chloro(2-cyanoethoxy)(*N,N*-diisopropylamino)phosphine (0.23 mL, 1.00 mmol) at room temperature, inside the vinyl glove bag. The mixture was stirred for 1 h at room temperature and white precipitate confirmed reaction completion. The reaction mixture was extracted with $CHCl_3$ and aqueous $NaHCO_3$ (saturated). The organic layer was washed with brine, dried with $Na_2SO_4$ and concentrated. The residue was purified by silica gel chromatography using hexane/ethyl acetate (2:1) to afford **23** (0.28 g, 0.37 mmol, 76%): $^{31}$P-NMR (202 MHz, $CDCl_3$) δ 149.984, 149.547.

**2,3,5-Tri-*O*-benzoyl-1-*O*-(4-fluorophenyl)-β-D-ribofuranose (9)**

To a stirred solution of 1-*O*-acetyl-2,3,5-tri-*O*-benzoyl-β-D-ribofuranose (3.02 g, 6.00 mmol) in dry $CH_2Cl_2$ (20 mL) at −30 ˚C, TMSOTf (1.95 mL, 10.8 mmol) and 4-fluorophenol (0.67 g, 6.00 mmol) were added. The reaction mixture was stirred for 17 h, quenched by saturated sodium bicarbonate and extracted with $CHCl_3$. The organic layer was washed with aqueous $NaHCO_3$ and brine, dried ($Na_2SO_4$) and solvent was evaporated under reduced pressure. The crude was purified by silica gel chromatography using hexane/ethyl acetate (5:1) to afford **9**

(2.85 g, 5.12 mmol, 85%): $^{1}$H-NMR (500 MHz, $CDCl_3$) δ 8.02-8.04 (m, 2H), 7.92-7.96 (m, 5H), 7.59 (t, *J* = 7.4 Hz, 1H), 7.42-7.55 (m, 5H), 7.34 (q, *J* = 8.2 Hz, 5H), 6.90-6.98 (m, 5H), 6.02 (dd, *J* = 7.2, 4.9 Hz, 1H), 5.90 (t, *J* = 6.0 Hz, 1H), 5.81 (s, 1H), 4.74-4.84 (m, 2H), 4.51 (dd, *J* = 11.7, 4.3 Hz, 1H); $^{13}$C-NMR (126 MHz, $CDCl_3$) δ 166.22, 165.55, 165.37, 152.45, 133.80, 133.67, 133.23, 129.98, 129.91, 129.85, 129.66, 129.12, 128.95, 128.70, 128.57, 128.40, 117.99, 117.93, 116.11, 115.93, 104.30, 79.82, 77.41, 76.90, 75.87, 72.07, 63.94.

**1-*O*-(4-Fluorophenyl)-β-D-ribofuranose (2)**

To a stirred solution of **9** (2.65 g, 4.76 mmol) in MeOH (14 mL) and $CH_2Cl_2$ (10 mL), a catalytic amount of 28% MeOH solution of sodium methoxide was added. The reaction mixture was stirred at room temperature for 20 h and quenched by using aqueous $NH_4Cl$ (saturated, 1 mL). The solvent was evaporated under reduced pressure and the resulting residue was purified by silica gel chromatography using $CHCl_3$/MeOH (10:1) to give **2** (1.02 g, 4.16 mmol, 88%): $^{1}$H-NMR (500 MHz, DMSO-$d_6$) δ 7.09-7.12 (m, 2H), 6.98-7.01 (m, 2H), 5.37 (s, 1H), 5.31 (d, *J* = 3.4 Hz, 1H), 5.01 (d, *J* = 5.2 Hz, 1H), 4.66-4.70 (m, 1H), 3.96-4.05 (m, 2H), 3.88 (q, *J* = 4.8 Hz, 1H), 3.51-3.55 (m, 1H), 3.36 (t, *J* = 6.0 Hz, 1H); $^{13}$C-NMR (126 MHz, DMSO-$d_6$) δ 158.11, 156.22, 152.96, 118.00, 117.93, 115.91, 115.73, 105.87, 84.62, 74.62, 70.57, 62.71, 40.02, 39.85, 39.68, 39.35, 39.19, 39.01.

**3,5-*O*-(Tetraisopropyldisiloxane)-1-*O*-(4-fluorophenyl)-β-D-ribofuranose (12)**

To a solution of **2** (0.97 g, 3.97 mmol) in pyridine (15 mL) stirred at room temperature, $TIPDSCl_2$ (1.36 mL, 4.37 mmol) was added. The mixture was stirred for 12 h and extracted with $CHCl_3$ and water. The organic layer was washed with aqueous $NaHCO_3$ (saturated), brine, dried with $Na_2SO_4$ and co-evaporated with toluene under vacuum to remove excess pyridine.

The residue was purified by silica gel chromatography using hexane/ethyl acetate (10:1) to give **12** (1.73 g, 3.55 mmol, 89%). $^{1}$H-NMR (500 MHz, $CDCl_3$) δ 6.91-6.99 (m, 4H), 5.53 (d, *J* = 5.7 Hz, 1H), 4.66 (t, *J* = 5.7 Hz, 1H), 4.25 (d, *J* = 4.6 Hz, 1H), 4.07-4.13 (m, 1H), 4.00 (dd, *J* = 11.5, 4.0 Hz, 1H), 3.72-3.77 (m, 1H), 3.07 (s, 1H), 1.03-1.12 (m, 32H); $^{13}$C-NMR (126 MHz, $CDCl_3$) δ 152.53, 117.93, 117.87, 116.11, 115.93, 104.92, 83.38, 77.42, 76.91, 76.19, 74.58, 65.74, 17.62, 17.57, 17.54, 17.48, 17.36, 17.16, 17.11, 13.47, 13.42, 13.00, 12.74.

**2-*O*-Methyl-3,5-*O*-(tetraisopropyldisiloxane)-1-*O*-(4-fluorophenyl)-β-D-ribofuranose (15)**

To a stirred solution of 12 (1.62 g, 3.33 mmol) in DMF (17 mL) was added NaH (60% in oil, 0.40 g, 9.99 mmol) at 0 ˚C. After 15 minutes, the reaction mixture was brought to room temperature and iodomethane (1.04 mL, 16.65 mmol) was added. The reaction mixture was stirred for 20 h at room temperature and partitioned between $CHCl_3$ and water. The organic layer was washed with aqueous $NaHCO_3$ (saturated), brine, dried with $Na_2SO_4$ and evaporated under reduced pressure. The crude was purified by silica gel chromatography using hexane/ethyl acetate (20:1) to yield **15** (0.75 g, 1.5 mmol, 49%). $^{1}$H-NMR (400 MHz, $CDCl_3$) δ 6.91-6.97 (m, 4H), 5.42 (s, 1H), 4.65 (q, *J* = 4.2 Hz, 1H), 4.07-4.10 (m, 1H), 3.87-3.97 (m, 2H), 3.83 (d, *J* = 4.0 Hz, 1H), 3.61 (d, *J* = 12.0 Hz, 3H), 1.02-1.13 (m, 33H); $^{13}$C-NMR (101 MHz, $CDCl_3$) δ 152.58, 118.10, 118.04, 116.07, 115.89, 103.39, 84.64, 81.67, 77.42, 76.91, 72.90, 62.97, 59.68, 17.58, 17.53, 17.48, 17.40, 17.22, 17.15, 13.63, 13.35, 12.87, 12.80.

**2-*O*-Methyl-1-*O*-(4-fluorophenyl)-β-D-ribofuranose (18)**

To a solution of **15** (0.71 g, 1.41 mmol) in THF (12 mL) stirred at room temperature, TEA·3HF (0.28 mL, 1.69 mmol) was added. The reaction mixture was stirred for 18 h at 40 ˚C and quenched with $NaHCO_3$ (saturated, 1 mL). $CHCl_3$ was added to the reaction mixture and

reduced under vacuum. The residue was purified by silica gel chromatography using $CHCl_3$ /methanol (15:1) to give **18** (0.31 g, 1.21 mmol, 86%): $^1$H-NMR (500 MHz, $CDCl_3$) δ 6.95-7.01 (m, 4H), 5.59 (s, 1H), 4.43-4.47 (m, 1H), 4.09-4.11 (m, 1H), 3.94 (dd, *J* = 5.2, 1.1 Hz, 1H), 3.80-3.84 (m, 1H), 3.64-3.69 (m, 1H), 3.56 (d, *J* = 4.6 Hz, 3H), 2.61 (d, *J* = 8.6 Hz, 1H), 1.76 (q, *J* = 4.4 Hz, 1H); $^{13}$C-NMR (126 MHz, $CDCl_3$) δ 152.52, 117.68, 117.61, 116.33, 116.14, 103.31, 85.99, 84.80, 77.42, 76.91, 70.45, 62.70, 58.90.

**2-*O*-Methyl-5-*O*-(4,4'-dimethoxytrityl)-1-*O*-(4-fluorophenyl)-β-D-ribofuranose (21)**

To a stirred solution of 18 (0.26 g, 0.99 mmol) in pyridine (8 mL) was added DMTrCl (0.40 g, 1.19 mmol) at room temperature. The reaction mixture was stirred for 12 h at room temperature and partitioned between EtOAc and water. The organic layer was washed with aqueous $NaHCO_3$ (saturated), brine, dried with $Na_2SO_4$ and evaporated under reduced pressure. The crude was purified by silica gel chromatography using hexane/ethyl acetate (2:1) to yield **21** (0.55 g, 0.99 mmol, quant.). $^1$H-NMR (500 MHz, $CDCl_3$) δ 7.41 (dd, *J* = 8.6, 6.9 Hz, 2H), 7.28-7.30 (m, 3H), 7.14-7.19 (m, 4H), 6.96-7.03 (m, 5H), 6.69 (dd, *J* = 8.6, 5.7 Hz, 4H), 5.65 (s, 1H), 4.37-4.41 (m, 1H), 4.14 (dd, *J* = 8.9, 5.4 Hz, 1H), 3.99 (d, *J* = 5.2 Hz, 1H), 3.80 (s, 1H), 3.75 (d, *J* = 2.3 Hz, 6H), 3.57 (s, 3H), 3.29 (dd, *J* = 10.0, 3.2 Hz, 1H), 3.14 (q, *J* = 5.2 Hz, 1H), 2.52 (d, *J* = 8.6 Hz, 1H); $^{13}$C-NMR (126 MHz, $CDCl_3$) δ 158.46, 145.03, 136.15, 135.97, 130.25, 130.15, 129.27, 128.31, 127.81, 126.76, 117.57, 117.52, 116.07, 115.88, 113.30, 113.11, 102.95, 86.08, 84.61, 84.56, 77.41, 76.90, 71.20, 64.32, 58.78, 55.28.

**2-*O*-Methyl-5-*O*-(4,4'-dimethoxytrityl)-3-*O*-[(2-cyanoethoxy)(N,N-diisoprylamino)] phosphanyl-1-*O*-(4-fluorophenyl)-β-D-ribofuranose (24)**

To a solution of **21** (0.38 g, 0.68 mmol) in THF (5 mL) was added *N,N*-diisopropylethylamine (0.59 mL, 3.40 mmol) and chloro(2-cyanoethoxy)(*N,N*-diisopropylamino)phosphine (0.32 mL,

1.36 mmol) at room temperature, inside the vinyl glove bag. The mixture was stirred for 1 h at room temperature and white precipitate confirmed reaction completion. The reaction mixture was extracted with $CHCl_3$ and aqueous $NaHCO_3$ (saturated). The organic layer was washed with brine, dried with $Na_2SO_4$ and concentrated. The residue was purified by silica gel chromatography using hexane/ethyl acetate (2:1) to afford **23** (0.40 g, 0.52 mmol, 77%): $^{31}$P-NMR (202 MHz, $CDCl_3$) δ 149.971, 149.545.

**2,3,5-Tri-*O*-benzoyl-1-*O*-(4-chlorophenyl)-β-D-ribofuranose (10)**

To a stirred solution of 1-*O*-acetyl-2,3,5-tri-*O*-benzoyl-β-D-ribofuranose (3.02 g, 6.00 mmol) in dry $CH_2Cl_2$ (20 mL) at −30 ˚C, TMSOTf (1.95 mL, 10.8 mmol) and 4-chlorophenol (0.77 g, 6.00 mmol) were added. The reaction mixture was stirred for 17 h, quenched by saturated sodium bicarbonate and extracted with $CHCl_3$. The organic layer was washed with aqueous $NaHCO_3$ and brine, dried ($Na_2SO_4$) and solvent was evaporated under reduced pressure. The crude was purified by silica gel chromatography using hexane/ethyl acetate (8:1) to afford 10 (2.54 g, 4.43 mmol, **74**%): $^1$H-NMR (500 MHz, $CDCl_3$) δ 8.02-8.04 (m, 2H), 7.90-7.94 (m, 5H), 7.58-7.61 (m, 1H), 7.41-7.55 (m, 6H), 7.30-7.37 (m, 5H), 7.18 (dd, *J* = 9.5, 2.6 Hz, 2H), 6.91-6.94 (m, 2H), 6.01 (dd, *J* = 7.2, 4.9 Hz, 1H), 5.90 (t, *J* = 4.0 Hz, 1H), 5.83 (s, 1H), 4.70-4.84 (m, 3H), 4.49 (dd, *J* = 12.0, 4.0 Hz, 1H); $^{13}$C-NMR (126 MHz, $CDCl_3$) δ 165.54, 133.83, 133.69, 133.24, 129.98, 129.92, 129.84, 129.61, 129.51, 128.91, 128.71, 128.58, 128.50, 128.39, 117.86, 103.76, 79.92, 77.42, 76.91, 75.82, 71.95, 63.73.

**1-*O*-(4-Chlorophenyl)-β-D-ribofuranose (3)**

To a stirred solution of **10** (1.90 g, 3.32 mmol) in MeOH (12 mL) and $CH_2Cl_2$ (8 mL), a catalytic amount of 28% MeOH solution of sodium methoxide was added. The reaction mixture was stirred at room temperature for 13 h and quenched by using aqueous $NH_4Cl$ (saturated, 1 mL).

The solvent was evaporated under reduced pressure and the resulting residue was purified by silica gel chromatography using $CHCl_3$/MeOH (12:1) to give **3** (0.78 g, 2.98 mmol, 90%): $^1$H-NMR (500 MHz, DMSO-$d_6$) δ 7.32 (qd, *J* = 5.0, 2.7 Hz, 2H), 6.99 (td, *J* = 6.3, 3.8 Hz, 2H), 5.42 (s, 1H), 5.33 (d, *J* = 4.6 Hz, 1H), 5.02 (d, *J* = 5.7 Hz, 1H), 4.67-4.71 (m, 1H), 3.94-4.01 (m, 2H), 3.87-3.92 (m, 1H), 3.52 (qd, *J* = 5.7, 4.0 Hz, 1H), 3.35 (d, *J* = 5.7 Hz, 1H); $^{13}$C-NMR (126 MHz, DMSO-$d_6$) δ 155.47, 129.23, 129.15, 125.33, 118.53, 118.13, 105.42, 100.64, 86.30, 84.73, 74.60, 71.52, 70.54, 69.28, 62.64, 40.03, 39.85, 39.69, 39.36, 39.19, 39.02.

**3,5-*O*-(Tetraisopropyldisiloxane)-1-*O*-(4-chlorophenyl)-β-D-ribofuranose (13)**

To a solution of **3** (0.74 g, 2.84 mmol) in pyridine (10 mL) stirred at room temperature, $TIPDSCl_2$ (0.98 mL, 3.13 mmol) was added. The mixture was stirred for 12 h and extracted with $CHCl_3$ and water. The organic layer was washed with aqueous $NaHCO_3$ (saturated), brine, dried with $Na_2SO_4$ and co-evaporated with toluene under vacuum to remove excess pyridine. The residue was purified by silica gel chromatography using hexane/ethyl acetate (10:1) to give **13** (1.20 g, 2.33 mmol, 82%). $^1$H-NMR (500 MHz, $CDCl_3$) δ 7.22 (td, *J* = 6.2, 3.6 Hz, 2H), 6.90 (td, *J* = 6.3, 3.8 Hz, 2H), 5.56 (d, *J* = 3.4 Hz, 1H), 4.65 (dd, *J* = 6.3, 5.2 Hz, 1H), 4.25 (d, *J* = 5.2 Hz, 1H), 4.09-4.12 (m, 1H), 3.98 (dd, *J* = 11.7, 3.7 Hz, 1H), 3.72 (dd, *J* = 11.5, 9.2 Hz, 1H), 3.07 (s, 1H), 1.08 (dtd, *J* = 20.4, 5.0, 2.7 Hz, 28H); $^{13}$C-NMR (126 MHz, $CDCl_3$) δ 155.00, 129.54, 127.26, 117.85, 104.40, 83.45, 77.42, 76.91, 76.16, 74.53, 65.69, 17.61, 17.56, 17.53, 17.47, 17.36, 17.16, 17.11, 13.47, 13.42, 13.00, 12.75.

**2-*O*-Methyl-3,5-*O*-(tetraisopropyldisiloxane)-1-*O*-(4-chlorophenyl)-β-D-ribofuranose (16)**

To a stirred solution of 13 (0.76 g, 1.51 mmol) in THF (8 mL) was added NaH (60% in oil, 0.09 g, 2.26 mmol) at 0 ˚C. After 15 minutes, the reaction mixture was brought to room temperature and iodomethane (0.12 mL, 1.81 mmol) was added. The reaction mixture was stirred for 6 h at room temperature and partitioned between $CHCl_3$ and water. The organic layer was washed with aqueous $NaHCO_3$ (saturated), brine, dried with $Na_2SO_4$ and evaporated under reduced pressure. The crude was purified by silica gel chromatography using hexane/ethyl acetate (20:1) to yield **16** (0.51 g, 0.97 mmol, 64%). $^1$H-NMR (500 MHz, $CDCl_3$) δ 7.21 (dd, *J* = 9.5, 2.6 Hz, 2H), 6.89-6.91 (m, 2H), 5.46 (s, 1H), 4.64 (q, *J* = 4.2 Hz, 1H), 4.07-4.10 (m, 1H), 3.94 (dd, *J* = 12.3, 3.2 Hz, 1H), 3.82-3.89 (m, 2H), 3.62 (s, 3H), 1.12 (t, *J* = 5.4 Hz, 7H), 1.03-1.08 (m, 22H); $^{13}$C-NMR (126 MHz, $CDCl_3$) δ 155.08, 129.50, 127.12, 117.94, 102.87, 84.60, 81.74, 77.42, 76.90, 72.87, 62.91, 59.70, 17.56, 17.53, 17.47, 17.39, 17.21, 17.14, 13.63, 13.34, 12.88, 12.79.

**2-*O*-Methyl-1-*O*-(4-chlorophenyl)-β-D-ribofuranose (19)**

To a solution of **16** (0.46 g, 0.90 mmol) in THF (8 mL) stirred at room temperature, TEA·3HF (0.22 mL, 1.35 mmol) was added. The reaction mixture was stirred for 8 h at 40 ˚C and quenched with $NaHCO_3$ (saturated, 1 mL). $CHCl_3$ was added to the reaction mixture and reduced under vacuum. The residue was purified by silica gel chromatography using $CHCl_3$ /methanol (15:1) to give **19** (0.24 g, 0.88 mmol, 98%): $^1$H-NMR (500 MHz, $CDCl_3$) δ 7.24 (s, 2H), 6.96 (d, *J* = 9.2 Hz, 2H), 5.61 (s, 1H), 4.43-4.47 (m, 1H), 4.08-4.11 (m, 1H), 3.94 (d, *J* = 5.2 Hz, 1H), 3.81 (td, *J* = 8.0, 4.2 Hz, 1H), 3.63-3.68 (m, 1H), 3.57 (s, 3H), 2.60 (d, *J* = 8.6 Hz,

1H), 1.69 (q, *J* = 4.4 Hz, 1H); $^{13}$C-NMR (126 MHz, $CDCl_3$) δ 154.98, 129.73, 127.61, 117.69, 102.85, 86.02, 84.75, 77.42, 76.91, 70.42, 62.67, 58.92

**2-*O*-Methyl-5-*O*-(4,4'-dimethoxytrityl)-1-*O*-(4-chlorophenyl)-β-D-ribofuranose (22)**

To a stirred solution of 19 (0.21 g, 0.76 mmol) in pyridine (8 mL) was added DMTrCl (0.31 g, 0.91 mmol) at room temperature. The reaction mixture was stirred for 6 h at room temperature and partitioned between EtOAc and water. The organic layer was washed with aqueous $NaHCO_3$ (saturated), brine, dried with $Na_2SO_4$ and evaporated under reduced pressure. The crude was purified by silica gel chromatography using hexane/ethyl acetate (3:1) to yield **22** (0.42 g, 0.73 mmol, 96%). $^1$H-NMR (500 MHz, $CDCl_3$) δ 7.39 (dd, *J* = 7.4, 2.3 Hz, 2H), 7.28 (s, 1H), 7.25 (d, *J* = 1.1 Hz, 3H), 7.16-7.18 (m, 3H), 7.00-7.02 (m, 2H), 6.67 (dd, *J* = 8.9, 7.2 Hz, 4H), 5.68 (s, 1H), 4.37-4.41 (m, 1H), 4.12-4.16 (m, 1H), 4.00 (d, *J* = 4.6 Hz, 1H), 3.75 (d, *J* = 3.4 Hz, 7H), 3.57 (s, 3H), 3.27 (dd, *J* = 10.3, 2.9 Hz, 1H), 3.13 (q, *J* = 5.2 Hz, 1H), 2.51 (d, *J* = 8.6 Hz, 1H); $^{13}$C-NMR (126 MHz, $CDCl_3$) δ 158.46, 155.54, 145.08, 136.11, 135.89, 130.25, 130.13, 129.51, 128.30, 127.82, 126.97, 126.79, 117.69, 113.11, 102.49, 86.08, 84.68, 84.57, 77.42, 76.91, 71.15, 64.31, 58.83, 55.31.

**2-*O*-Methyl-5-*O*-(4,4'-dimethoxytrityl)-3-*O*-[(2-cyanoethoxy)(N,N-diisoprylamino)] phosphanyl-1-*O*-(4-chlorophenyl)-β-D-ribofuranose (25)**

To a solution of **22** (0.25 g, 0.43 mmol) in THF (4 mL) was added *N,N*-diisopropylethylamine (0.38 mL, 2.15 mmol) and chloro(2-cyanoethoxy)(*N,N*-diisopropylamino)phosphine (0.19 mL, 0.86 mmol) at room temperature, inside the vinyl glove bag. The mixture was stirred for 1 h at room temperature and white precipitate confirmed reaction completion. The reaction mixture was extracted with $CHCl_3$ and aqueous $NaHCO_3$ (saturated). The organic layer was washed with brine, dried with $Na_2SO_4$ and concentrated. The residue was purified by silica gel

chromatography using hexane/ethyl acetate (2:1) to afford **25** (0.26 g, 0.34 mmol, 78%): $^{31}$P-NMR (202 MHz, $CDCl_3$) δ 149.974, 149.543.

**Synthesis of the controlled pore glass (CPG) solid support (26-28)**

*N,N*-Dimethyl-4-aminopyridine (DMAP) (49 mg, 0.4 mmol), and succinic anhydride (80 mg, 0.8 mmol) were added to a solution of **20** (0.11 g, 0.2 mmol) in pyridine (4 mL) under argon atmosphere and the mixture was stirred for 20 h at room temperature. The mixture was extracted with $H_2O$ and EtOAc. The organic layer was washed with sat. $NaHCO_3$ solution, brine, dried over $Na_2SO_4$ and concentrated in vacuo. The residue was purified by column chromatography on silica gel (hexane:ethyl acetate, 2:1) to give succinate mixture as a colorless, viscous liquid in quantitttive yield. Aminopropyl controlled pore glass (0.33 g, 50 μmol) and 1-ethyl-3-[3-(dimethylamino)propyl] carbodiimide hydrochloride (38 mg, 0.2 mmol) were added to a solution of succinate in DMF and the mixture was kept at room temperature for 4 days. This resin was washed with pyridine, 15 mL of capping solution (0.1 M DMAP in pyridine: $Ac_2O$, 9:1) were added to the resin and the mixture was kept at room temperature for 1 day. The resin was washed with pyridine, ethanol, acetonitrile and dried under vacuum to give solid support **26**. Similarly, solid supports 27 and 28 were also synthesized for analogs 2 and **3**. The amount of nucleoside loaded to the solid support was calculated by release of dimethoxytrityl cation using solution of 70% $HClO_4$: EtOH (3:2, v/v).

## 6.3. Experimental procedure

### 6.3.1. RNA synthesis

Synthesis was carried out with a DNA/RNA synthesizer by phosphoramidite method according to the normal protocol. Post synthesis, the oligomers were cleaved from CPG beads and deprotected with concentrated $NH_3$ solution/40% methylamine (1:1, v/v) for 10 min at 65 ˚C. 2'-*O*-TBDMS groups were removed by $Et_3N{\cdot}3HF$ in DMSO at 65 ˚C for 1.5 h. The reaction was quenched with 0.1 M TEAA buffer (pH 7.0) and the mixture desalted using Sep-Pak C18 cartridge. The oligonucleotides were later purified by 20% denaturing PAGE to give highly purified RNAs.

### 6.3.2. Thermal denaturation study

The solution containing 3.0 μM duplex in a buffer of 10 mM sodium phosphate (pH 7.0) containg 100 mM NaCl was heated at 100 ˚C, then gradually cooled to room temperature and used for this study. Thermally induced transitions of each mixture were monitored at 260 nm with a UV/Vis spectrometer fitted with temperature controller in quartz cuvettes with a path length of 1.0 cm. The sample temperature was increased by 0.5 ˚C/min.

### 6.3.3. Dual-luciferase reporter assay

HeLa cells were transfected with the psiCHECK-2 (Promega) reporter and the pcDNA3.1 containing a hygromycin resistance gene (Thermo Fisher Scientific). Cells were cultured in the presence of 0.5 mg/mL hygromycin for one week. Stable HeLa-psiCHECK-2 cells expressing both *Renilla* and firefly luciferases were grown in Dulbecco's Modified Eagle Medium (D-MEM) supplemented with 10% bovine serum (BS) and 0.25 mg/mL hygromycin at 37 ˚C. HeLa-psiCHECK-2 cells ($8.0 \times 10^4$/mL) were cultured on a 96-well microplate (100 μL/well)

for 24 h and transfected with siRNA targeting the *Renilla* luciferase gene using lipofectamine RNAi max in Opti-MEM I reduced serum medium. Transfection without siRNA was used as a control. After 1 h, each well was seeded with 50 µL of D-MEM containing 10% BS and cells were further incubated for another 12 h and 24 h as per the treatment. The activities of *Renilla* and firefly luciferases in the cells were determined with Dual-Luciferase Reporter Assay System (Promega) according to a manufacture's protocol. The activity of Renilla luciferase was normalized by the firefly luciferase activity. The results were confirmed by at least three independent transfections and expressed as the average from four experiments as mean±SD.

### 6.3.4. Molecular Modelling

We obtained the initial atomic coordinates of the PAZ domain-siRNA complex from the Protein Data Bank (PDB); the entry 1SI3 was used for preparing the structure. The PAZ domain-siRNA complex prepared for calculation consists of PAZ domain (Mse224-Gln295, Val302-Arg349) and a 9-mer RNA (5'-CGUGACUCU-3'). Missing hydrogen atoms and side chains were added and optimized their positions with the Tripos force field using the molecular modelling software SYBYL-X. Three-dimensional data for 3'-end modified siRNA were constructed by replacing native siRNA. The coordinates of the modified and neighboring nucleotides were again refined by energy minimization using the Tripos force field (Vinter *et al.*, 1987; Hammarström *et al.*, 1988; Matthew *et al.*, 1989).

The *ab initio* Fragment Molecular Orbital (FMO) calculations was adopted to evaluate the specific interactions and binding affinity between PAZ domain and siRNA. This method is a quantum-chemical calculation method to study the electronic states and the interactions of large biomolecule with high accuracy. In the FMO calculation, each amino acid residue in PAZ domain was treated as a single fragment, and each nucleotide for siRNA was divided into

backbone fragments (phosphate + sugar) and base fragments, because this fragmentation enables to analyse the base-residues interaction. All FMO calculations were performed with the PAICS program, where we employed the second-order Møller-Plesset (MP2) perturbation methods with the basis set of 6-311G** (Mochizuki *et al.*, 2004).

### 6.3.5. Enzyme-linked immunosorbent assay (ELISA)

A solution of dsRNAs (100 nM, 50 μL), modified with biotin at the 3'-end of the passenger strand, were added to a streptavidin-coated 96-well plate. After 15 min, each well was washed three times with a solution (200 μL x 3) of 0.05% Tween 20 in PBS (pH 7.4) and then a solution (100 μL) of 3% BSA in PBS buffer (pH 7.4) was added. After 2 h, each well was washed and then a solution of the PAZ domain protein (100 nM, 50 μL) in PBS buffer (pH 7.4) contained 1% BSA was added. The plate was incubated at 37 ˚C for 10 min. Each well was washed and then a solution of the anti-His tag antibody conjugated horseradish peroxidase (50 μL) in PBS containing 1% BSA was added. After 1 h, each well was washed and then a peroxidase (POD) substrate (50 μL) was added. After 10 min, a stop solution (1 M $H_2SO_4$, 50 μL) was added and then an absorbance of each well at 450 nm was measured by a microplate reader.

### 6.3.6. Partial digestion of RNAs by 3'-exonuclease SVPD

Each ON (600 pmol) labeled with fluorescein at the 5'-end was incubated with SVPD (0.075 unit) in a buffer (150 μL) comprising 0.1 M Tris-HCl (pH 8.0) and 20 mM $MgCl_2$ at 37 ˚C. After 0, 1, 5, 10, 30, 60, 120, or 240 min, an aliquot (5 μL) of the reaction mixture was mixed with the loading buffer (15 μL), comprising Tris-borate-EDTA (TBE) buffer and 20% glycerin, on ice. Each sample was analyzed by 20% denaturing PAGE at room temperature for 2 h at 20 mA. Similarly the experiment was executed for branched RNAs also. But, the analysis was

performed with 6% denaturing PAGE for 2 h at 20 mA. The gel was visualized by use of a Luminescent Image analyzer LAS-4000 (Fujifilm).

### 6.3.7. Dynamic light scattering

Hydrodynamic diamters of siRNAs were determined by dynamic light scattering (DLS) using a Zetasizer nano ZS (Malvern Instruments, UK). siRNA solutions (9 nmol in 1 mL PBS) were analysed at 25 ˚C in triplicate. Correspondingly, the bident and trident branching siRNAs solution were also formed by annealing of equimolar amounts of each.

### 6.3.8. HPLC analysis of RNAs

The RNA strands were purified by reversed-phase C-18 HPLC using a linear gradient of 5−50% of MeCN in 0.1 M TEAA buffer at pH 7.0. Also, the lipophilicity analysis of the modified siRNAs was performed with the similar conditions of RP-HPLC.

# Publications

Akash Chandela, Taeko Watanabe, Kenji Yamagishi, Yoshihito Ueno (2019). Synthesis and characterization of small interfering RNAs with haloalkyl groups at their 3'-dangling ends. *Bioorganic & Medicinal Chemistry* 27 (2019); 1341-1349.

Akash Chandela, Yoshihito Ueno (2019). Systemic Delivery of Small Interfering RNA Therapeutics: Obstacles and Advances. *Reviews in Agricultural Science* 2019, Volume 7, Pages 10-28.

Akash Chandela, Yoshihito Ueno (2019). Design, synthesis and evaluation of novel, branched trident small interfering RNA nanostructures for sequence-specific RNAi activity (under review)

# Acknowledgement

I am greatly indebted to my mentor, Prof. Yoshihito Ueno for his tireless efforts and guidance during my years of study at Gifu University. I appreciate the time he took to supervise me and direct my efforts in a constructive way to procure comprehensive knowledge of the subject. Regular input of suggestions and comments from him, helped me throughout during the completion of my doctoral degree.

I acknowledge the efforts of my co-supervisors; Prof. Shingo Kawai and Assoc. Prof. Yanase Emiko, who constantly provided their precious time and reviewed my research progress at regular intervals. Their critical inputs helped me in designing and assessing the various factors for the successful accomplishment of my experiments.

Special thanks to Prof. Yoko Hirata for supplying the cells and providing the technical guidance during the gene silencing assays. Also, I am very grateful to Prof. Kenji Yamagishi and his student Ms. Taeko Watanabe (Nihon University) for assisting with the molecular modelling studies of the modified siRNAs with PAZ domain.

My heartfelt thanks is also extended to my bachelor's and master's project mentor, Prof. Rakhi Chaturvedi (IIT Guwahati) for building up my scientific interests and guiding me throughout my experimental problems. Her dedication to her work and diligence played a great role in intensifying my interest in biological sciences.

During my stay in Japan, over the span of closely 3 years, I always had the constant support of my lab members. They helped me throughout my journey of the doctoral degree and trained me with all the instruments, required during the course of my experiments. My seniors, Dr. Yusuke Maeda and Dr. Kosuke Nakamoto always provided me with the opportunity for scientific discussions and guided me through some of the experimental problems. Ryohei Kajino (master graduate) always provided me help during my experiments and as a tutor, also

Kajino (master graduate) always provided me help during my experiments and as a tutor, also took very nice care of me. Masashi Yamaguchi, a graduate student from our lab, always helped me with the learning of language and maintained a positive environment. Other master graduates, Toshifumi Kano, Koki Ozaki, Nazuki Niwa, Hiyuki Yanase, Kenji Honda and Kana Koizumi, were all very helpful and kind during the course of my program. I am also thankful to Dr. Arindam Chakrabarty, who helped me with dynamic light scattering experiments.

Foremost, I would like to extend my heartfelt thanks to my parents, especially my late mother for her constant support, efforts and belief in me. The kind of support and unequalled sacrifice she made are unmatched. I also appreciate the fervour support my family has always provided me. The list of friends to thank is endless, so I will leave it unwritten here but always in my heart.

Finally, and most important of all, thanks be to God, because it is only through Him that all of this work has been possible.

# References

Ambardekar, V. V., Han, H.Y., Varney, M.L., Vinogradov, S. V., Singh, R.K., and Vetro, J.A. 2011. The modification of siRNA with 3' cholesterol to increase nuclease protection and suppression of native mRNA by select siRNA polyplexes. *Biomaterials* **32**: 1404–1411.

Aviñó, A., Ocampo, S.M., Perales, J.C., and Eritja, R. 2011. Branched RNA: A New Architecture for RNA Interference. *J. Nucleic Acids* **2011**: 1–7.

Bienk, K., Hvam, M.L., Pakula, M.M., Dagnæs-Hansen, F., Wengel, J., Malle, B.M., Kragh-Hansen, U., Cameron, J., Bukrinski, J.T., and Howard, K.A. 2016. An albumin-mediated cholesterol design-based strategy for tuning siRNA pharmacokinetics and gene silencing. *J. Control. Release* **232**: 143–151.

Borna, H., Imani, S., Iman, M., and Azimzadeh Jamalkandi, S. 2015. Therapeutic face of RNAi: in vivo challenges. *Expert Opin. Biol. Ther.* **15**: 269–85.

Chakraborty, C., Sharma, A.R., Sharma, G., Doss, C.G.P., and Lee, S.S. 2017. Therapeutic miRNA and siRNA: Moving from Bench to Clinic as Next Generation Medicine. *Mol. Ther. - Nucleic Acids* **8**: 132–143.

Chandela, A., and Ueno, Y. 2019. Systemic Delivery of Small Interfering RNA Therapeutics: Obstacles and Advances. *Rev. Agric. Sci.* **7**: 10–28.

Chandela, A., Watanabe, T., Yamagishi, K., and Ueno, Y. 2019. Synthesis and characterization of small interfering RNAs with haloalkyl groups at their 3′-dangling ends. *Bioorganic Med. Chem.* **27**.

Chang, C. Il, Lee, T.Y., Kim, S., Sun, X., Hong, S.W., Yoo, J.W., Dua, P., Kang, H.S., Kim, S., Li, C.J., et al. 2012. Enhanced intracellular delivery and multi-target gene silencing

triggered by tripodal RNA structures. *J. Gene Med.* **14**: 138–146.

Chernikov, I. V., Gladkikh, D. V., Meschaninova, M.I., Ven'yaminova, A.G., Zenkova, M.A., Vlassov, V. V., and Chernolovskaya, E.L. 2017. Cholesterol-Containing Nuclease-Resistant siRNA Accumulates in Tumors in a Carrier-free Mode and Silences MDR1 Gene. *Mol. Ther. - Nucleic Acids* **6**: 209–220.

Crombez, L., Aldrian-Herrada, G., Konate, K., Nguyen, Q.N., McMaster, G.K., Brasseur, R., Heitz, F., and Divita, G. 2009. A new potent secondary amphipathic cell-penetrating peptide for siRNA delivery into mammalian cells. *Mol. Ther.* **17**: 95–103.

Cryan, S.-A., McKiernan, P.J., Yadav, A.B., Kelly, C., and Greene, C.M. 2013. RNAi in Respiratory Diseases In: Advanced Delivery and Therapeutic Applications of RNAi. pp. 391–416.

Eberle, F., Peter, M., Richert, C., Dalpke, A.H., Giessler, K., Deck, C., and Heeg, K. 2014. Modifications in Small Interfering RNA That Separate Immunostimulation from RNA Interference. *J. Immunol.* **180**: 3229–3237.

Elbashir, S.M., Harborth, J., Lendeckel, W., Yalcin, A., Weber, K., and Tuschl, T. 2001a. Duplexes of 21 ± nucleotide RNAs mediate RNA interference in cultured mammalian cells. *Nature* **411**: 494–498.

Elbashir, S.M., Lendeckel, W., and Tuschl, T. 2001b. RNA interference is mediated by 21- and 22-nucleotide RNAs. *Genes Dev.* **15**: 188–200.

Eldredge, A.C., Johnson, M.E., Cao, Y., Zhang, L., Zhao, C., Liu, Z., Yang, Q., and Guan, Z. 2018. Dendritic peptide bolaamphiphiles for siRNA delivery to primary adipocytes.

*Biomaterials* **178**: 458–466.

Elkayam, E., Kuhn, C., Tocilj, A., Haase, A.D., Greene, E.M., and Hannon, G.J. 2012. The Structure of Human Argonaute-2. *Cell* **150**: 100–110.

Fire, A. 1999. RNA-triggered gene silencing. *Trends Genet.* **15**: 358–363.

Fire, A., Xu, S., Montgomery, M.K., Kostas, S.A., Driver, S.E., and Mello, C.C. 1998. Potent and specific genetic interference by double-stranded RNA in Caenorhabditis elegans. *Nature* **391**: 806–811.

França, N.R. de, Mesquita, D., Lima, A.B., Pucci, F.V.C., Andrade, L.E.C., and Silva, N.P. 2010. RNA interference: A new alternative for rheumatic diseases therapy. *Rev. Bras. Reumatol.* **50**: 702–709.

Frank, F., Sonenberg, N., and Nagar, B. 2010. Structural basis for 5 9 -nucleotide base-specific recognition of guide RNA by human AGO2. *Nature* **465**: 818–822.

Garba, A.O., and Mousa, S.A. 2010. Bevasiranib for the treatment of wet, age-related macular degeneration. *Ophthalmol. Eye Dis.* **2**: 75–83.

Gresham, D. 2003. RNAi on or off target? *Nat. Genet.* **34**: 133.

Grøtli, M., Eritja, R., and Sproat, B. 1997. Solid-phase synthesis of branched RNA and branched DNA/RNA chimeras. *Tetrahedron* **53**: 11317–11346.

Gvozdeva, O. V., Gladkih, D. V., Chernikov, I. V., Meschaninova, M.I., Venyaminova, A.G., Zenkova, M.A., Vlassov, V. V., and Chernolovskaya, E.L. 2018. Nuclease-resistant 63-bp trimeric siRNAs simultaneously silence three different genes in tumor cells. *FEBS Lett.* **592**:

122–129.

Hammarström, L. -G, Liljefors, T., and Gasteiger, J. 1988. Electrostatic interactions in molecular mechanics (MM2) calculations via PEOE partial charges I. Haloalkanes. *J. Comput. Chem.* **9**: 424–440.

Hammond, S.M., Caudy, A.A., and Hannon, G.J. 2001. Post-transcriptional gene silencing by double-stranded RNA. *Nat. Rev. Genet.* **2**: 110–9.

Haraszti, R.A., Miller, R., Didiot, M.C., Biscans, A., Alterman, J.F., Hassler, M.R., Roux, L., Echeverria, D., Sapp, E., DiFiglia, M., et al. 2018. Optimized Cholesterol-siRNA Chemistry Improves Productive Loading onto Extracellular Vesicles. *Mol. Ther.* **26**: 1973–1982.

Haussecker, D. 2014. Current issues of RNAi therapeutics delivery and development. *J. Control. Release* **195**: 49–54.

He, X.-X. 2017. Macrophage migration inhibitory factor siRNA inhibits hepatic metastases of colorectal cancer cells. *Front. Biosci.* **22**: 4549.

Hutvágner, G., and Zamore, P.D. 2002. A microRNA in a multiple-turnover RNAi enzyme complex. *Science (80-. ).* **297**: 2056–2060.

Inada, N., Nakamoto, K., Yokogawa, T., and Ueno, Y. 2015. Synthesis of small interfering RNAs containing acetal-type nucleoside analogs at their 3???-ends and analysis of their silencing activity and their ability to bind to the Argonaute2 PAZ domain. *Eur. J. Med. Chem.* **103**: 460–472.

Kandeel, M., and Kitade, Y. 2013. In silico molecular docking analysis of the human

Argonaute 2 PAZ domain reveals insights into RNA interference. *J. Comput. Aided. Mol. Des.* **27**: 605–614.

Khairuddin, N., Gantier, M.P., Blake, S.J., Wu, S.Y., Behlke, M.A., Williams, B.R., and McMillan, N.A. 2012. SiRNA-induced immunostimulation through TLR7 promotes antitumoral activity against HPV-driven tumors in vivo. *Immunol. Cell Biol.* **90**: 187–196.

Kosmas, C., Muñoz Estrella, A., Sourlas, A., Silverio, D., Hilario, E., Montan, P., and Guzman, E. 2018. Inclisiran: A New Promising Agent in the Management of Hypercholesterolemia. *Diseases* **6**: 63.

Kruspe, S., and Giangrande, P. 2017. Aptamer-siRNA Chimeras: Discovery, Progress, and Future Prospects. *Biomedicines* **5**: 45.

Leachman, S.A., Hickerson, R.P., Hull, P.R., Smith, F.J.D., Milstone, L.M., Lane, E.B., Bale, S.J., Roop, D.R., McLean, W.H.I., and Kaspar, R.L. 2008. Therapeutic siRNAs for dominant genetic skin disorders including pachyonychia congenita. *J. Dermatol. Sci.* **51**: 151–157.

Li, Y., Zhang, J., Wang, B., Shen, Y., and Ouahab, A. 2016. Co-delivery of siRNA and hypericin into cancer cells by hyaluronic acid modified PLGA-PEI nanoparticles. *Drug Dev. Ind. Pharm.* **42**: 737–746.

Liebow, A., Li, X., Racie, T., Hettinger, J., Bettencourt, B.R., Najafian, N., Haslett, P., Fitzgerald, K., Holmes, R.P., Erbe, D., et al. 2017. An Investigational RNAi Therapeutic Targeting Glycolate Oxidase Reduces Oxalate Production in Models of Primary Hyperoxaluria. *J. Am. Soc. Nephrol.* **28**: 494–503.

Lingel, A., Simon, B., Izaurralde, E., and Sattler, M. 2003. Structure and nucleic-acid binding

of the Drosophila Argonaute 2 PAZ domain. 465–469.

Liu, X., and Peng, L. 2016. Dendrimer nanovectors for siRNA delivery In: Methods in Molecular Biology. pp. 127–142.

Liu, X., Wang, Y., Chen, C., Tintaru, A., Cao, Y., Liu, J., Ziarelli, F., Tang, J., Guo, H., Rosas, R., et al. 2016. A Fluorinated Bola-Amphiphilic Dendrimer for On-Demand Delivery of siRNA, via Specific Response to Reactive Oxygen Species. *Adv. Funct. Mater.* **26**: 8594–8603.

Ma, D. 2014. Enhancing endosomal escape for nanoparticle mediated siRNA delivery. *Nanoscale* **6**: 6415–6424.

Ma, J.B., Ye, K., and Patel, D.J. 2004. Structural basis for overhang-specific small interfering RNA recognition by the PAZ domain. *Nature* **429**: 318–322.

Makita, Y., Murata, S., Katou, Y., Kikuchi, K., Uejima, H., Teratani, M., Hoashi, Y., Kenjo, E., Matsumoto, S., Nogami, M., et al. 2017. Anti-tumor activity of KNTC2 siRNA in orthotopic tumor model mice of hepatocellular carcinoma. *Biochem. Biophys. Res. Commun.* **493**: 800–806.

Martínez, T., González, M.V., Roehl, I., Wright, N., Pañeda, C., and Jiménez, A.I. 2014. In vitro and in vivo efficacy of SYL040012, a novel siRNA compound for treatment of glaucoma. *Mol. Ther.* **22**: 81–91.

Matranga, C., Tomari, Y., Shin, C., Bartel, D.P., and Zamore, P.D. 2005. Passenger-Strand Cleavage Facilitates Assembly of siRNA into Ago2-Containing RNAi Enzyme Complexes. **123**: 607–620.

Matthew, C., Richard III, D.C., and Nicole Van, O. 1989. Validation of the general purpose tripos 5.2 force field. *J. Comput. Chem.* **10**: 982–1012.

Mello, C.C., and Conte, D. 2004. Revealing the world of RNA interference. *Nature* **431**: 338–342.

Mochizuki, Y., Nakano, T., Koikegami, S., Tanimori, S., Abe, Y., Nagashima, U., and Kitaura, K. 2004. A parallelized integral-direct second-order Møller-Plesset perturbation theory method with a fragment molecular orbital scheme. *Theor. Chem. Acc.* **112**: 442–452.

Molitoris, B.A., Dagher, P.C., Sandoval, R.M., Campos, S.B., Ashush, H., Fridman, E., Brafman, A., Faerman, A., Atkinson, S.J., Thompson, J.D., et al. 2009. siRNA Targeted to p53 Attenuates Ischemic and Cisplatin-Induced Acute Kidney Injury. *J. Am. Soc. Nephrol.* **20**: 1754–1764.

Moreno-Montañés, J., Bleau, A.M., and Jimenez, A.I. 2018. Tivanisiran, a novel siRNA for the treatment of dry eye disease. *Expert Opin. Investig. Drugs* **27**: 421–426.

Murchison, E.P., and Hannon, G.J. 2004. miRNAs on the move: miRNA biogenesis and the RNAi machinery. *Curr. Opin. Cell Biol.* **16**: 223–229.

P.N. Pushparaj, J.J. Aarthi, J.Manikandan, S.D.K. 2008. siRNA, miRNA, and shRNA: *Crit. Rev. Oral Biol. Med.* **87**: 992–1003.

Paroo, Z., and Corey, D.R. 2004. Challenges for RNAi in vivo. *Trends Biotechnol.* **22**: 390–394.

Pecot, C. V., Calin, G.A., Coleman, R.L., Lopez-Berestein, G., and Sood, A.K. 2011. RNA

interference in the clinic: Challenges and future directions. *Nat. Rev. Cancer* **11**: 59–67.

Peng, S.F., Hsu, H.K., Lin, C.C., Cheng, Y.M., and Hsu, K.H. 2017. Novel PEI/Poly-γ-gutamic acid nanoparticles for high efficient siRNA and plasmid DNA co-delivery. *Molecules* **22**.

Pfeifer, A., and Lehmann, H. 2010. Pharmacological potential of RNAi - Focus on miRNA. *Pharmacol. Ther.* **126**: 217–227.

Pruijn, G.J.M. 2006. The RNA interference pathway: A new target for autoimmunity. *Arthritis Res. Ther.* **8**.

Robbins, M., Judge, A., Liang, L., McClintock, K., Yaworski, E., and MacLachlan, I. 2007. 2′-O-methyl-modified RNAs act as TLR7 antagonists. *Mol. Ther.* **15**: 1663–1669.

Sajeesh, S., Lee, T.Y., Kim, J.K., Son, D.S., Hong, S.W., Kim, S., Yun, W.S., Kim, S., Chang, C., Li, C., et al. 2014. Efficient intracellular delivery and multiple-target gene silencing triggered by tripodal RNA based nanoparticles: A promising approach in liver-specific RNAi delivery. *J. Control. Release* **196**: 28–36.

Schirle, N.T., and MacRae, I.J. 2012. The Crystal Structure of Human Argonaute2. *Science (80-. ).* **336**: 1037–1040.

Schütze, N. 2004. siRNA technology. *Mol. Cell. Endocrinol.* **213**: 115–119.

Shchepinov, M.S., Mir, K.U., Elder, J.K., Frank-kamenetskii, M.D., and Southern, E.M. 1999. Oligonucleotide dendrimers : stable nano-structures. **27**: 3035–3041.

Shchepinov, M.S., Udalova, I.A., Bridgman, A.J., and Southern, E.M. 1997. Oligonucleotide dendrimers : synthesis and use as polylabelled DNA probes. **25**: 4447–4454.

Song, J.J., Liu, J., Tolia, N.H., Schneiderman, J., Smith, S.K., Martienssen, R.A., Hannon, G.J., and Joshua-Tor, L. 2003. The crystal structure of the Argonaute2 PAZ domain reveals an RNA binding motif in RNAi effector complexes. *Nat. Struct. Biol.* **10**: 1026–1032.

Tushir-Singh, J. 2017. Antibody-siRNA conjugates: drugging the undruggable for anti-leukemic therapy. *Expert Opin. Biol. Ther.* **17**: 325–338.

Tuttolomondo, M., Casella, C., Hansen, P.L., Polo, E., Herda, L.M., Dawson, K.A., Ditzel, H.J., and Mollenhauer, J. 2017. Human DMBT1-Derived Cell-Penetrating Peptides for Intracellular siRNA Delivery. *Mol. Ther. - Nucleic Acids* **8**: 264–276.

Ueno, Y., Inoue, T., Yoshida, M., Yoshikawa, K., Shibata, A., Kitamura, Y., and Kitade, Y. 2008. Synthesis of nuclease-resistant siRNAs possessing benzene-phosphate backbones in their 3′-overhang regions. *Bioorganic Med. Chem. Lett.* **18**: 5194–5196.

Ueno, Y., Watanabe, Y., Shibata, A., Yoshikawa, K., Takano, T., Kohara, M., and Kitade, Y. 2009. Synthesis of nuclease-resistant siRNAs possessing universal overhangs. *Bioorganic Med. Chem.* **17**: 1974–1981.

Utagawa, E., Ohkubo, A., Sekine, M., and Seio, K. 2007. Synthesis of branched oligonucleotides with three different sequences using an oxidatively removable tritylthio group. *J. Org. Chem.* **72**: 8259–8266.

Valencia-Serna, J., Landry, B., Jiang, X., and Uludag, H. 2014. Potential of siRNA Therapy in Chronic Myeloid Leukemia In: Intracellular Delivery II. pp. 435–473.

Valenzuela, R.A.P., Onizuka, K., Ball-Jones, A.A., Hu, T., Suter, S.R., and Beal, P.A. 2016. Guide Strand 3′-End Modifications Regulate siRNA Specificity. *ChemBioChem* **17**: 2340–

2345.

Valenzuela, R.A.P., Suter, S.R., Ball-Jones, A.A., Ibarra-Soza, J.M., Zheng, Y., and Beal, P.A. 2014. Base modification strategies to modulate immune stimulation by an siRNA. *ChemBioChem* **16**: 262–267.

Vinter, J.G., Davis, A., and Saunders, M.R. 1987. Strategic approaches to drug design. I. An integrated software framework for molecular modelling. *J. Comput. Aided. Mol. Des.* **1**: 31–51.

Wagner, E. 2012. Polymers for siRNA delivery: Inspired by viruses to be targeted, dynamic, and precise. *Acc. Chem. Res.* **45**: 1005–1013.

Wang, J., Lu, Z., Wientjes, M.G., and Au, J.L.-S. 2010. Delivery of siRNA Therapeutics: Barriers and Carriers. *AAPS J.* **12**: 492–503.

Wang, T., Shigdar, S., Al, H., Gantier, M.P., Yin, W., Xiang, D., Wang, L., Zhou, S., Hou, Y., Wang, P., et al. 2017. Challenges and opportunities for siRNA-based cancer treatment. *Cancer Lett.* **387**: 77–83.

Wang, Y., Juranek, S., Li, H., Sheng, G., Tuschl, T., and Patel, D.J. 2008. Structure of an argonaute silencing complex with a seed-containing guide DNA and target RNA duplex. *Nature* **456**: 921–926.

Whitehead, K.A., Dahlman, J.E., Langer, R.S., and Anderson, D.G. 2011. Silencing or Stimulation? siRNA Delivery and the Immune System. *Annu. Rev. Chem. Biomol. Eng.* **2**: 77–96.

Wu, S.Y., Lopez-Berestein, G., Calin, G.A., and Sood, A.K. 2014. RNAi therapies: Drugging the undruggable. *Sci. Transl. Med.* **6**.

Xu, L., Wang, X., He, H., Zhou, J., Li, X., Ma, H., Li, Z., Zeng, Y., Shao, R., Cen, S., et al. 2015. Structure-based design of novel chemical modification of the 3′-overhang for optimization of short interfering RNA performance. *Biochemistry* **54**: 1268–1277.

Yang, Y., Yang, Y.F., Xie, X.Y., Wang, Z.Y., Gong, W., Zhang, H., Li, Y., Yu, F.L., Li, Z.P., and Mei, X.G. 2015. Dual-modified liposomes with a two-photon-sensitive cell penetrating peptide and NGR ligand for siRNA targeting delivery. *Biomaterials* **48**: 84–96.

Zhou, J., Li, H., Li, S., Zaia, J., and Rossi, J.J. 2008. Novel dual inhibitory function aptamer-siRNA delivery system for HIV-1 therapy. *Mol. Ther.* **16**: 1481–1489.

Zuckerman, J.E., Choi, C.H.J., Han, H., and Davis, M.E. 2012. Polycation-siRNA nanoparticles can disassemble at the kidney glomerular basement membrane. *Proc. Natl. Acad. Sci.* **109**: 3137–3142.